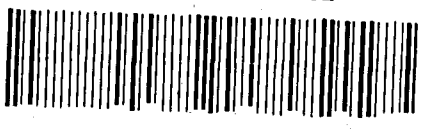

OXIDATION STUDIES INVOLVING SILVER ELECTRODES

by

JOHN RICHARD MORLEY Dip.Tech., D.L.C., A.R.I.C.

Supervisors:- Dr. N. A. Hampson
Dr. J. B. Lee

Submitted for the degree: Doctor of Philosophy of Loughborough University of Technology; on 31st October 1969.

SUMMARY

The kinetics of the electrochemical oxidation of silver in alkali have been studied. The oxidation of silver to Ag_2O at low coverage (of Ag_2O) is charge transfer controlled being second order w.r.t. silver. Adsorption of OH^- is indicated. The oxidation to AgO is controlled by a classical electrocrystallisation process.

The oxidation of organic compounds at silver oxide electrodes are also discussed. The electrode shows very strong catalytic activity in the oxidation of amines. Primary amines react by either of two overall oxidation paths, each of which can be chosen by suitable adjustment of the electrochemical parameters. The oxidation mechanisms for aliphalic amines and alcohols are discussed.

ACKNOWLEDGEMENT

There are many people who have contributed in many ways towards my completion of this work.

My most sincere thanks go to my supervisors Dr. Noel Hampson and Dr. Barry Lee who have been unstintingly generous in their guidance and inspiration throughout the last three years; to Dr. Bernard Scanlon who has helped me in so many ways; to my fellow research students (past and present) for their good companionship and for the long hours of discussion (not just on Chemistry) we have had; to Professor R. F. Phillips for providing the opportunity and facilities for this work; to the University for financial assistance; to the technical staff of the Chemistry Department for their cheerful cooperation; to the staff of the Computer Centre (L.U.T.) - especially Mr. John Sawbridge - for their help in unravelling the intricacies of Fortran; and finally to Miss Marian Buxton who has typed this manuscript so well.

CONTENTS

INDEX OF FIGURES

INDEX OF TABLES

INTRODUCTION

The study of the electrochemical behaviour of organic compounds is historically well founded (128). It is, however, only within the last 25 years that rigorous theoretical and experimental treatments of the problem have been made. Dropping mercury polarography has provided a very powerful technique for the study of electro-organic reductions, from mechanistic and kinetic standpoints, and this method is now at a very advanced stage (163). Polarography cannot be used at potentials more positive than +0.2 V. N.H.E. (due to the formation of oxide films), and as a consequence, cannot be used for the study of very many oxidations.

The development of the Fuel Cell, and the realisation that many catalytic reactions are electrochemical in nature, has stimulated much recent interest in organic electrochemical reactions at 'inert' solid electrodes (the platinum group metals (29) and vitreous carbon (162)).

The realisation of the importance of complete system cleanliness (12) and the development of new electrochemical techniques such as cyclic voltammetry (158), rotating electrode systems (136) and potentiostatic methods (7,65) has enabled valid kinetic and mechanistic studies of complex electrode systems to be made.

Studies of organic electrode reactions have shown that the nature of the electrode greatly affects the

reaction kinetics (42), i.e. the electrode has a catalytic effect on the electrochemical reaction. A study of the electrochemical oxidation of organic compounds at catalytically active electrodes might yield reactions of potential industrial interest.

Choice of electrode material is limited to those which will not dissolve or form insulating oxides at anodic potentials. Silver is a very important oxidation catalyst (26) and certain silver complexes are selective oxidising agents (104). Silver oxides are formed anodically under alkaline conditions but these are not insulators (103).

It was therefore decided to study the oxidation of simple organic compounds in aqueous electrolytes at silver electrodes.

SECTION 1

THEORETICAL PRINCIPLES AND PRELIMINARY CONSIDERATIONS

CHAPTER 1

OXIDATION MECHANISMS

The term 'oxidation', in modern usage, defines those reactions in which the electropositive character of the species under question is increased (16). An oxidation reaction cannot occur without involving a corresponding reduction (i.e. increase in electronegative character) of another species.

This definition is very readily applied to inorganic reactions, as charged inorganic ions are generally stable. This stability is due entirely to the coordination of these ions with suitable ligands or solvent molecules to form complexes (157). Consider, for example, the oxidation of cobalt. In vacuo the energy required for oxidation to take place (the Ionisation Potential, I) increases with increasing oxidation state:- I_1 = 7.86 eV, I_2 = 17.0 eV, I_3 = 33.4 eV (102). In solution the relative stability of the ions depends entirely upon the chemical nature of the ligand present. (In the presence of CN^- ions $\left[Co^{III}(CN)_6\right]^{3-}$ is more stable than $\left[Co^{II}(CN)_6\right]^{4-}$ (117)). The constitution of the complex may depend on the oxidation state of the metal ion (e.g. manganese^{II} is stable as the hydrated cation while manganese^{VII} is

stable only as the oxyanion MnO_4^-).

Organic oxidation processes cannot be defined in this manner as organic compounds are covalent and do not exist in formal oxidation states.

Organic oxidation process are defined as reactions involving the substitution of an atom (or functional group) with a more electronegative atom (or functional group) within the organic molecule[82]. Dehydrogenation (i.e. desaturation or the formation of π bonds) is also considered to be an oxidation (155). Many organic oxidations do occur through the generation of (transitory) electron deficient centres, but these processes are always associated with chemical rearrangements (antecedent and/or subsequent to the charge transfer). The oxidation step in an organic reaction sequence is very rarely at equilibrium and, as a consequence organic electrode processes cannot be treated in a classical kinetic manner (see Ch. 3.1)

Organic oxidations may be divided into two general classes:-
inter-molecular and intra-molecular oxidations. Intra-molecular oxidations are usually homogeneous reactions (i,e. they take place within one phase), and involve a transition state within which the oxidation reaction occurs, e.g.:-

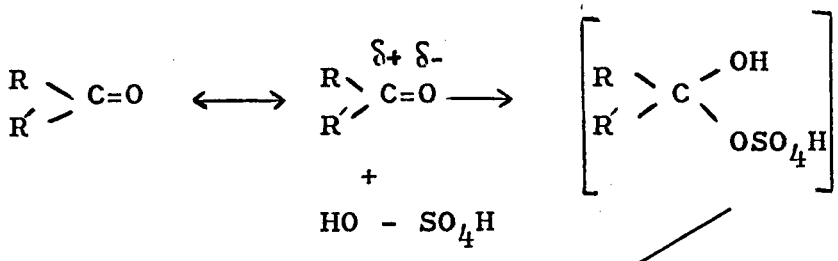

(Oxidation Step)

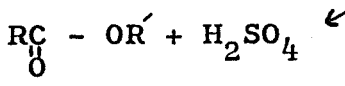

[2.1] (18)

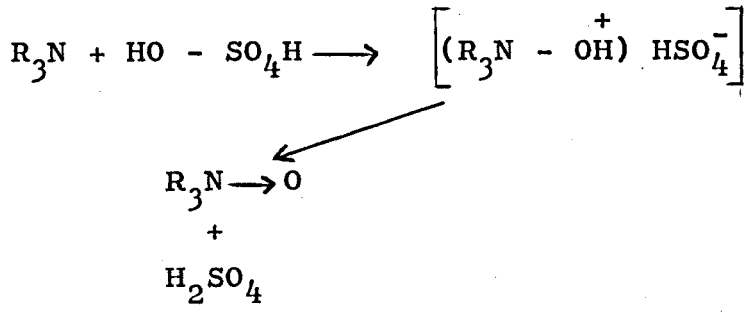

[2.2] (146)

The inter molecular reactions involve the definite transfer of charge yielding an electron deficient species which undergoes rapid chemical rearrangement. These reactions can be either homogeneous or heterogeneous and usually involve a transition metal. The organic molecule forms a complex (homogeneous or heterogeneous) with the metal ion (in a high oxidation state) and is oxidised (the metal ion being reduced). Examples of homogeneous reactions are the silver catalysed persulphate oxidations:-

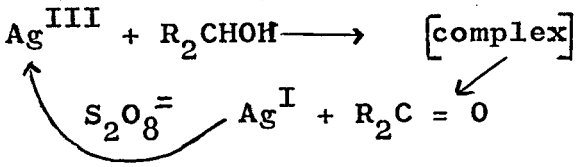

[2.3] (88)

and the Sandmeyer reaction:-

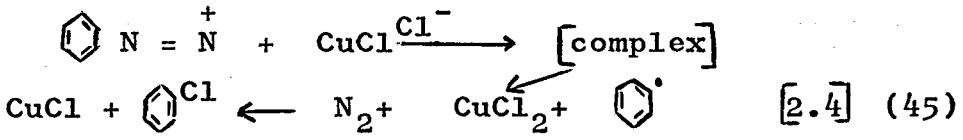

[2.4] (45)

Examples of heterogeneous reactions are the silver catalysed gaseous oxidation of alcohols to aldehydes (61) and the Zeigler-Natta polymerisation of alkenes which, although not a true oxidation proceeds through the generation and propagation of electron deficient centres (119).

Oxidations which involve the intermolecular transfer of electrons (especially those which occur rapidly at ambient temperatures) should be particularly amenable to study using electrochemical methods. Such investigations would not yield rigorous thermodynamic data. Those oxidations which proceed intra-molecularly would be more difficult to study electrochemically.

CHAPTER 2

THE PROPERTIES OF THE ELECTRODE - ELECTROLYTE INTERPHASE

A chemical electrode may be defined as a two phase system, both components of which are conductors of electricity. An electrode is usually a metal in contact with an electrolyte (The electrolyte may be aqueous or non-aqueous, the metal may be solid, liquid or even a semi-conductor). An electrode is thus associated with an interphase with a consequent difference in electrical potential between the two phases. Two different interfacial potential differences may be defined:-

(a) The Galvani potential ($\Delta\phi_i$) is the electrical work required to transfer a unit charge from the bulk of one phase to the bulk of the second phase.

(b) The Volta potential ($\Delta\psi_i$) is the work required to transfer a unit charge from the bulk of one phase to the interphase .

$\Delta\psi_i$ can be measured abolutely, $\Delta\phi_i$ cannot be measured absolutely, but differences in $\Delta\phi_i$ are manifested as the E.M.F. of galvanic cells.

The existance of a potential difference at an interphase implies that there is a difference in electrical charge density (q_i) at the interphase which, for an electrode in which the charges are mobile, is manifested as a difference in sign. (The numerical values of the two charge densities being equal to preserve macroscopic

electrical neutrality).

An electrode is termed 'ideally polarisable' if there is no net faradaic current flow when the potential at the interphase is changed (i.e. a change in $\Delta\phi_i$). An ideally polarisable electrode can only arise when the activity of each electroactive species is finite within one phase only (75); and thus the system is equivalent to an electrical capacitor, and its capacitance can be measured by conventional techniques.

Electrode capacitance measurements are readily resolvable into the interphase components only when all the charge due to one phase (usually the metal) is at the interphase. Capacitance measurements made at semiconductor electrodes are difficult to resolve (116). The electrode capacitance (intuitively) depends upon the area of the electrode/electrolyte interphase, and thus accurate measurements can be made only with systems whose interfacial area is clearly defined, i.e. at liquid metal electrodes. Mercury is an ideal electrode (75) and the theory of the structure of the metal/aqueous interphase has been developed from data measured at the mercury/electrolyte interphase. Liquid gallium has proved to be experimentally difficult (77) to use as an electrode. Measurements made at solid metal electrodes involve several uncertainties (inter alia the true surface area of the interphase).

Fig. 1 The HELMHOLTZ Model for the Double Layer

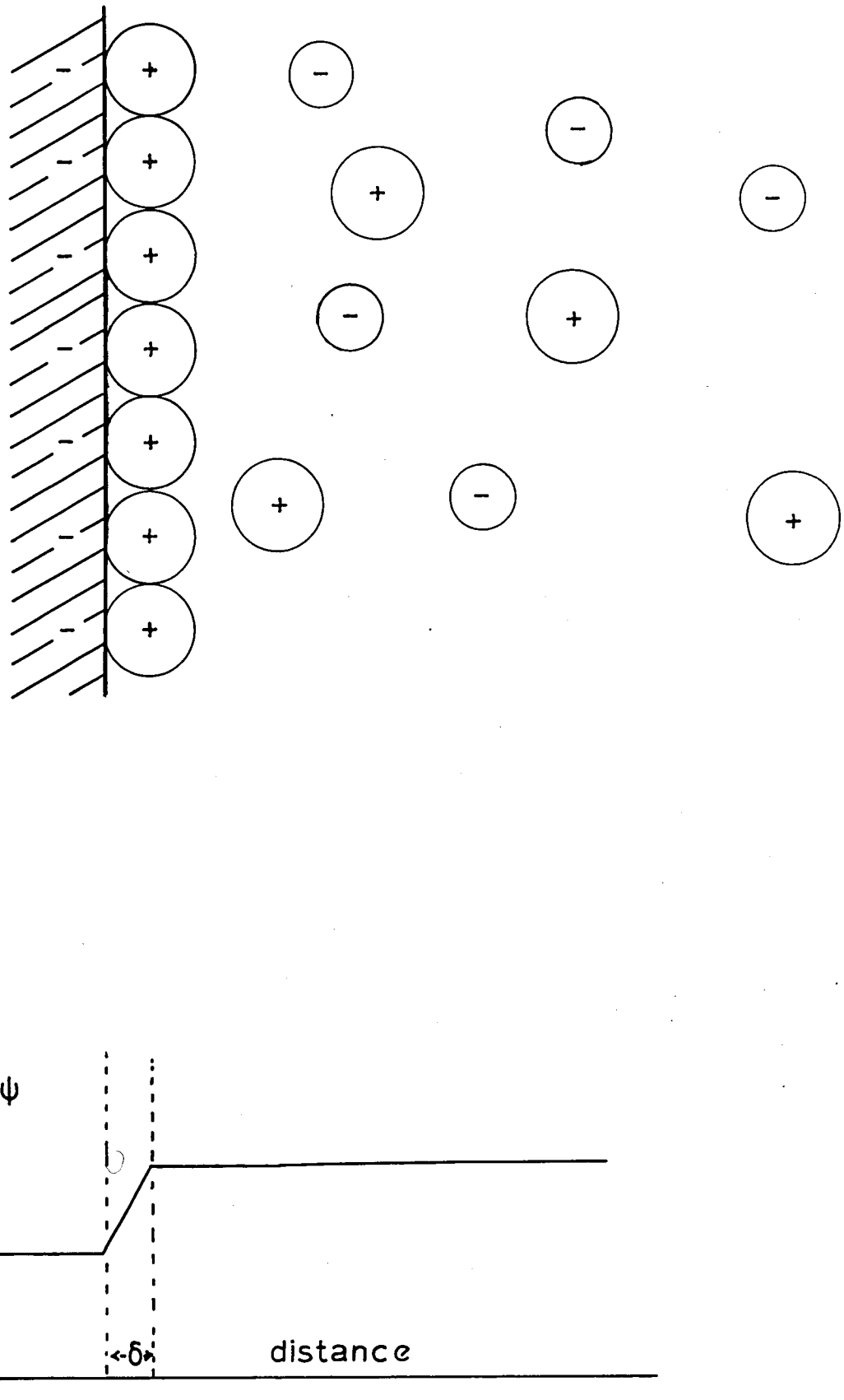
ψ
δ
distance

Fig. 2 The GOUY-CHAPMAN Model for the Double Layer

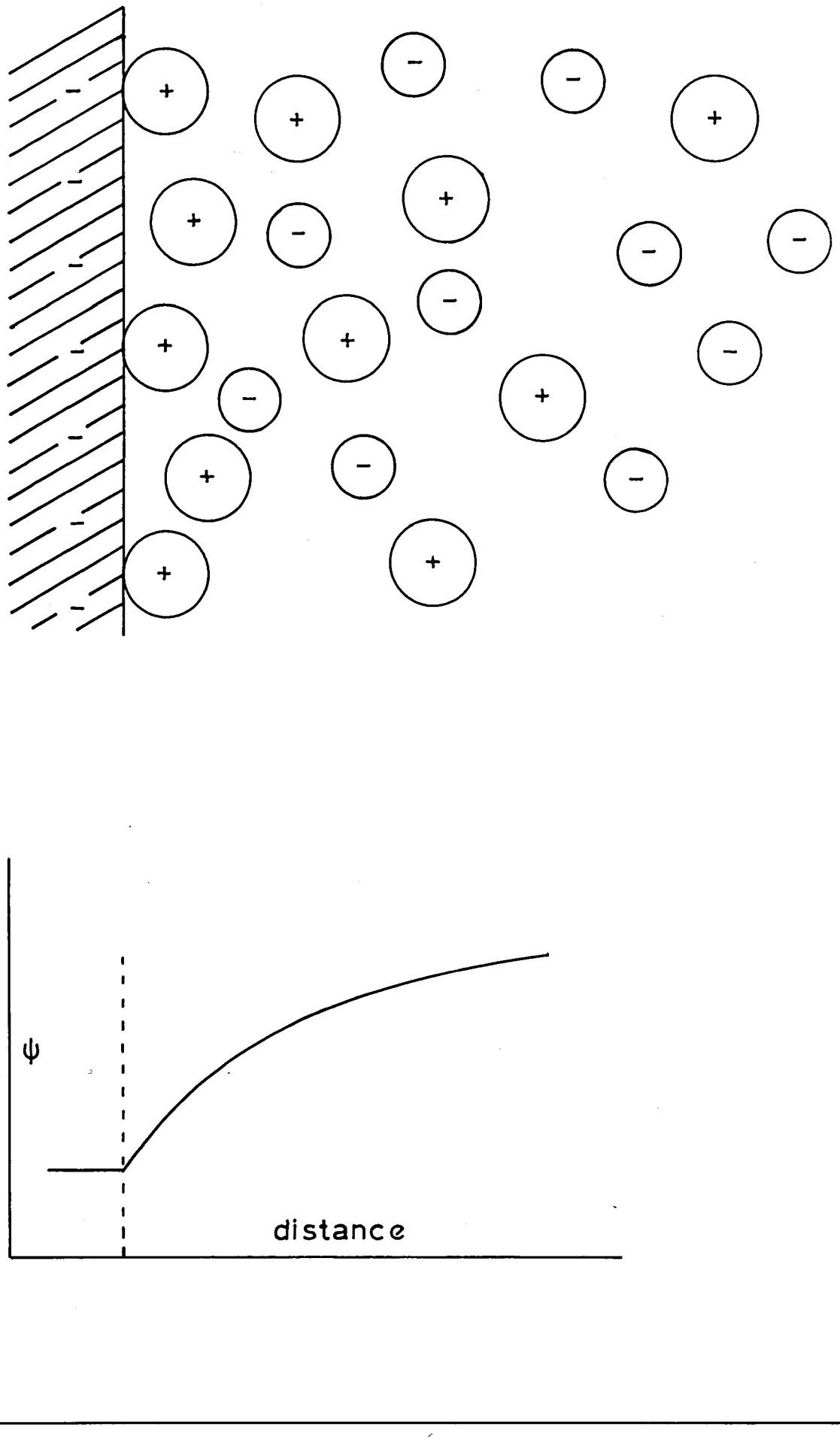
ψ
distance

Fig. 3 The STERN Model for the Double Layer

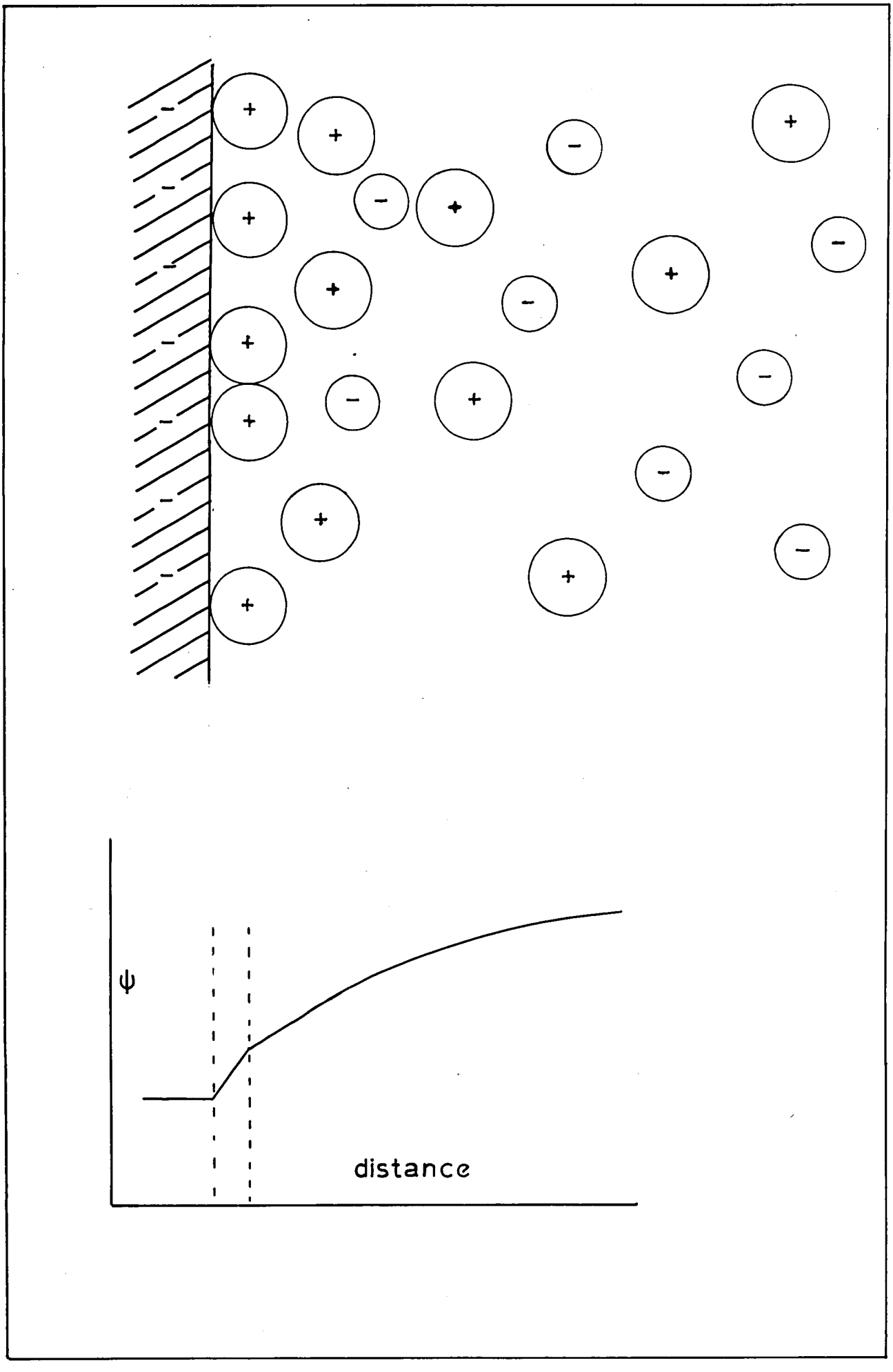
Ψ
distance

2.1 Models of the Uncomplicated Interphase

The original model for the metal/electrolyte interphase, proposed by HELMHOLTZ (87) was a simple 'double layer' in which the charge on the electrode is exactly balanced by a discrete layer of counter ions (Fig. 1). The charge separation, δ, was thought to be the hydrated radius of the counter ions. Such a system is not stable from thermodynamic considerations and values for C_L calculated using this model did not agree with those found experimentally. GOUY (78) and CHAPMAN (35) proposed a model in which the charged electrolyte component of the double layer is diffuse (Fig. 2). C_L values calculated from this model agree with experimental data at low q_e, but there are large discrepancies at high values for q_e. These anomalies were explained by STERN (143) in terms of a combined Helmholtz/Gouy-Chapman model (Fig. 3). The C_L vs. q_e curve predicted from Stern theory agrees very well with that measured at Mercury in non interacting electrolytes (75).

2.2 The adsorption of Ions at the Interphase

Certain electrolytes affect the shape of the C_L - q_e curve. At positive potentials (w.r.t. E_z) the deviations are caused by certain anions and at negative potentials by

Fig. 4 The Currently Accepted Model for the Double Layer. δ_1 Distance of Closest Approach of Specifically Adsorbed cations; δ_2 Distance of Closest Approach of Hydrated Cations.

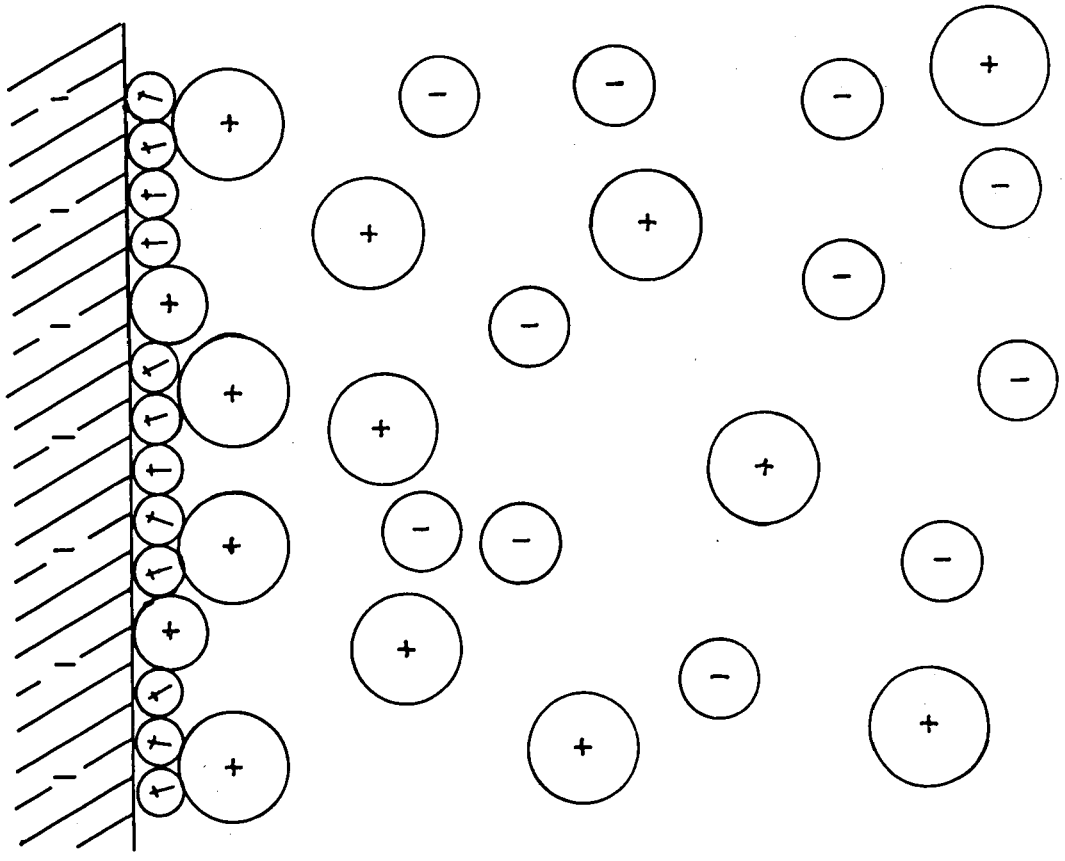

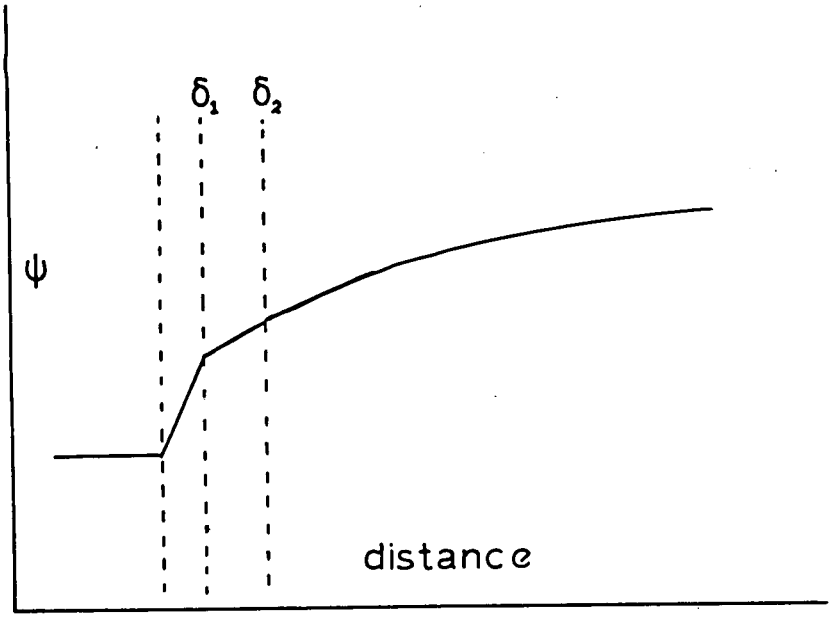
δ1
δ2
ψ
distance

Fig. 5 Schematic Representation of the Effect of Organic Compounds on a Differential Capacitance Curve ..... Without Addition; —— after Addition of Organic Compound.

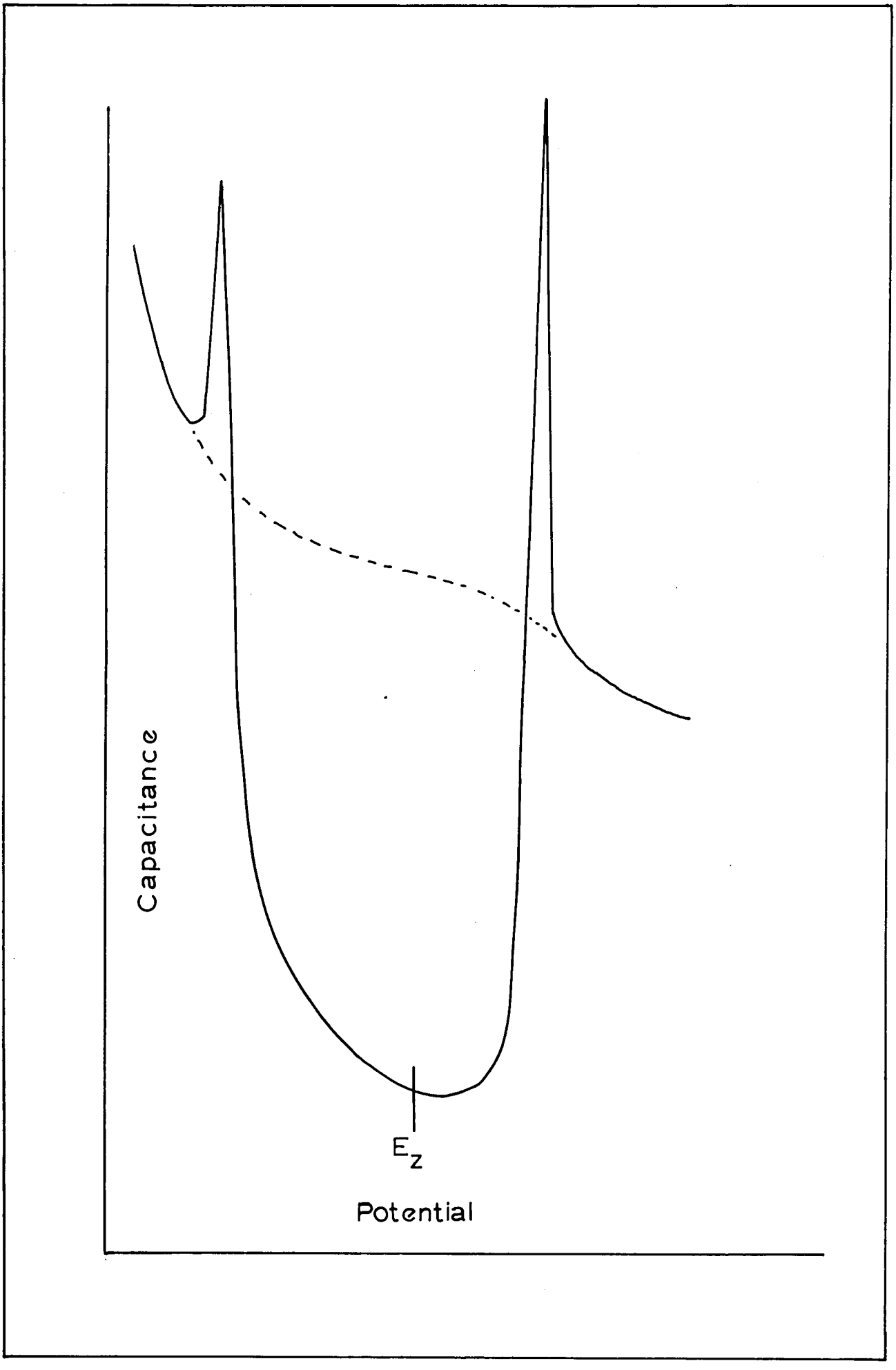
Capacitance
E_z
Potential

certain cations (75). These effects are due to the 'specific' adsorption of these ions at the electrode. The degree of specific adsorption has been shown to depend on the ionic radius and polarisability indicating that hydration energy may be an important parameter (24).

2.3 The Adsorption of Dipoles at the Interphase

The absolute values for C_L can be equated with the expected charge separation (the hydrated ionic radius of the counter ions) only if the dielectric constant at the interphase is ~ 6 (for liquid water $\epsilon \sim 80$ at $20^{\circ}C$, and for ice $\epsilon \sim 3$ at $-15^{\circ}C$). This anomaly is explained by postulating an ice-like ordered monolayer of water at the interphase. This monolayer is penetrated by specifically adsorbed, dehydrated ions (24) (Fig. 4)

2.4 The Adsorption of Neutral Molecules at the Interphase

The low dielectric constant at the electrode lowers the Free Enthalpy of adsorption of neutral molecules at the electrode. This effect is significant when considering the presence of organic compounds in the electrolyte, which are generally strongly adsorbed in the potential region aroung $q_e = 0$. Neutral molecule adsorption has a pronounced effect on the capacitance-potential curve for an electrode (Fig. 5). At a certain potential (either side of E_z) the solvent dipoles interact very strongly and the neutral molecules desorb, causing the capacitance

'spikes'. Attempts have been made to derive adsorption isotherms from the concentration dependance of the capacitance curves (47,50).

There have been several theoretical treatments of the adsorption of neutral molecules at electrodes (25, 33, 67). That of BOCKRIS, GILEADI and MÜLLER (25) is perhaps the most comprehensive and takes into account changes in orientation (hence surface coverage) of the solvent and adsorbate, with changes in field strength at the interphase.

2.5 The Application of Electrode Capacitance Data

A knowledge of the structure of the electrode-electrolyte interphase and in particular the value for E_z is a prerequisite to the study of the kinetics of electrode reactions (50.)

C_L - E curves are very easily measured and give a ready indication of the usefulness of electrode preparation technique and of the electrolyte cleanliness (131) - semi-conducting films and electrode roughness effects are easily diagnosed from a comparison of C_L - E curves. A reproducible 'clean' electrode surface is of prime importance in the study of charge transfer reactions.

CHAPTER 3

THE KINETICS OF ELECTROCHEMICAL REACTIONS

3.1 Charge Transfer Reactions

3.1.a. Kinetic Equations

From Transition State theory (43) the absolute rate of heterogeneous reaction is given by:-

$$V = \left[\gamma \frac{kT}{h} \exp -\frac{\Delta G^*}{RT}\right](1-\theta) \cdot C_R^* \qquad [3.1]$$

$$= K \cdot C_R^* \qquad [3.2]$$

The rate of an electrochemical reaction involving n electrons per mole. is given by:-

$$V_e = i/nF \qquad [3.3]$$

combining [3.2] and [3.3.]

$$i = nF\, K_e' \cdot C_R^* \qquad [3.4]$$

The electrochemical rate constant K_e' is directly analogeous to the chemical rate constant K, however, the activation energy term also involves electrochemical as well as chemical energy. This electrochemical energy is related directly to the electrical potential difference across the interphase. No definite value for the electrochemical free enthalpy of activation (ΔG_e^*) can be calculated a priori as this would require a detailed model for the transition state. It is assumed (50) that ΔG_e^* is some fraction, α, of the Free Enthalpy difference between the oxidised and reduced states of the species at the plane of closest approach to the electrode. (a reduction is conventionally the forward reaction (i, +ve) and is associated with α in the activation term.)

Equation [3.4] becomes

$$\vec{i} = nFC_o^{*}\vec{K} \exp\left(\frac{-\alpha nF}{RT} \cdot E\right) \qquad [3.6]$$

and $$\overleftarrow{i} = nFC_R^{*}\overleftarrow{K} \exp\left(\frac{(1-\alpha)nF}{RT} \cdot E\right) \qquad [3.7]$$

The electrical potential, E, in Eq. [3.6] and [3.7] is referred to the Nernst(equilibrium) potential (121) for the system, E_r, and the overpotential given by:-

$$\eta = E - Er \qquad [3.8]$$

Equation [3.6] becomes:-

$$\vec{i} = nFC_o^{*}\vec{K} \exp\left(\frac{-\alpha nF}{RT} \cdot Er\right) \exp\left(\frac{-\alpha nF}{RT}\eta\right) \qquad [3.9]$$

$$= i_o \exp\left(\frac{-\alpha nF}{RT}\eta\right) \qquad [3.10]$$

Similarly Equation [3.7] becomes:-

$$\overleftarrow{i} = i_o \exp\left(\frac{(1-\alpha)nF}{RT}\eta\right) \qquad [3.11]$$

The net current flowing is given by:-

$$i = \vec{i} - \overleftarrow{i}$$

$$= i_o \left[\exp\left(\frac{-\alpha nF}{RT}\eta\right) - \exp\left(\frac{(1-\alpha)nF}{RT}\eta\right)\right] \qquad [3.12]$$

If η is small (i.e. $RT \gg \alpha nF\eta$) Eq. [3.12] becomes:-

$$i = -i_o \cdot \frac{nF}{RT}\eta \qquad [3.13]$$

If η is large Eq [3.12] becomes:-

$$\ln\left(\frac{i}{i_o}\right) = \frac{-\alpha nF}{RT}\eta \qquad [3.14]$$

or $$\ln\left(\frac{|i|}{i_o}\right) = \frac{(1-\alpha)nF}{RT}\eta \qquad [3.15]$$

Fig. 6. Hypothetical P.E. Curves for a C.T. system
A- at Equilibrium; B- Cathodic Applied Overpotential.

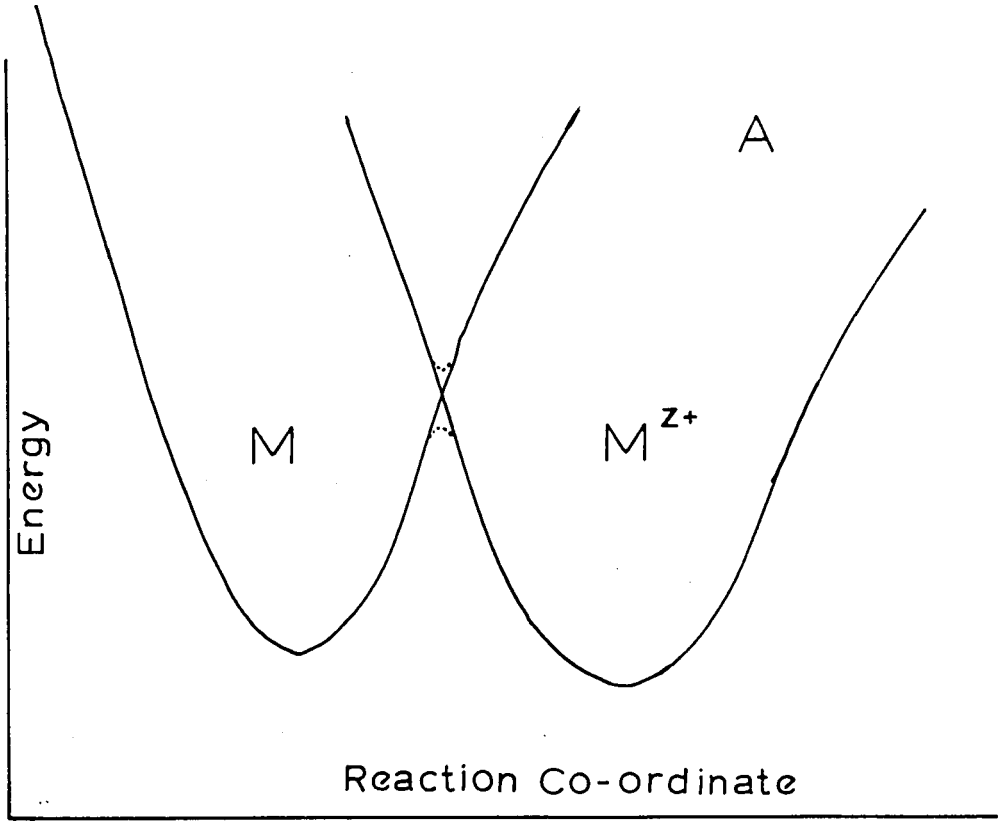
A
Energy
M
M^z+
Reaction Co-ordinate

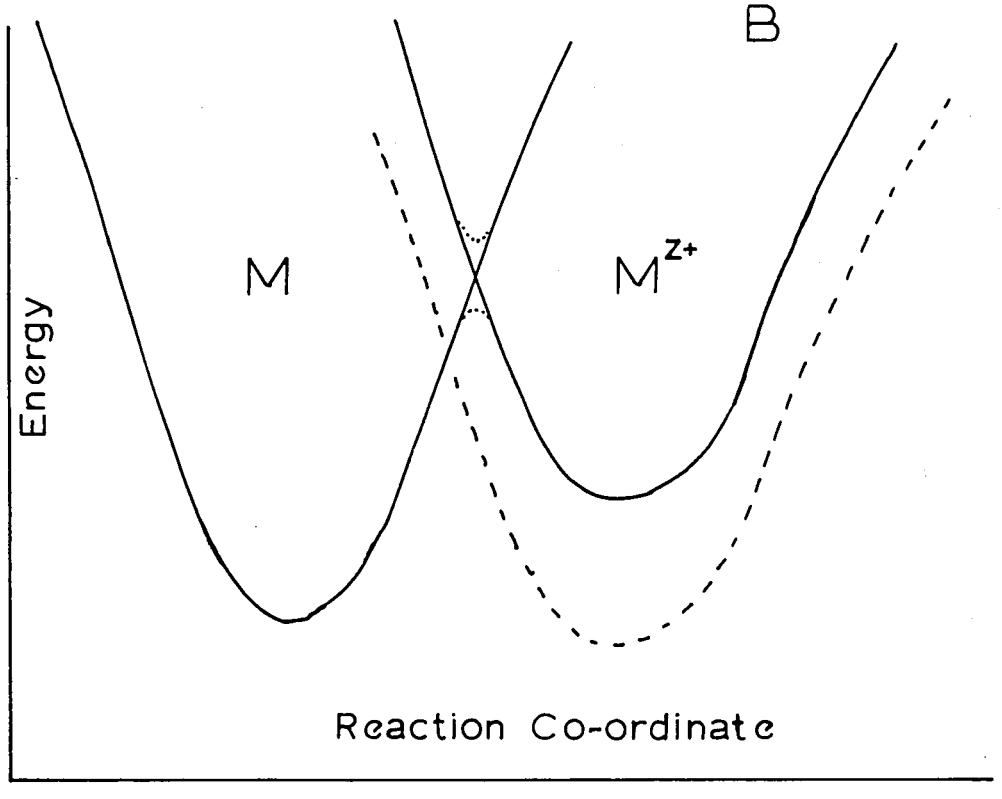
B
Energy
M
M^z+
Reaction Co-ordinate

The apparent Exchange Current, i_o, (50) is related to the apparent Rate Constant, k^o, by:-

$$i_o = nF\, k^o\, C_K^{\alpha}\, C_o^{(1-\alpha)} \qquad [3.16]$$

The correlation of reaction rate with overpotential (equations [3.12] to [3.15]) is valid only if:-

(a) the overpotential measured is uncomplicated by diffusion, reaction, etc. effects i.e. is the true charge-transfer overpotential.

(b) there is negligible "double layer effect" (50)

(c) the postulated Langmiur-type isotherm (43) is obeyed for the electroactive species.

3.1.b. The Physical Meaning of α and i_o

i_o, introduced in Eq. [3.10] , has the dimension of current density and was thus called the Exchange Current (32). The existance of actual exchange reactions has been shown by the use of radio tracer techniques (31).

There have been many attempts to correlate Eq. [3.12] in terms of a potential energy diagram for the exchange reaction (17). Perhaps the best of these; that due to HORIUTI and POLANYI (89), is shown in Fig. 6. The charge transfer coefficient, α, is considered to be related to relative slopes of the P.E. curves at their intersection (113).

3.2 Diffusion Controlled Reactions

Liquid-phase diffusion is probably the most common rate controlling process in any (liquid) heterogeneous system. Electrochemical methods readily provide diffusion

data (91).

The problem of diffusion was formulated by FICK (60):-

$$\frac{dn_i}{dt} = -D_i\left(\frac{\partial C_i^*}{\partial x}\right) \qquad [3.17]$$

$$\frac{dC_i^*}{dt} = D_i\left(\frac{\partial^2 C_i^*}{\partial x^2}\right) \qquad [3.18]$$

Complete solution of these equations is complex, however, Eq. [3.17] is valid when $t \rightarrow \infty$, while Eq. [3.18] can be applied when $t \rightarrow 0$ (i.e. in transient experiments (21)).

3.3 Electrocrystallisation

The formation of a solid phase usually occurs most readily when the new phase is formed at a growing crystal face (or faces). Thus the rate controlling process might well be the rate of crystallisation and this may be either the rate of growth of the crystallites or the rate of formation of new crystallites (nucleation). The growth of crystallites may occur in either one dimension, two dimensions or three dimensions.

An analysis of crystallisation rates at constant potential has been made by, inter alia, FLEISCHMANN and THIRSK (66) in terms of current-time responses. If it is assumed that the nucleation rate equation is of the form:-

$$N = N_o\,(1 - \exp(-At)) \qquad [3.19]$$

and that the neuclei grow in an ideal manner:- 1-D as needles, 2-D as plates and 3-D as hemispheres, six basic

rate equations are obtained:-

(a) Instantaneous Nucleation (A large)

1-D $i = nFkN_oS$ [3.20]

2-D $i = \frac{2nF\pi MhN_ok^2}{\rho} .t$ [3.21]

3-D $i = \frac{2nF\pi M^2N_ok^3}{\rho^2} .t^2$ [3.22]

(b) Slow Nucleation (A Small)

1-D $i = nFAN_okS . t$ [3.23]

2-D $i = \frac{nF\pi MhAN_oK^2}{\rho} . t^2$ [3.24]

3-D $i = \frac{2nF\pi M^2AN_oK^3}{3\rho^2} . t^3$ [3.25]

Thus an analysis of the i-t response to a constant potential may be diagnostic (in the case of $i \propto t^o$ and $i \propto t^3$) of the mode of crystal growth.

Under conditions where the rates of charge transfer and crystallisation are both fast, the rate determining process may be the diffusion of an atom, after charge transfer, along the electrode surface to a crystallisation growth site. Such species have been termed 'adatoms' (or adions) (108). Rate control by the 'adatom' diffusion process is usually observed in studies of the exchange reactions of metals with a high K^o (110). The rate of a reaction controlled by 'adatom' diffusion is proportional to the surface concentration, C_{ad}, of adatoms at the electrode. C_{ad} is potential dependent (150) but is

independent of the concentration of electroactive species in the electrolyte (108). Thus 'adatom' diffusion controlled reactions obey an equation of the form Eq. [3.12] but not Eq. [3.16].

3.4 Reaction Rate Control by a Chemical Reaction Coupled with the Charge Transfer Process.

Coupled chemical reactions occur predominantly in organic electrochemical reactions in which metastable species are readily produced. Such systems have been studied theoretically by several groups (93, 122, 137, 159). Even for the simplest case of a single C.T. - chemical reaction process there are three possible mechanisms (a,b,c) which are further complicated by the fact that in each of these either the chemical or C.T. step or both may be reversible or irriversible:-

(a) Chemical Step antecedent:-

$$A \longrightarrow B \xrightarrow{\pm e} C$$

(b) C.T. Step antecedent:-

$$A \xrightarrow{\pm e} B \longrightarrow C$$

(c) Parallel reactions

$$A \begin{cases} \xrightarrow{\pm e} B \\ \longrightarrow C \end{cases}$$

Case (b) is formally similar to an 'adatom diffusion process, and it could be that the discharge rate of an ion is controlled by the rate of loss of the 'solvent sheath' from an 'adatom'.

Organic electrode reactions are rarely as simple as in these three cases; usually there are several chemical -C.T. processes occurring. The possibility does exist of controlling a reaction path and hence the products by control of the C.T. and chemical reactions occurring at the electrode through control of the electrode potential and mass transfer at the electrode (7, 65).

Fig. 7 D.C. Polarised Schering Bridge Circuit used for Differential Capacitance and Faradaic Impedance Studies. (The reference electrode system is not shown for simplicity).

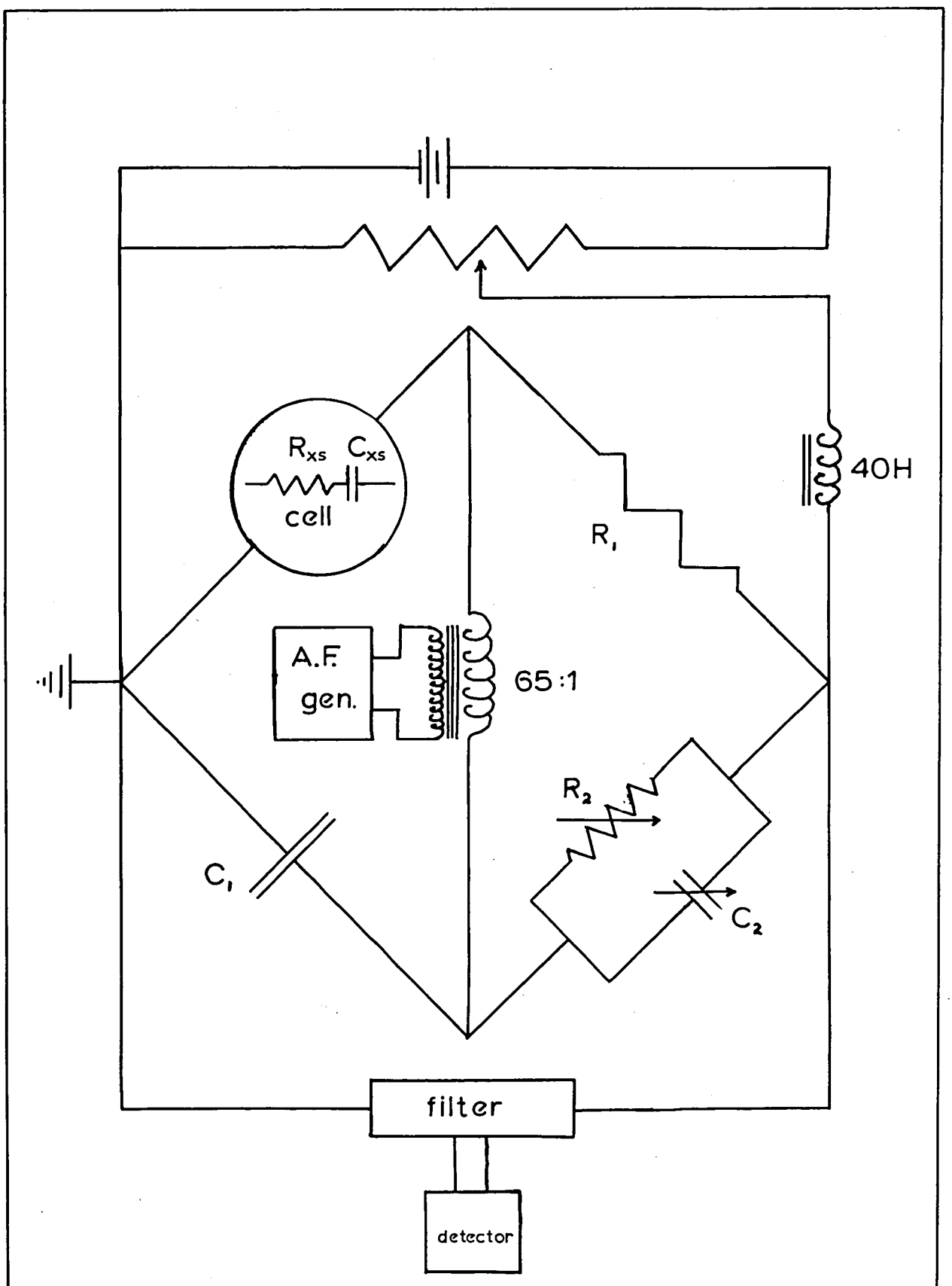
R_{xs} C_{xs}
cell
40H
R_1
A.F.
gen.
65:1
R_2
C_1
C_2
filter
detector

CHAPTER 4

THE MEASUREMENT OF ELECTROCHEMICAL PARAMETERS

The rate of an electrochemical reaction may be determined by any one of several different processes (see Ch. 3). As a consequence, to elucidate the reaction rate parameters, relaxation techniques have to be used.

There are two main classes of relaxation techniques:- (1) Steady State methods, and (2) Perturbation methods.

4.1 Steady State Methods

In the steady state methods the electrode is either peturbed symmetrically from equilibrium by a regular sinusoidal or triangular potential waveform or the mass transfer at the electrode is artificially controlled so that the electrical response of the electrode is time-independent.

4.1.a. The Faradaic Impedance Technique

This is the classical steady state technique and was developed for the study of electrochemical reactions by RANDLES (133). The impedance of the electrode is measured over a range of frequencies by means of a Schering bridge (79) (Fig. 7). A Low amplitude ($\sim$7mV pp.) sinusoidal A.C. signal is applied and the electrode potential is maintained at its equilibrium value by means of a D.C. potentiometer circuit.

If the electrolyte contains no electroactive species (see Ch. 2), i.e. there is no electrode reaction, the

Fig. 8 Electrical Analogue of a Simple Charge Transfer Reaction. Frequency Dependence of Non-Linear Components.

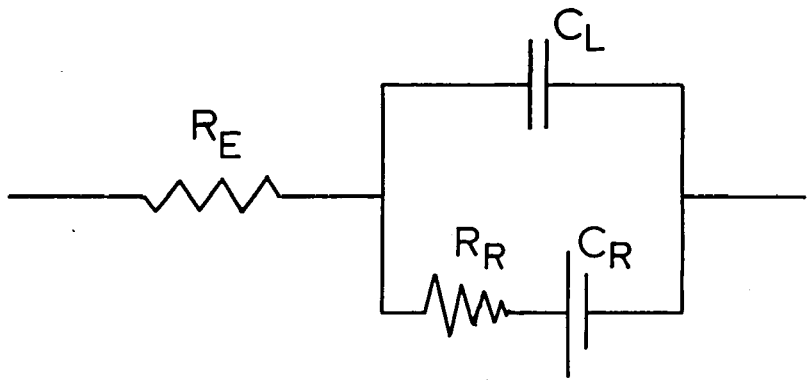
C_L
R_E
R_R
C_R

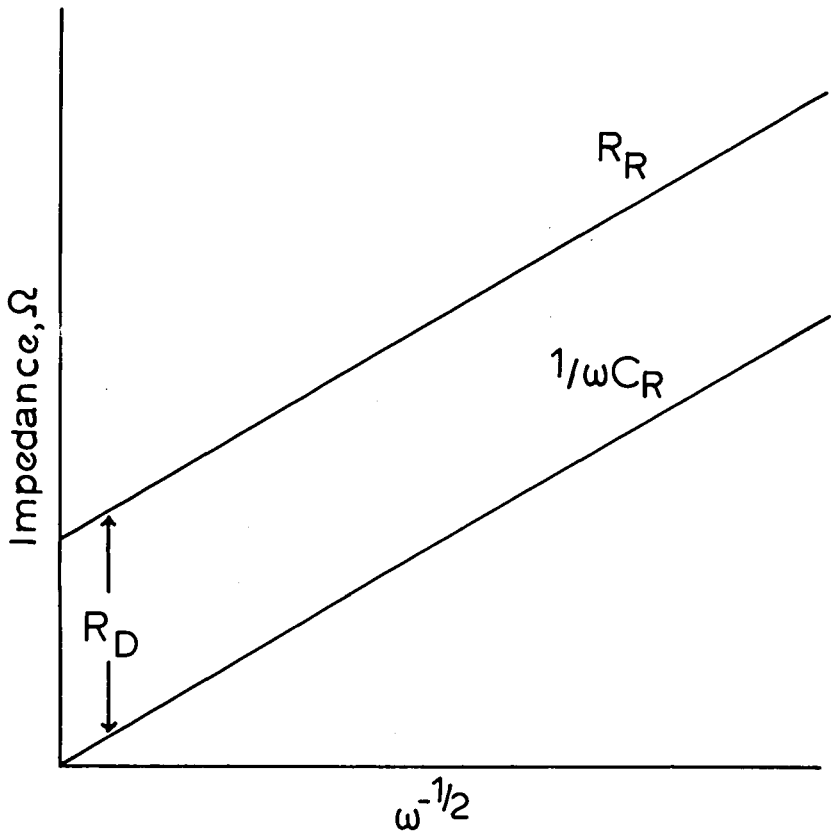
R_R
$1/\omega C_R$
Impedance, Ω
R_D
$\omega^{-1/2}$

bridge measurements correspond to C_L, the electrode capacitance (Ch. 2), and R_E, the electrolyte resistance (130). Very accurate electrode capacitance measurements are possible using this technique (75), and the potential is continuously variable enabling accurate differential capacitance curves to be derived and, as a consequence, valid data concerning the structure of the double layer may be deduced.

If an electrode reaction does occur the measured capacitance and resistance values approach C_L and R_E only at very high frequency. The equivalent electrical circuit for a faradaic reaction is shown in Fig. 8 (133). R_R and C_R are non linear components which vary with A.C. frequency and are related to R_D the charge transfer resistance:-

$$R_R = R_D + 1/\omega C_R \qquad [4.1]$$

$$R_D = \frac{RT}{nF} \cdot 1/i_o \qquad [4.2]$$

R_R and $i/\omega C_R$ increase linearly with $\omega^{-\frac{1}{2}}$; a plot of R_R and $1/\omega C_R$ against $\omega^{-\frac{1}{2}}$ yields two parallel straight lines with separation: R_D, and slope: $\frac{RT}{n^2F^2} \sum \frac{\nu_i^2}{C_i^* D_i^{\frac{1}{2}}}$ (151) as shown in Fig. 8: Thus in addition to i_o, the diffusion coefficient of the electroactive species is derived from faradaic impedance data. The charge transfer coefficient, α, is not obtained directly but can be derived from the dependence of i_o on concentration (Eq. [3.16]).

If the reaction is not completely charge transfer/diffusion controlled, plots of R_R and $1/\omega C_R$ against $\omega^{-\frac{1}{2}}$ do not give straight lines and analysis is more complicated (100, 109).

4.1.b. Potential Sweep Voltammetry

This technique is best suited to the study of reactions at 'inert' electrodes (e.g. platinum (158) or glassy carbon (162)), and in particular, organic-electrochemical reactions. The electrode potential, controlled potentiostatically, is varied linearly with time in a 'saw-tooth' wave form, and the current response of the electrode recorded oscillographically.

The shape of the current-potential oscillogram is diagnostic of the rate controlling mechanism (137); variation of the oscillogram with potential sweep rate enables kinetic parameters to be elucidated (122, 137, 142, 159). This method is only readily applicable to relatively simple C.T.-chemical reaction schemes, however qualitative deductions concerning the mechanisms of more complicated systems can be made from P.S.V. data.

4.1.c. Rotating Disc and Rotating Ring-Disc Electrode Systems.

The change in reaction at an electrode resulting from mass transfer effects is the most frequently observed electrochemical phenomonon, and as a consequence of the form of the diffusion laws (Eq. [3.17] and [3.18]), the

most difficult to elucidate accurately. In Faradaic Impedance and P.S.V. techniques diffusion, although on average zero, is instantaneously finite and thus these methods are not true steady state methods.

The theory of mass transfer at a rotating disc was developed by LEVICH (106) and a nearly ideal practical electrode developed by RIDDIFORD (136). The rate of an electrochemical reaction is measured directly as a function of mass transfer and as a consequence the absolute reaction rate under conditions of infinite diffusion can be determined.

The rotating ring-disc electrode developed by FRUMKIN (69) et al. (2), can be used for the detection and study of unstable intermediates generated at the disc electrode.

Electrodes, to function properly, have to be inert, and their shape and mechanical finish carefully controlled (23). If these factors are not observed the system will not follow the mathematical theory. Thus in practice specially fabricated 'inert' electrodes (usually of Pt) have to be used.

4.2 Perturbation Methods

In these techniques the electrode is perturbed from equilibrium by means of a pulse of potential or of current, and the relaxation of the current or potential recorded oscillographically. Both of these techniques

Fig. 9 The Galvanostatic Technique. Ideal and Real Potential Responses to an applied Current Step Function.

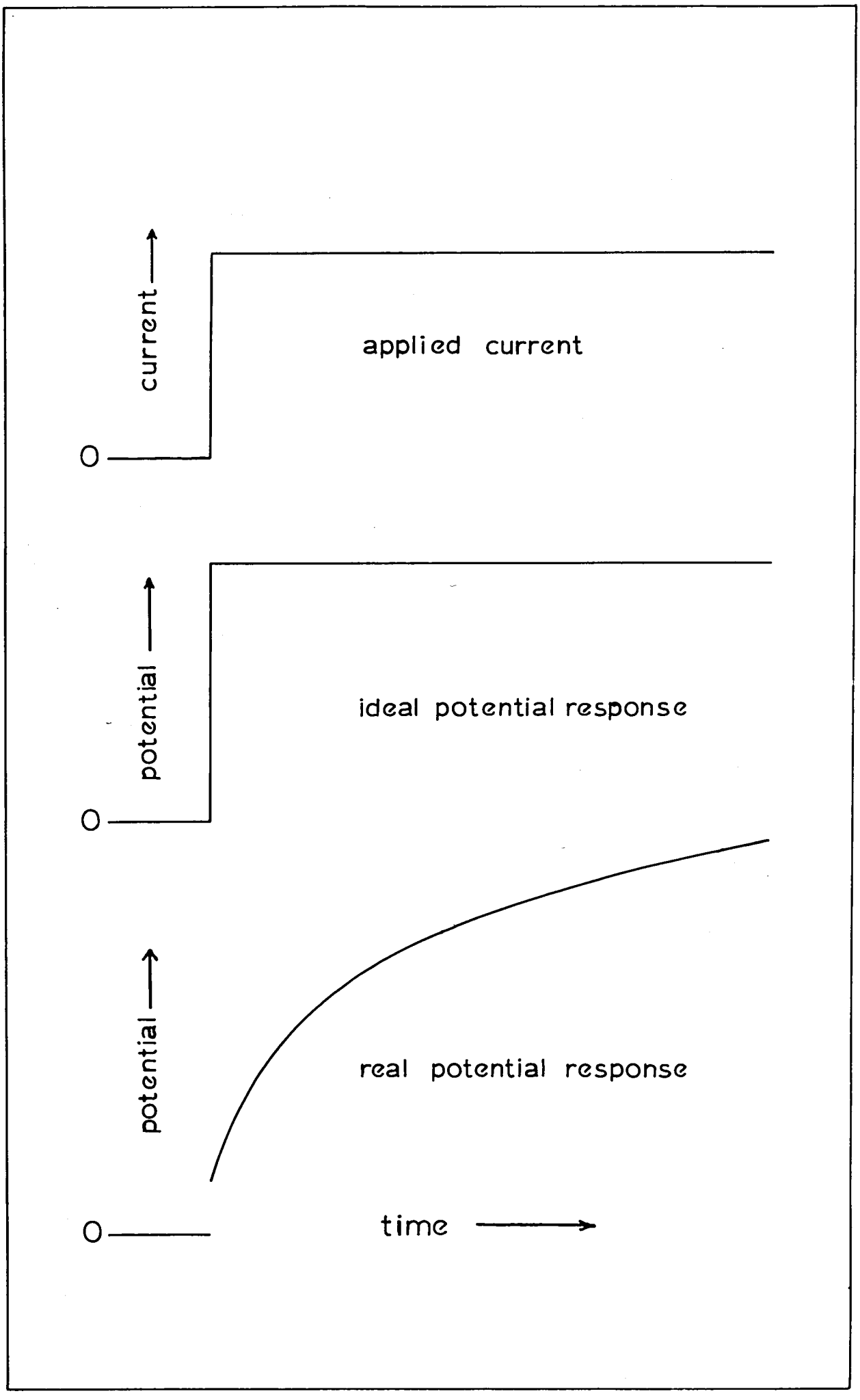
current
applied current
O
potential
ideal potential response
O
potential
real potential response
O
time

are complicated by the rapid intrusion of mass transfer polarisation (71) when applied to the study of fast electrode reactions, and use in conjunction with a R.D.E. system can be an advantage in this instance.

4.2.a. The Galvanostatic Method

When a current-time step-function is applied to an electrode the resultant potential-time response would be a step-function also, if charge transfer were the only rate controlling process. In practice at least three factors intrude and the potential-time response is complex (Fig. 9):- A. The resistance of the electrolyte between the tip of the Luggin capillary and the test electrode results in a higher than expected potential. This appears, in practice, as a vertical gap in the trace (70) and can be readily corrected. B. The capacitance of the electrode requires a finite current flow before the new activation potential is attained. The slope of the potential time trace at zero time yields the electrode capacitance (152) according to:-

$$\left(\frac{\partial E}{\partial t}\right)_{t \to 0} = \frac{-i}{C_L} \qquad [4.3]$$

This capacitance is a true differential capacitance only when the current rise-time is very small (i.e. the effective frequency is high (see Ch. 4.1.a.). This method does not yield accurate values for C_L. C. Changes in the concentration of the electroactive species at the electrode cause a further time dependent potential change.

The potential-time response for a charge transfer system near equilibrium ($|\eta| < 10mV$) has been derived by BERZINS and DELAHAY (21). For fast reactions η varies with $t^{\frac{1}{2}}$ and the true activation overpotential η_D can be derived by extrapolation to zero time. When the exchange reaction is slow ($i_o < 10^{-2}$ Acm^{-2}) the overpotential is found to increase linearly with time (83) and extrapolation to derive η_D is relatively easy. When the exchange reaction is very fast ($i_o > 10A\ cm^{-2}$) the double layer charging process (B) intrudes on the reaction making analysis of η - t curves diffucult. GERISCHER and KRAUSE (72) have developed a double pulse technique in which a short, intense pulse of current is used to charge the double layer before application of the main pulse. This method is experimentally very cumbersome as the prepulse has to be controlled precisely in magnitude with respect to the main pulse to achieve the desired effect.

If the electrode reaction is partially controlled by 'adatom' diffusion the rise-time and steady state for η - t curves are considerably greater than expected (135). The 'adatom' diffusion parameters can be derived from a complete analysis of the η - t curve.

When the electrode reaction is partially controlled by electrocrystallisation 'superpolarisation' peaks are observed (19).

4.2.b. The potentiostatic Method

This technique is analogeous to the Galvanostatic method. A pulse of potential, controlled by a fast response potentiostat (22), is applied to the electrode and the current-time response recorded oscillographically.

Falling current-time transients are observed for rate control by charge-transfer and by 'adatom' diffusion (86, 93). The current is initially high due to the rapid charging of the double layer and then falls as $\sqrt{t}$ (92) for C.T. controlled reactions. Extrapolation of $i - \sqrt{t}$ curves to $t = 0$ yields the current corresponding to the applied potential (Eq. [3.12]).

If the electrode reaction is controlled by an electrocrystallisation mechanism rising current-time transients are observed according to Eqs. [3.20] to [3.25] (66). Unambiuous assignment of mechanism from the current-time relationship is possible only in the case of i = constant (Eq. [3.20]) and $i \propto t^3$ (Eq. [3.25]). The assignment of mechanisms for the $i \propto t$ and $i \propto t^2$ cases can be made by using and 'L' double pulse technique (66). The first pulse is adjusted in magnitude and length so that N_o neuclei are formed, and these grow at the second potential according to a zero or 1^{st} order of time (Eq. [3.20] or [3.21]). The kinetic parameters A and K can be elucidated from the relative slopes of i-t^n curves at different potentials.

4.3 General Experimental Precautions

Electrochemical exchange reactions, especially those involving an M/M^{z+} exchange, generally occur at discrete 'active' centres on the electrode. These active centres very readily adsorb neutral organic molecules over a very wide potential region (131) and, in addition, the surface concentration of these active centres generally depends very strongly upon the electrode pre-treatment history. It is thus of prime importance to use an electrode pretreatment procedure which results in eleectrodes of uniform and reproducible activity and also to ensure that electrolytes contain a minimum level (20) of surfactants. The best procedure for attaining these low levels ($< 10^{-9}$M) of surfactants is the charcoal absorption procedure developed by BARKER (12), coupled with care in cleaning all glasswear, the use of the highest quality of water available (i.e. multiple-distilled) and in general a high standard of 'house-keeping'.

In reactions which are very slow (e.g. the Hydrogen exchange at certain metals) concentrations of cations which are active w.r.t. the h.e.r. have to be reduced to a low level. Pre-electrolysis using an additional rèmovable electrode has to be used in addition to the other techniques described.

CHAPTER 5

THE ELECTROCHEMICAL AND PHYSICAL PROPERTIES OF SILVER AND ITS OXIDES

5.1 The Electrochemical Equilibria of Silver

In acidic or neutral electrolytes which do not contain halide (or pseudo-halide) anions, silver behaves as a reversible metal-ion electrode (E^{o} = 0.799V (126)).

In halide (or pseudo-halide) electrolytes, silver behaves as a reversible halogen electrode. This is due to the very low solubility of silver-halides - the activity of the potential determining ion (Ag^{+}) being inversely proportional to the activity of the halide ion (X^{-}):-

$$Ag^{+} = S/[X^{-}] \qquad [5.1]\ *$$

$$\therefore \quad E = E^{o} + \frac{RT}{F} \ln S - \frac{RT}{F} \ln [X^{-}] \qquad [5.2]$$

$$= E^{o\prime} - \frac{RT}{F} \ln [X] \qquad [5.3]$$

In alkaline electrolytes two stable oxides exist, one corresponding to Ag(I), Ag_2O (107), and the second a higher oxidation state of silver, AgO(11). These two oxides are slightly soluble in aqueous electrolytes and, as a consequence, silver behaves as two different electrodes reversible to OH^{-}:-

$$Ag_2O + H_2O + 2e \longrightarrow 2Ag + 2OH^{-}, \quad E^{o} = 0.338V(53) \qquad [5.4]$$

$$2AgO + H_2O + 2e \longrightarrow Ag_2O + 2OH^{-}, \quad E^{o} = 0.599V(54) \qquad [5.5]$$

* It is assumed that the activity coefficients are unity.

5.2 Physical Properties of Silver and its Oxides

These properties are summarised in Table I.

The higher oxide of Silver, AgO, is of considerable interest, Although the stoichiometry indicates that the oxidation state of Silver is +2 (electronic state: $4d^9$) AgO is diamagnetic (120) and thus cannot be in the +2 oxidation state. Also R.D.E. experiments (129) show that Ag^{II} is unstable in alkaline electrolytes. 'X' ray and neutron diffraction experiments (74, 138) have shown that Silver exists in the +1 and +3 oxidation states in AgO. This accounts for the higher electron conductivity of AgO compared with Ag_2O (5). AgO dissolves in very strongly alkaline solutions (> 5M $[OH^-]$) to give the tetrahydroxy argentate^{III} anion $[Ag(OH)_4]^-$ (41), however this species is not stable in weakly alkaline and neutral electrolytes.

TABLE I

THE PHYSICAL PROPERTIES OF SILVER AND ITS OXIDES

Property	Silver	Ag_2O	AgO
Melting Point	968.8°C	300°C decomposes(3)	~80°C (4) decomposes
Electrical Conductivity	6.3×10^5 mho cm^{-1} (141)	10^{-8} mho cm^{-1} (103)	7×10^{-2} mho cm^{-1} (96)
Crystal Structure	FCC	Cuprite	Monoclinic
Interatomic Distances	Ag-Ag: 1441Å (140)	Ag-Ag: 3.3 Å (5) Ag-O: 2.06Å	Ag-Ag: 3.28 & 3.39Å (74, 138) Ag-O: 2.18+2.0 (138)
Solubility in 1M NaoH	-	1.8×10^{-4}M (94)	2×10^{-4}M (57)
Species in Solution	-	$Ag(OH)_2^-$ (57)	$Ag(OH)_2^-$ (57, 62)

CHAPTER 6

THE STRUCTURE OF THE SILVER/AQUEOUS SOLUTION INTERPHASE

6.1 Introduction

A study of the differential capacitance of an electrode is an essential preliminary to the study of the kinetics of electrochemical reactions at the electrode (50). Differential capacitance studies in non-interacting (1:1) electrolytes enable estimates of the microscopic roughness (154) and of E_z to be made. For interacting electrolytes information concerning the specific adsorption of ions (58) and neutral molecules (47) at the electrode is obtained. Differential capacitance studies, therefore, enable relevant comparisons between electrode preparation and pretreatment techniques to be made.

Studies of the differential capacitance of silver in a variety of electrolytes have been carried out (27, 105, 115, 132, 149, 154). Values given for E_z lie in the range +0.5V to -0.7V and for the roughness factor for silver from $\sim$2.5 to $\sim$10. Certain of these studies were made in solutions of ions which would be expected to interact strongly with silver (154). A value for E_z = -0.7V (105, 132) in neutral electrolytes appears to be experimentally well substaniated and correlates with E_z-work function data (68) for other metals.

The present studies were carried out under conditions of ultra purity (84) and over a range of pH from neutral to 14 in an attempt to obtain meaningful data. The effect of the adsorption of n-Butylamine at the electrode was also studied.

6.2 Experimental Techniques

Type I cells (Appendix 1) were used. The reference electrode, $Ag_2O/Ag/OH$ (1M) (See Appendix 2) was contained in a removable 'thimble', the liquid junction being made through an asbestos fibre. The counter electrode was platinum gauze; the working microelectrode is described in Appendix 3.

Electrolytes were prepared from A.R. chemicals and conductivity water (twice distilled in quartz from deionised stock). Stock solutions, 1M NaOH and 1M $NaClO_4$, were made; concentrations in the cell were changed by the removal of aliquots and re-addition of conductivity water. The aliquots were analysed by titration (for $[OH^-]$) and flame photometry (for $[Na^+]$).

All glassware (including cells) was cleaned in HNO_3/H_2SO_4(1:1) for $\sim$7 days, thoroughly washed in conductivity water and dried at 120°C before use.

Electrolyte was circulated continuously through activated charcoal (see Appendix 4) by means of a nitrogen lift pump. Electrolytes were saturated with, and under an atmosphere of, oxygen free nitrogen.

Fig. 10 Schering Bridge for A.C. Measurements.
a- Nitrogen Purification Furnaces; b- A.F. Generator;
c- Electrometer; d- 50 c/sec Filter, e- Detector,
g- Galvanometer; h- R_1; i- C_2; j- R_2

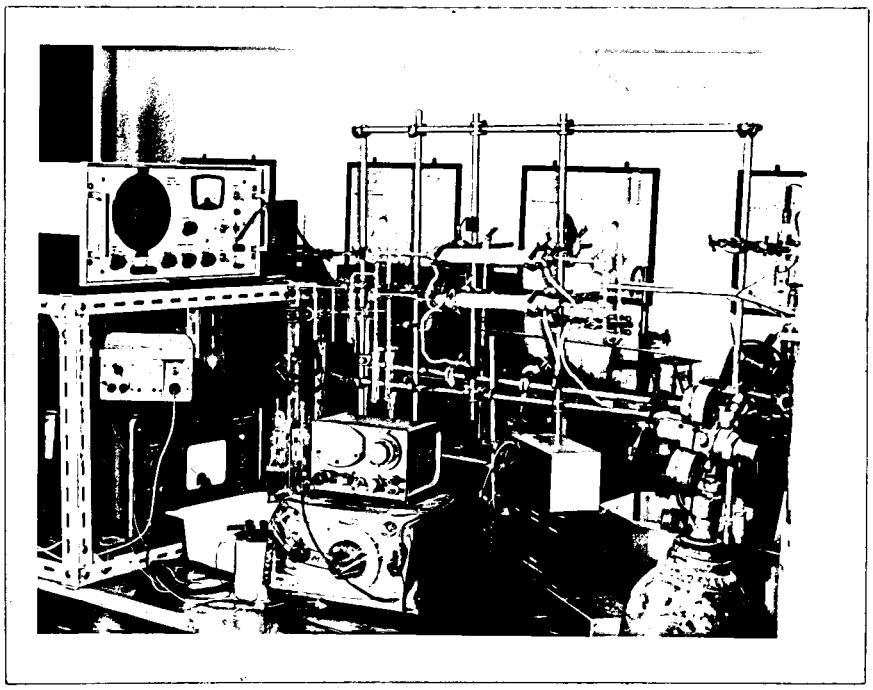

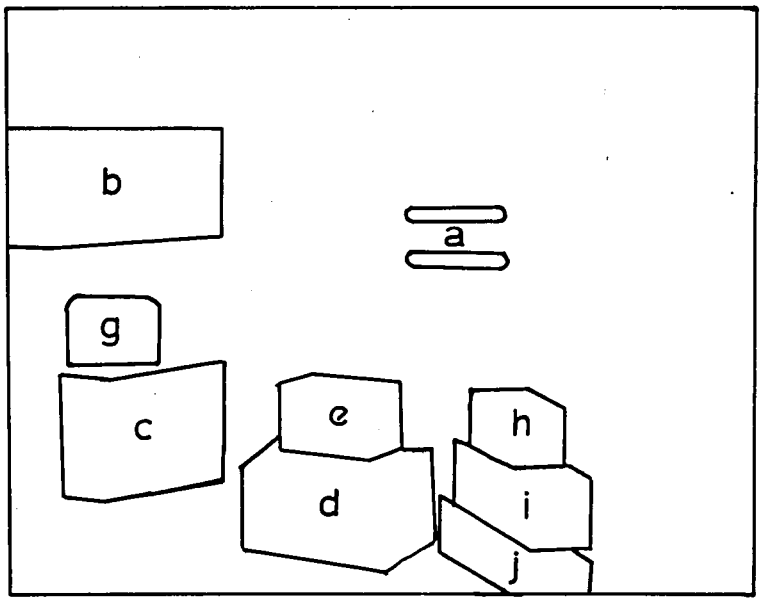
b
a
g
c
e
h
d
i
j

Fig. 11 Differential Capacitance Equilibration of Silver in 1.0M $NaClO_4$, 23°C, 212c/sec.

Fig. 12 Faradaic Current Curves for Silver in NaOH and $NaClO_4$ showing Polarisable Regions.

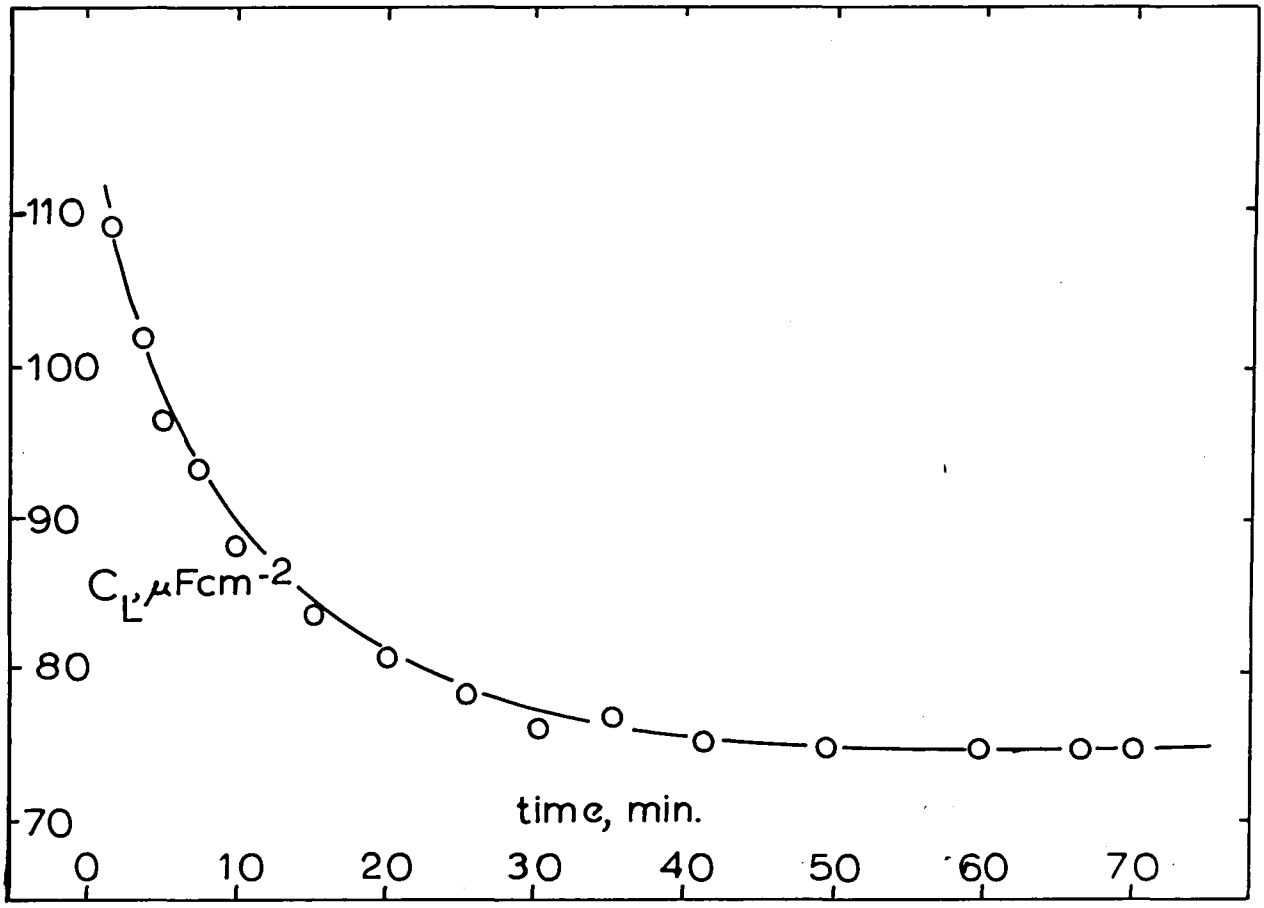
110
100
90
80
70
C_L, μFcm^{-2}
time, min.
0
10
20
30
40
50
60
70

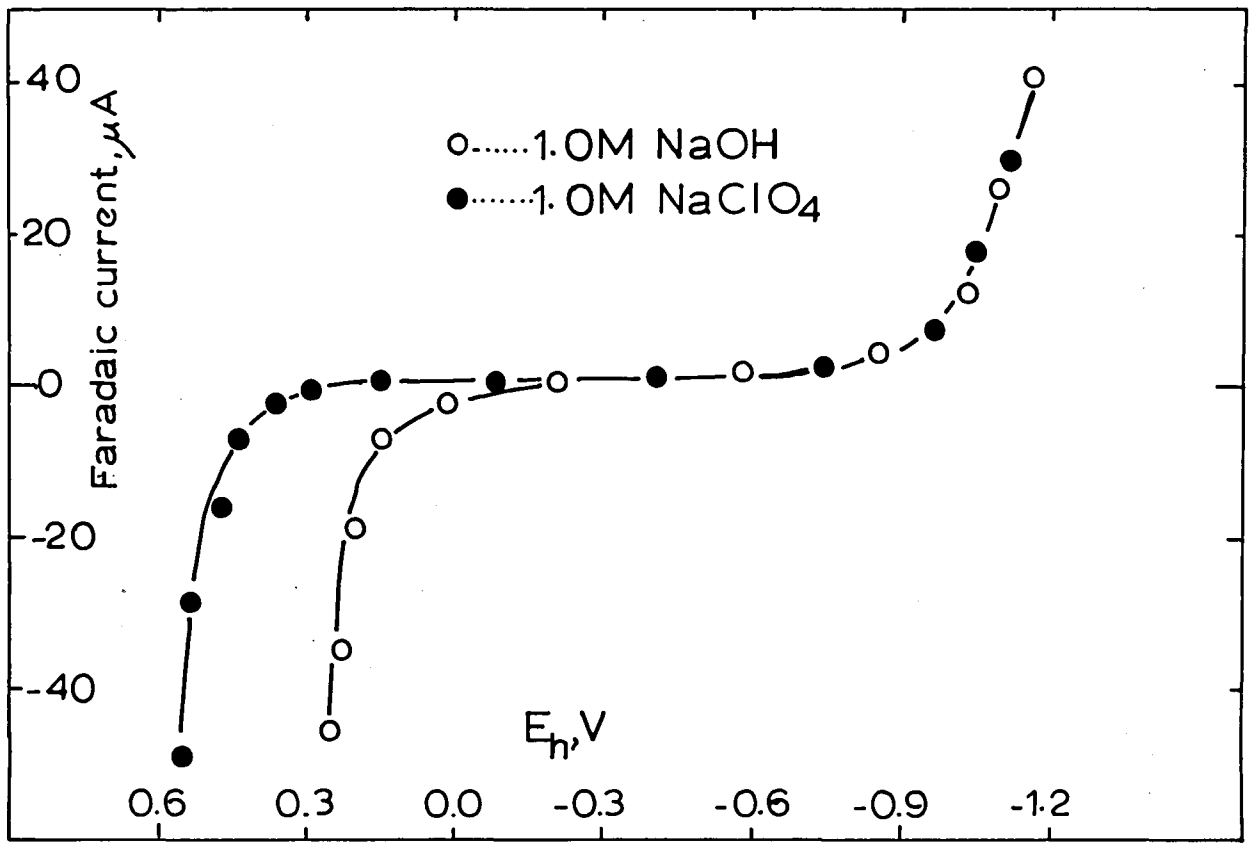
40
20
0
-20
-40
Faradaic current, μA
o.....1.0M NaOH
●.....1.0M $NaClO_4$
E_h, V
0.6
0.3
0.0
-0.3
-0.6
-0.9
-1.2

Capacitance measurements were made with a Schering bridge (Fig. 10). The cell was polarised by means of a DC potentiometer (the A.C. being filtered with a 4OH choke). The bridge accuracy was 99% up to frequencies of 1kc; above this frequency the errors in measurement became more pronounced, as shown below:-

Frequency c/sec	170	320	680	1000	3000	9000
Error %	-0.1	-0.1	-0.2	-0.3	-2.0	-15.0

These errors were in the capacitance values; resistance readings were accurate to within $\pm$ 0.5% over the whole range.

6.3 Results and Discussion

6.3.a. Electrode Pretreatment and Equilibrium

Electrodes were polished on roughened glass under conductivity water and etched in a number of ways (see Table II) before insertion into the cell. The differential capacitance at the 'rest' potential fell rapidly with time after initial electrode/electrolyte contact (see e.g. Fig. 11), eventually reaching a stable value. Under conditions of exhaustive electrolyte cleaning (i.e. treatment with charcoal for 2/3 months) this final capacitance was stable for long periods (up to 48 hours). The equilibration time and, to a certain extent, the stable capacitance value depended on the electrode pre-treatment (Table II). Electrochemical etches gave electrodes which exhibited differential capacitance curves indicative of an adsorbed film at the electrode (85).

Fig. 13 Differential Capacitance of Silver in Neutral $NaClO_4$ Electrolytes at 23°C.

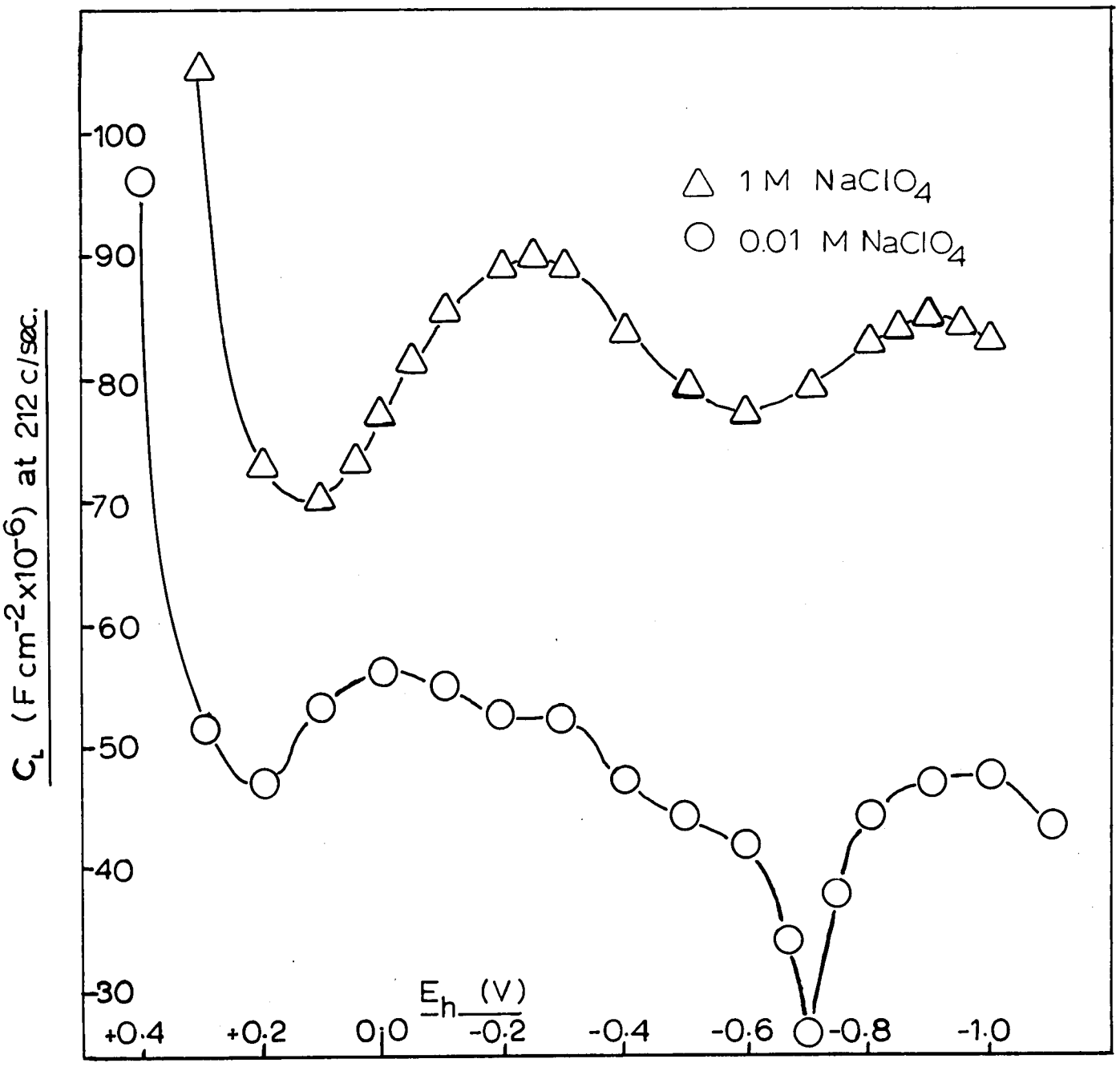
△ 1 M NaClO4
○ 0.01 M NaClO4
100
90
80
70
60
50
40
30
Cl (F cm-2 x10-6) at 212 c/sec.
+0.4
+0.2
0.0
-0.2
-0.4
-0.6
-0.8
-1.0
Eh (V)

Fig. 14 The Differential Capacitance of Silver in NaOH Effect of Dilution. 23°C, 1000c/sec

Fig. 15 Frequency Dispersion of Capacitance of Silver in 1 M NaOH, 23°C.

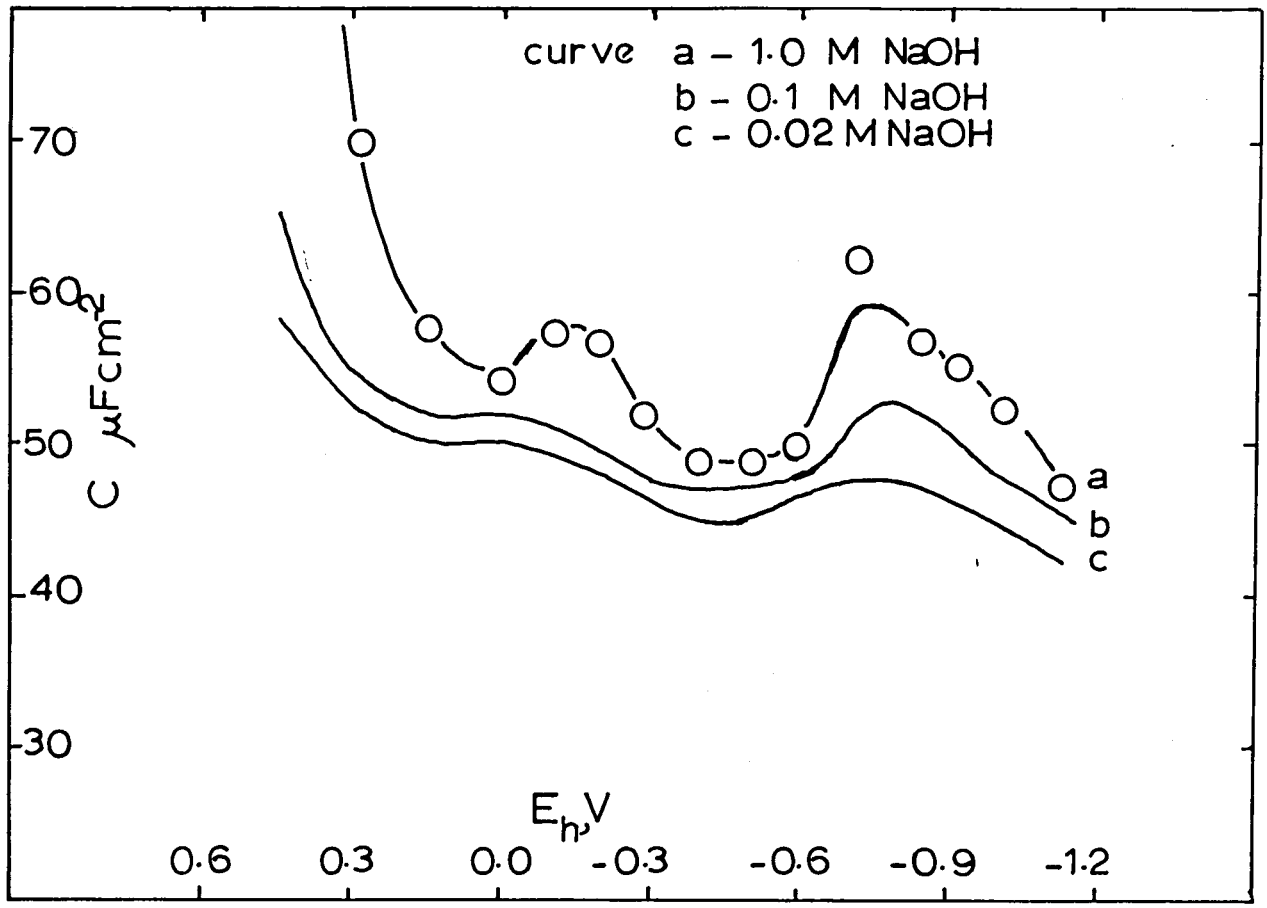
curve a – 1·0 M NaOH
b – 0·1 M NaOH
c – 0·02 M NaOH
70
60
50
40
30
C μFcm⁻²
a
b
c
E_h,V
0·6
0·3
0·0
-0·3
-0·6
-0·9
-1·2

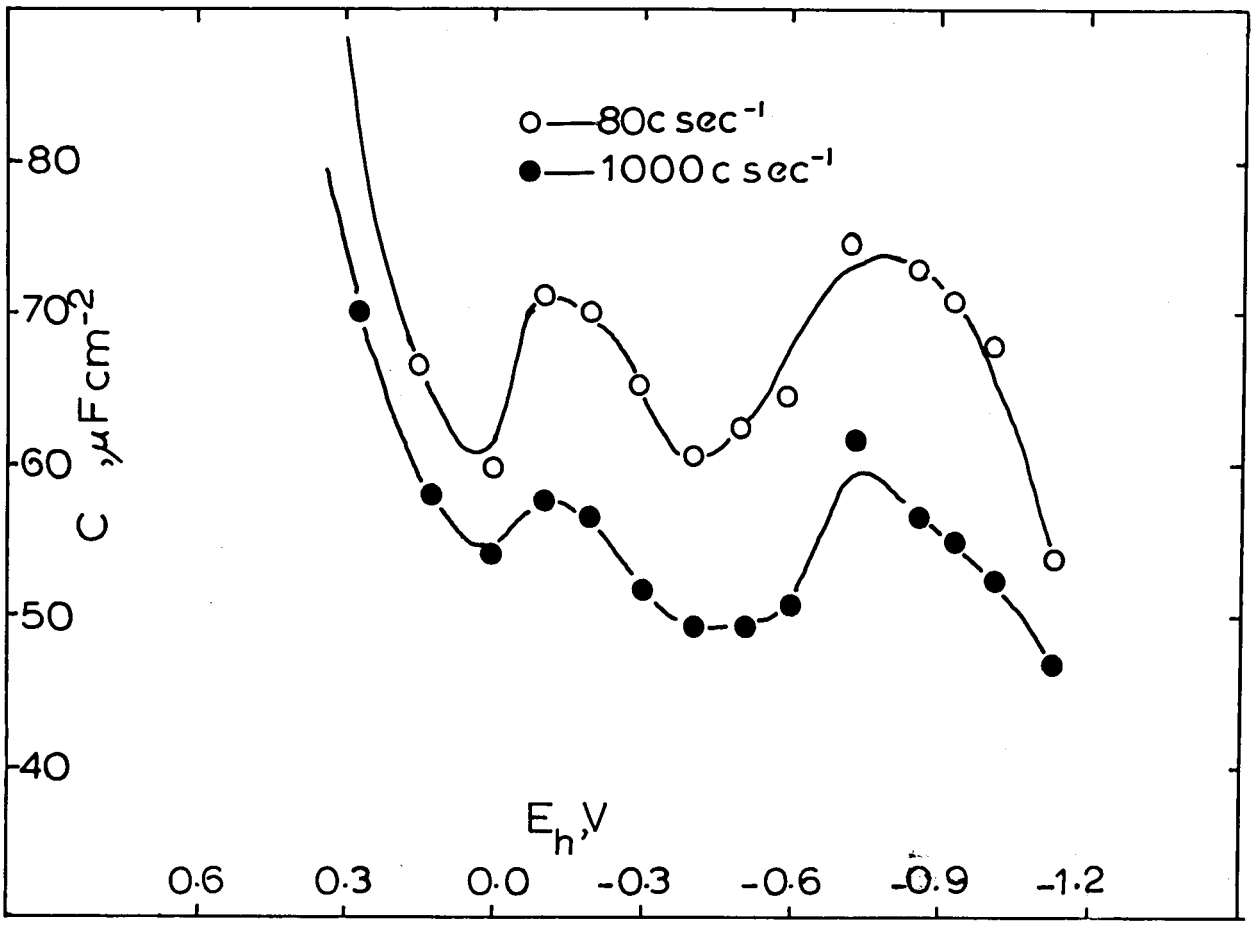
o—80c sec⁻¹
●—1000c sec⁻¹
80
70
60
50
40
C μFcm⁻²
E_h,V
0·6
0·3
0·0
-0·3
-0·6
-0·9
-1·2

Mineral acid etches gave the best results. HNO_3 etches resulted in electrodes with reproducible equilibrium times ($\sim$40 mins) and electrode capacitances.

6.3.b. Differential Capacitance Studies in Alkaline and Neutral Electrolytes.

Current-potential curves (Fig. 12) show that the electrode is polarisable over a considerable potential range, even in alkaline electrolytes.

The differential capacitance curves in 1.0M NaOH and 1.0M $NaClO_4$ are formally very similar (Figs 13, 14) and indicate that silver, pretreated as described (Ch. 6.3.a), has a roughness factor of 2.5-3. (Liquid mercury has an average differential capacitance of $\sim 17\ \mu F\ cm^{-2}$ at potentials removed from E_z (75)). This value for the roughness factor agrees with that found by RAMALEY and ENKE (132) using similar methods, and also with that reported by ZHUTAEVA and SHUMILOVA (160) who used a P.S.V. technique.

The differential capacitance curves exhibit relatively slight frequency dispersion (Fig. 15) except at their extremes (of potential) where faradaic reaction is starting to occur (Fig. 12), and thus do represent differential capacitances. The relatively slight frequency dispersion is attributable to electrode roughness effects (51).

Electrolyte dilution causes a reduction in capacitance values. In $NaClO_4$ electrolytes a capacitance minimum appeared at -0.7V N.H.E. on Dilution (Fig. 13) the potential of the minimum remaining unchanged with dilution. It was therefore concluded that this potential (-0.7V) represents

Fig. 16 The Effect of n-Butylamine on the Differential Capacitance of Silver in 1M $NaClO_4$. 1000c/sec, 23°C.

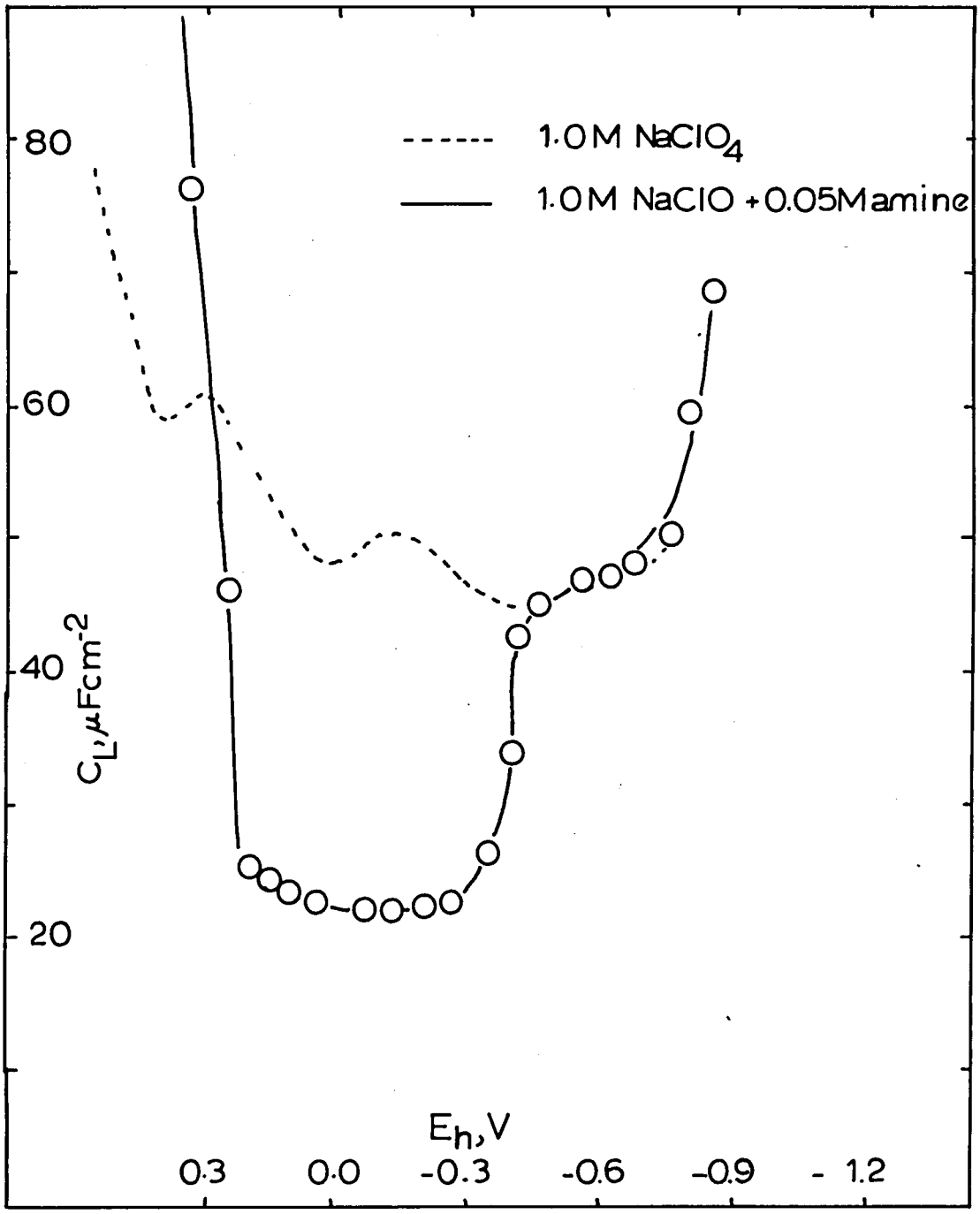
80
60
40
20
$C_L, \mu Fcm^{-2}$
1.0M $NaClO_4$
1.0M NaClO +0.05Mamine
E_h, V
0.3
0.0
-0.3
-0.6
-0.9
- 1.2

Fig. 17 The Effect of n-Butylamine on the Differential Capacitance of Silver in 1.0M NaOH, 23°C, 1000c/sec.

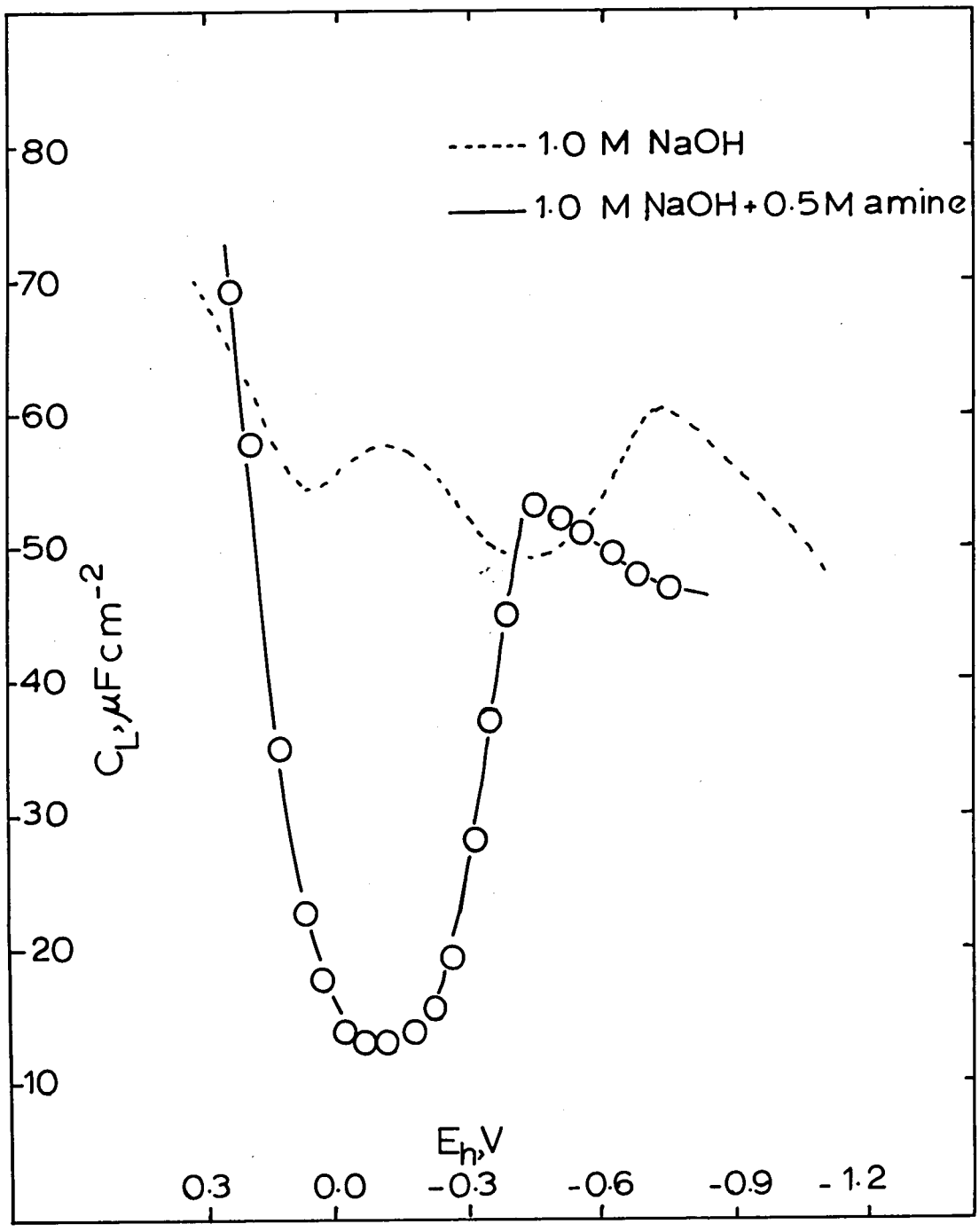
1.0 M NaOH
1.0 M NaOH + 0.5 M amine
80
70
60
50
40
30
20
10
C_L, μF cm^{-2}
E_h, V
0.3
0.0
-0.3
-0.6
-0.9
-1.2

E_z. No such effect was observed in NaOH electrolytes (Fig. 14) down to concentrations where the bridge sensitivity limits the accuracy of measurements ($\sim 10^{-3}$M).

These results would appear to confirm the previously accepted value for E_z (-0.7V) with the reservation that the interphase is complicated in the presence of NaOH - due possibly to OH^- adsorption.

6.3.c. Differential Capacitance Curves in the Presence of a Neutral Organic Compound.

Neutral organic molecules are adsorbed at electrodes at potentials around E_z(75) and have a very marked effect on differential capacitance curves (47).

Additions of n-butylamine* to the electrolyte had a very marked effect on the differential capacitance curves of Silver in 1.0M $NaClO_4$ (Fig. 16) and 1.0M NaOH (Fig. 17). This effect was, in both cases, the appearance of a very deep capacitance minimum. This minimum occurred, identically, at $\sim$ -0.1 V N.H.E. and suggests that this potential represents E_z for silver. It is significant that this result was obtained in both neutral and alkaline electrolytes.

* The adsorption of n-butylamine was investigated as it was of interest from an electrosynthesis aspect (Ch. 8)

6.4 The Structure of the Interphase at Silver Electrodes

The Electrode-electrolyte interphase is complicated even in neutral electrolytes. Although E_z is perhaps $\sim$ - 0.1V, no capacitance minimum becomes apparent at this potential on dilution of the electrolyte, indeed a capacitance minimum at -0.7V in neutral electrolytes is well authenticated (85, 105). This capacitance minimum is difficult to explain, but it is propably not due to $q_e = 0$ at this potential.

The absence of a capacitance minimum at E_z is probably due to the electrode-electrolyte interactions discussed in Ch. 7.

TABLE II

Electrode Pretreatment Techniques - Effect on Equilibration Time and Final Electrode Capacitance (at the rest potential)

1.0M $NaClO_4$

Treatment	Time to equilibrate	C_L at 1000c/sec.
1. Mechanical polish on roughened glass	75 hrs	130
2. Mechanical polish, 2 min etch in $HClO_4$ (A.R.)	2 hrs	56
3. Mechanical polish, 10 min etch in $HClO_4$ (A.R.)	1 hr	54
4. Mechanical polish, 10 sec etch in HNO_3 (conc.)	$\frac{1}{2}$ hr	55
5. Mechanical polish, 30 sec etch in HNO_3 (conc.)	$\frac{1}{2}$ hr	70
6. Mechanical polish, electropolish in HNO_3	$\frac{1}{4}$ hr	20
7. Mechanical polish, electropolish in $HClO_4$	$\frac{1}{4}$ hr	18

1.0M NaOH Electrolyte

8. Mechanical polish, 10 sec etch in HNO_3 (conc)	$\frac{1}{2}$ hr	56
9. Mechanical polish, 2 min etch in $HClO_4$ (A.R.)	2 hrs	54
10. Mechanical polish, electropolish in HNO_3 (conc.) (C_L rising with time)	3 hrs	48

CHAPTER 7

THE ANODIC OXIDATION OF SILVER ELECTRODES IN ALKALINE ELECTROLYTES

7.1 Introduction

7.1.a. General Features of the Electrochemical Oxidation of Silver

The galvanostatic oxidation of silver in 1M NaOH was first studied by LUTHER and POKORNEY (111). Under these conditions a potential-time curve of the form shown in Fig. 18 is obtained. Two regions of approximately constant potential (before oxygen evolution becomes dominant) are observed, with a relatively rapid transition between them. These two 'constant' potential regions have been ascribed to the formation of Ag_2O (at the lower potential) and of AgO (28, 52). The potential 'overshoot' spike at the start of the formation of AgO is thought to be due to an electrocrystallisation process (97).

DIRKSE and DeVRIES studied the electrochemical oxidation of silver by means of a potential sweep technique. A current-potential response of the form shown in Fig. 19 was observed. In addition to the expected faradaic current flow due to the formation of Ag_2O and AgO (peaks 'b' and 'c') an additional (minor) (56) current peak ('a') was observed at a lower potential than that for the formation of Ag_2O and was ascribed to the formation of AgOH (hitherto unreported). The appearance

Fig. 18 The Galvanostatic Oxidation of Silver in 1.0M NaOH, 23°C. Applied Current Density = 3.4 $mAcm^{-2}$.

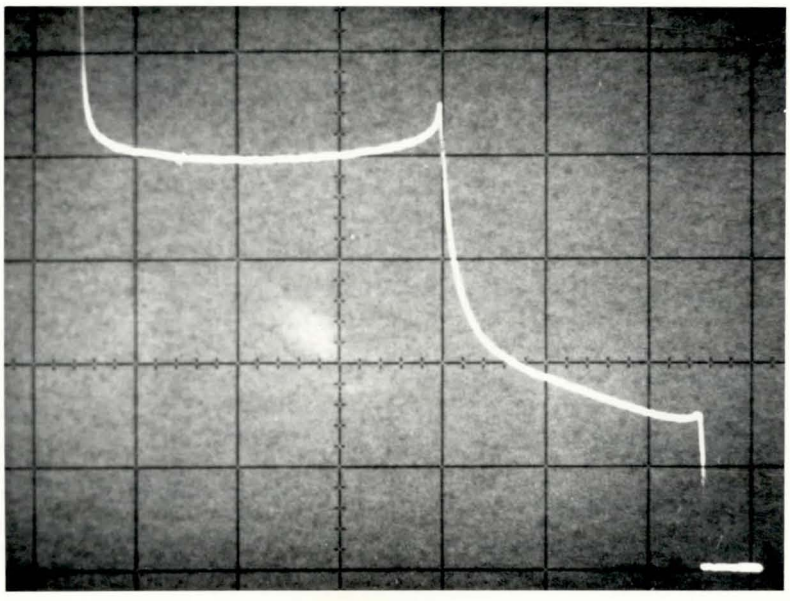

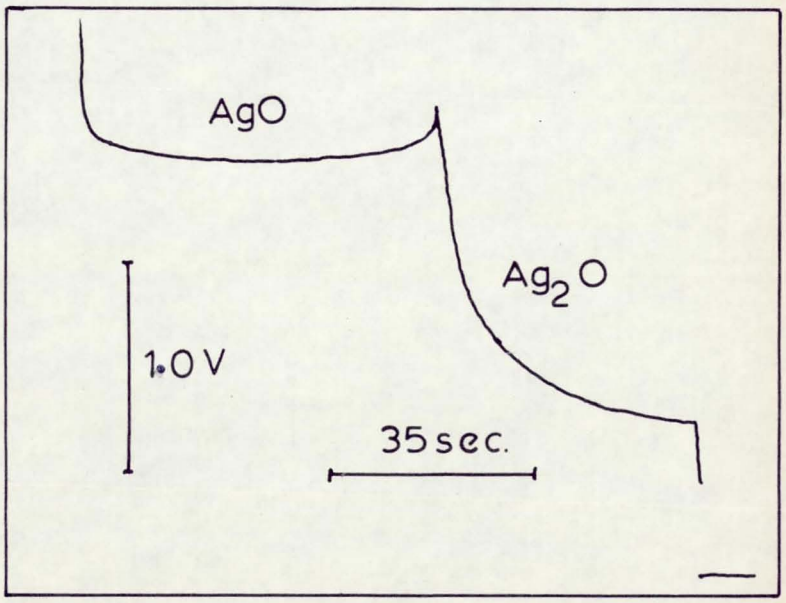
AgO
Ag_2O
1.0 V
35 sec.

Fig. 19 P.S.V. Current-Potential Trace for Silver in 1.0M NaOH, 23°C, 6 x 10^{-4} V sec^{-1} (Trace runs from R - L) Start at + 0.338V. A- Preliminary Reaction Peak; B- Massive Ag_2O Formation; C- Massive AgO Formation.

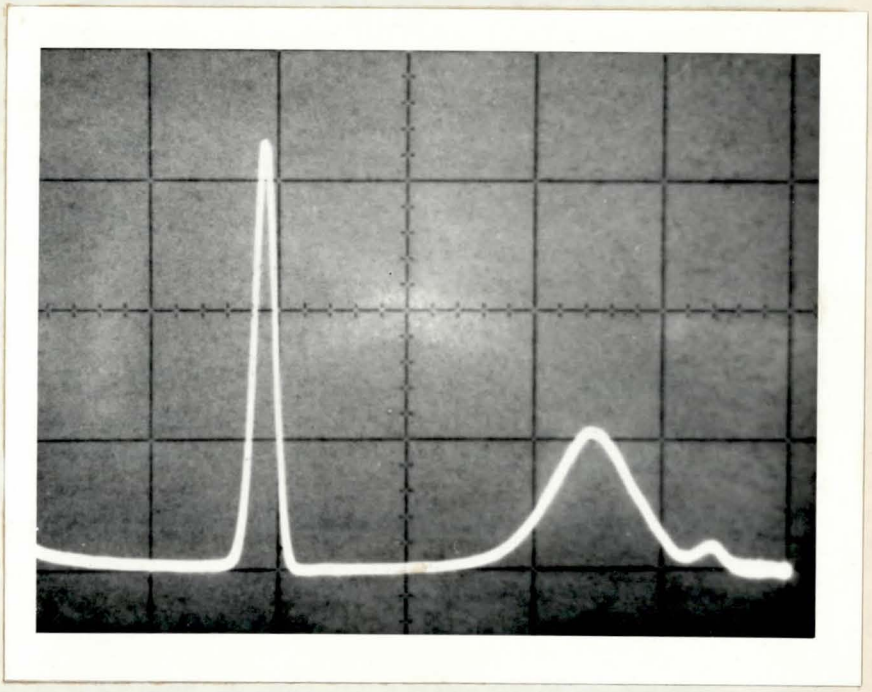

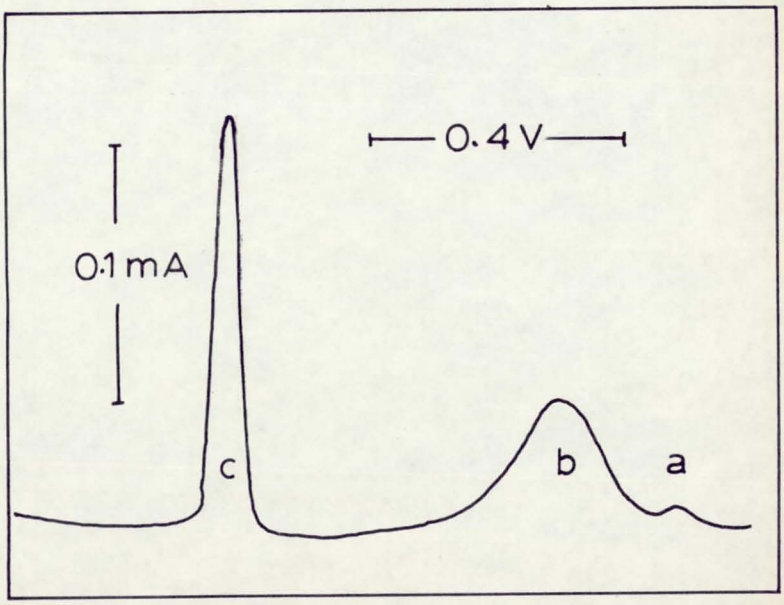
0.4 V
0.1 mA
c
b
a

of current peaks rather than waves indicates that the electrode reactions are self-inhibiting and explains the rapid transition in mechanism under galvanostatic conditions.

7.1.b. Studies of the formation of Ag_2O

The kinetics of the formation of Ag_2O have been studied by several groups of workers using different techniques.

DIRKSE et al. (55), using the galvanostatic pulse technique at low overpotential found a value for $i_o \sim 2mAcm^{-2}$; however a linear overpotential-current density plot extending to 50mV was given. Such a large linear region is inconsistent with the kinetic theory of charge transfer reactions (see Ch. 3.1.a.).

FLEISCHMANN et al. (63) studied the electrode reaction using potentiostatic pulse techniques. Falling current-time transients were observed and it was deduced that the rate controlling process for the formation of Ag_2O is solid-state ionic diffusion.

STONEHART (144) and OSHE (123) have studied the formation of Ag_2O by P.S.V. techniques. STONEHART derived a value for the transfer coefficient, $\alpha = 0,7$ and concluded that the reaction is second order with respect to silver. OSHE studied the effect of electrolyte concentration on the rate of reaction and showed (in agreement with other workers (63, 100, 148))

that the rate controlling process is solid-state ionic diffusion.

7.1.c. Studies of the Formation of AgO

The rate determining process for the formation of AgO has been shown to be electrocrystallisation (64) (or autocatalysis (145)) although BARRADAS and FRASER have interpreted Tafel plots (14) in terms of ionic diffusion/migration at the AgO/Ag_2O interphase (15).

7.1.d. Summary of Previous Work

The mechanism and kinetics of the electrochemical oxidation of silver appear to be unresolved. There are indications of uncharacterised 'low' overpotential faradaic processes. Conflicting mechanisms have been proposed for the formation of Ag_2O, possibly due to changes in mechanism with electrode coverage and film thickness. The formation of AgO appears to be controlled by an electrocrystallisation process; however this mechanism is not fully accepted.

A complete knowledge of the 'substrate' electrode reaction is a prerequisite to a study of the electrochemical oxidation of organic compounds. Such a study of the silver electrode in alkali was undertaken and is reported in this chapter.

7.2 Experimental Methods

7.2.a. Apparatus and Chemicals

The electrochemical cell used was made from borosilicate glass and was of Type II (see appendix 1). All glassware was thoroughly cleaned before use (see Ch. 6.2).

The micro test electrode and reference electrode ($Ag_2O/Ag/OH^-$ (1M) are described in appendix 2 and 3. The counter electrode was silver gauze.

Electrolytes, made from A.R. NaOH and $NaClO_4$, were maintained at constant $[Na+]$ = 1.0M, except in experiments using electrolytes of $[OH^-] > 1.0M$. Stock solutions of 1.0M NaOH and 1.0M $NaClO_4$ were made up as described in Ch. 6.2. Electrolytes were initially 1.0M NaOH - the $[OH^-]$ being changed by the removal of aliquots from the cell and addition of 1.0M $NaClO_4$. The electrolytes were continuously circulated over activated charcoal (see appendix 4) and were saturated with, and under an atmosphere of, oxygen-free nitrogen.

7.2.b. Experimental Procedure

Potentiometric measurements were made using a high input impedance electrometer (Pye 11088). The test electrode was polished on roughened glass under conductivity water, etched in HNO_3 and inserted into the cell. The potential was allowed to reach equilibrium and was then recorded. Equilibrium was usually reached within 20 minutes.

Fig. 20 Potentiostat used for Kinetic Measurements.
a - Potentiostat; b- Linear Sweep Generator; C- Double Pulse Generator; d- Oscilloscope

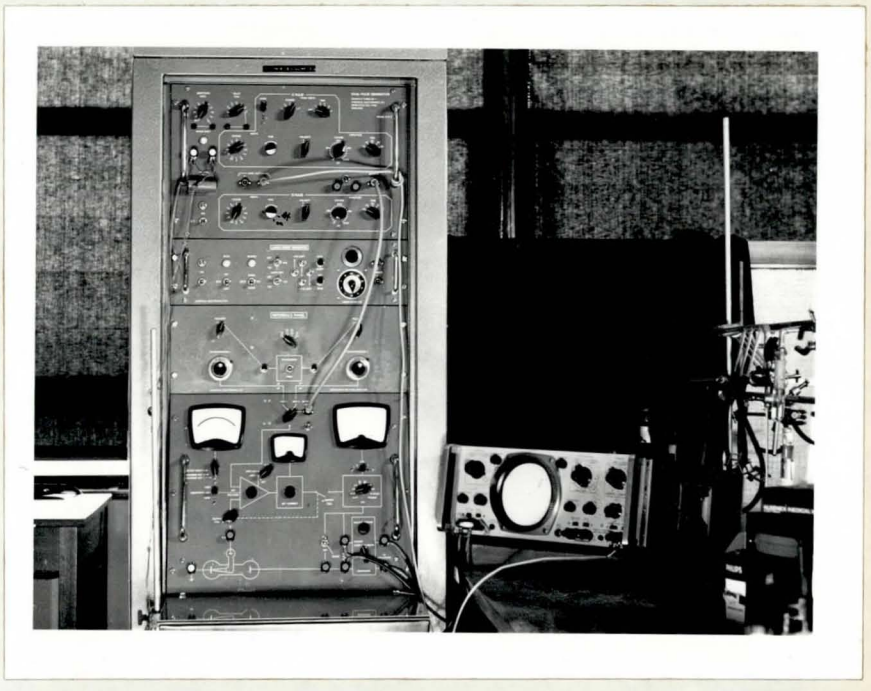

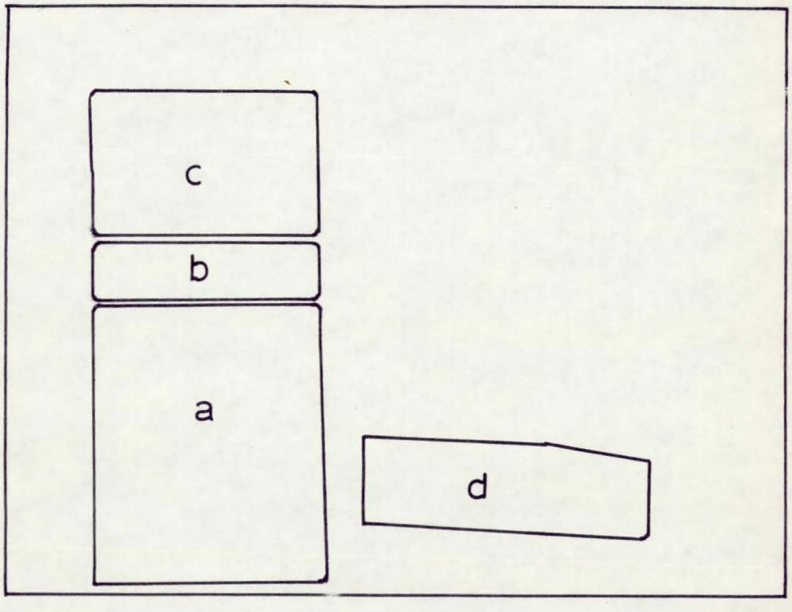
c
b
a
d

For electrode-kinetic measurements (galvanostatic and potentiostatic) of the rate of formation of Ag_2O, the electrode was held in the cell after polishing and etching for 60 mins before electrical connection was made. A single current pulse (rise-time $\sim 0.5 \times 10^{-6}$ sec. from a Solatron GO 1005 pulse generator), or potential pulse (Chemical Electronics Ltd. potentiostat and pulse generator; rise-time $\sim 10^{-6}$ sec (Fig. 20)) was applied to the electrode, the potential-time or current-time response recorded oscillographically (Hewlett Packard 130C oscilloscope and camera), and the electrode re-polished and etched.

The faradaic impedance of the Ag_2O/Ag equilibrium was measured using the cell and apparatus described in Ch. 6.2. The test electrode was polished, etched and inserted into the cell without connecting electrically. After 1 hour the test electrode was connected into circuit and its potential brought to that of the reversible $Ag_2O/Ag/OH^-$ electrode by means of the D.C. potentiometer (see Fig. 7). C_{xs} and R_{xs} values were measured over a range of A.C. frequencies.

Kinetic data on the formation of AgO were obtained potentiostatically. The polished, etched electrode, was held in the cell for 20 mins and then oxidised to Ag_2O galvanostatically (current density = 2.5 $mAcm^{-2}$) until the potential started to rise rapidly. The cell was then

connected to the potentiostat and the electrode held at a potential of +0.550V N.H.E. for 10 mins. A potential pulse was then applied, the current response being recorded oscillographically. The electrode was then re-polished and etched.

P.S.V. experiments were carried out using a linear sweep generator in conjunction with the potentiostat. Electrodes were allowed to equilibriate in the cell for 20 minutes after polishing and etching (unless equilibration experiments were being carried out). Current-potential curves were recorded either oscillographically (X-Y mode) or as current-time curves on a chart recorder. There was no parasitic interaction between the potentiostat and chart recorder (or oscilloscope). Each P.S.V. experiment was repeated 4-5 times and the average of the I_m and E_m values taken. Reproducibility was $\pm$ 10%.

7.3 Faradaic Processes Occurring at Relatively Low Potentials

7.3.a. Potentiometric Measurements

When a polished, etched silver electrode is brought into contact with an NaOH electrolyte the steady state potential attained is not that due to the $Ag_2O/Ag/OH^-$ electrode reaction (Fig. 21). This potential does not obey the expected (Nernst) dependence on $[OH^-]$ (Fig. 50) and as a consequence cannot be due to a simple electrochemical exchange reaction. This rest potential is

probably a mixed or corrosion potential (99). Such potentials have been observed for silver in oxygen saturated solutions (90) and were attributed to the dissolution of silver:-

$$Ag \longrightarrow Ag^+ + e \qquad [7.1]$$

and the reduction of dissolved oxygen:-

$$2H_2O + O_2 + 4e \longrightarrow 4OH^- \qquad [7.2]$$

The reduction of dissolved oxygen would not seem a valid electrode process under conditions of exhaustive nitrogen purging. Oxygen adsorbed at the electrode has been shown to exist under similar experimental conditions (160) as has adsorbed hydrogen (161); these species are probably produced by the interaction of the electrolyte with the electrode and the potential determining reactions are thus:

$$H_2O + e \longrightarrow OH^- + H_{ads} \qquad [7.3]$$

$$H_2O \longrightarrow 2H^+ + O_{ads} + 2e \qquad [7.4]$$

The fact that the potential - log $[OH^-]$ curve lies between the values for the reversible Oxygen and Hydrogen electrodes (Fig. 21) lends support to this mechanism.

7.3.b. Potential Sweep Measurements

Potentiodynamic current curves show that, under certain conditions, faradaic reaction occurs at potentials below that for the formation of thick films of Ag_2O (56, 144) although these potentials are still more positive than the $Ag_2O/Ag/OH^-$ equilibrium

Fig. 21 The Dependence of the Rest Potential for Silver on $[OH^-]$. Comparison with the Reversible Hydrogen and Oxygen Electrodes.

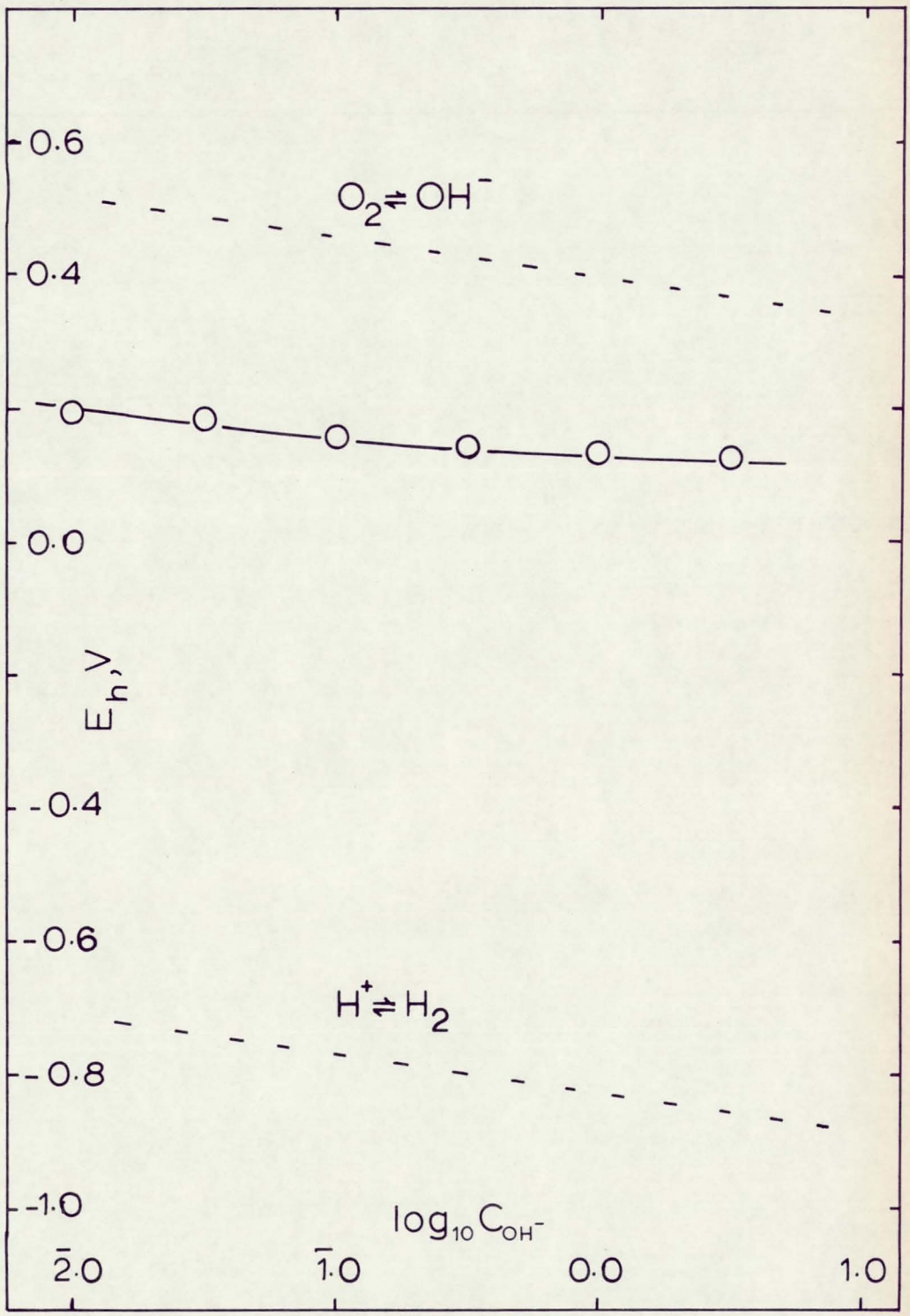
0.6
0.4
0.0
-0.4
-0.6
-0.8
-1.0
E_h, V
$O_2 \rightleftharpoons OH^-$
$H^+ \rightleftharpoons H_2$
$\log_{10} C_{OH^-}$
$\bar{2}.0$
$\bar{1}.0$
0.0
1.0

(Figs. 19 and 22). This faradaic reaction, observed as a current peak, is usually equivalent to the oxidation of ~1 monolayer of silver and could be due to any one (or more) of four different oxidation processes.

i. the formation of AgOH at the electrode surface (56, 144)
ii. The formation of a monolayer of Ag_2O
iii. The oxidation of adsorbed hydrogen
iv. the prior oxidation of active areas of the electrode

The essential difference between mechanisms i and ii is that the latter requires the disruption of the silver lattice while the former does not.

The appearance of the 'preliminary' peak can be seen to be very dependent upon electrode pretreatment (Table III) Although the peak is enhanced by preliminary etching and cathodic reduction of oxide, the prior cathodic evolution of hydrogen at a mechanically polished surface does not increase the magnitude of the peak, which thus cannot be due to mechanism iii.

ASTLEY, HARRISON and THIRSK (6) observed for the deposition of metals onto substrates, similar double peaks, which they interpreted in terms of the deposition of a monolayer occurring at a lower energy of activation (i.e. mechanism i or ii). Table III shows that if an electrode, prepared under conditions that would enhance the formation of the 'pre-peak', is allowed to remain

Fig. 22 The Effect of Electrode Pretreatment on the P.S.V. Current Curves for Silver in 1.0M NaOH at 23°C. Potential Sweep Rate = 6×10^{-4}V sec^{-1}. A-Polish and Etch; B- Polish, Etch and Nold for 30 mins; C- Reduce an AgO Electrode; D- As C; hold for 14 hrs.

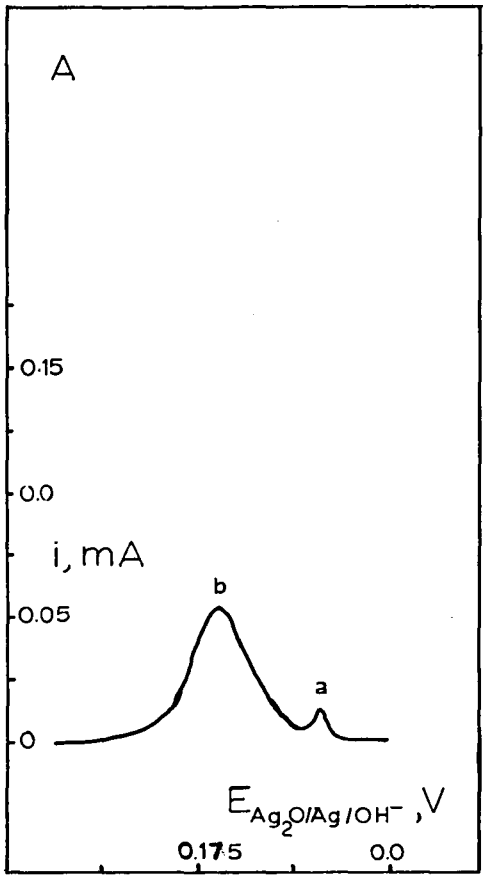
A
0.15
0.0
i, mA
b
0.05
a
0
$E_{Ag_2O/Ag/OH^-}$, V
0.175
0.0

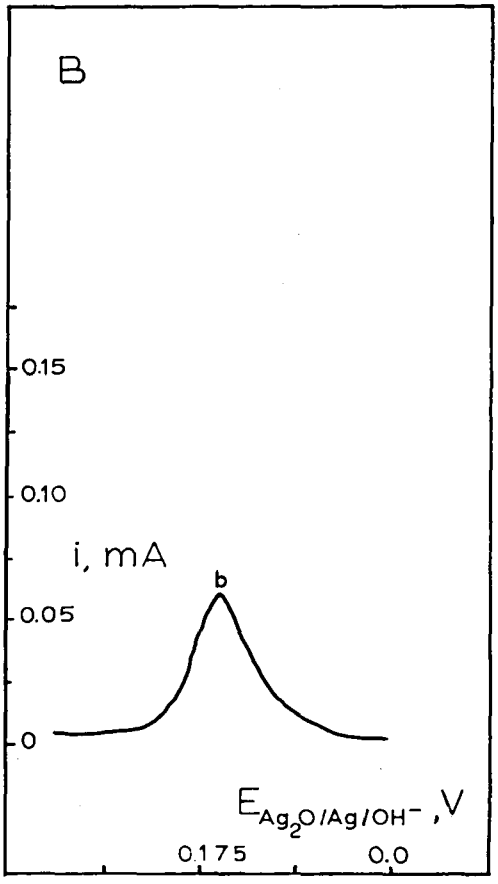
B
0.15
0.10
i, mA
b
0.05
0
$E_{Ag_2O/Ag/OH^-}$, V
0.175
0.0

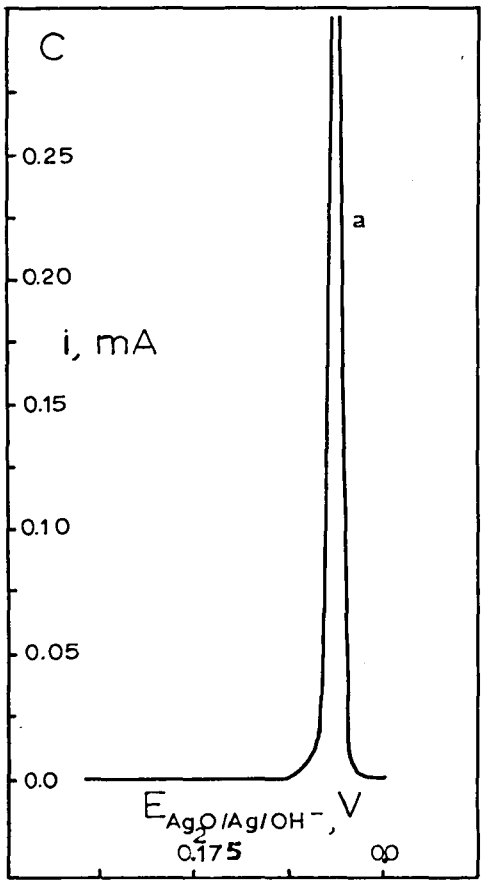
C
0.25
a
0.20
i, mA
0.15
0.10
0.05
0.0
$E_{Ag_2O/Ag/OH^-}$, V
0.175
0.0

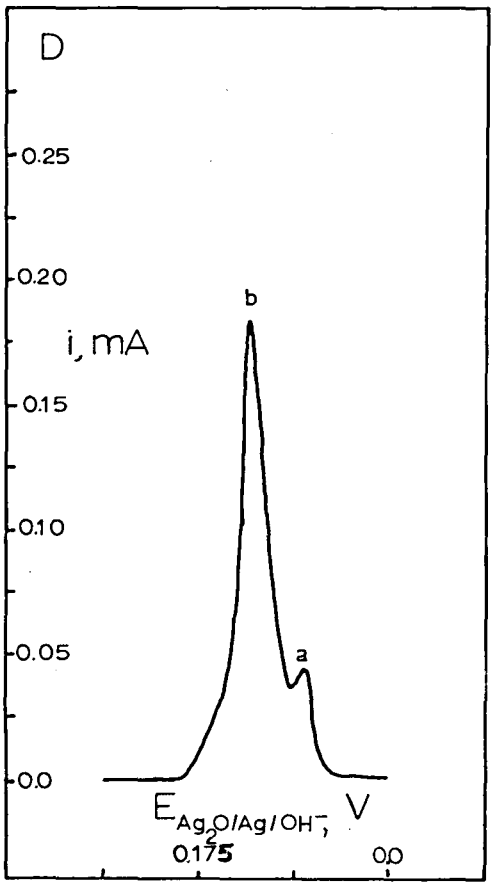
D
0.25
0.20
b
i, mA
0.15
0.10
a
0.05
0.0
$E_{Ag_2O/Ag/OH^-}$, V
0.175
0.0

TABLE III

The Effect of Electrode Pretreatment on the Potentiodynamic Current Curve for the Oxidation of Silver To Ag_2O in 1.0M NaOH, 23°C. Potential Sweep Rate = 6×10^{-4} V sec^{-1}. Electrode Area = $4.45 \times 10^{-2} cm^2$.

Pretreatment*	Peak 'a'		Peak 'b'		Total Charge
	Em, V**	Im, mA	Em, V**	Im, MA	mC
1	0.06	0.01	0.135	0.055	~5
2	0.06	0.02	0.135	0.06	~5
3	0.06	0.04	0.135	0.06	~5
4	—	—	0.135	0.05	~5
5	0.04	0.35	—	—	~8.5
6	0.06	0.02	0.110	0.18	~14

*Pretreatments
A:- Mechanical polish (on glass)
B:- Polish followed by cathodic Hydrogen evolution
C:- Polish and etch in 50% HNO_3
D:- Polish, etch and equilibrate in situ for 30 mins.
E:- Reduce AgO film
F:- As E then equilibrate in situ for 14 hrs

** W.R.T. the reversible $Ag_2O/Ag/OH^-$ potential

in contact with the electrolyte for long periods (10 - 20 mins for an etched electrode, > 12 hrs for a 'reduced oxide' electrode) the preliminary peak does not appear (see also Fig. 22). If mechanism i or ii is obeyed the electrode should exhibit a reversible AgOH/Ag/OH^- or Ag_2O/Ag/OH^- potential after such long electrolyte contact periods, as the non-appearance of the peak must be due to the prior spontaneous formation of AgOH or Ag_2O. This is not observed (Ch. 7.3.a.).

It would seem that mechanism iv represents the true behaviour of the electrode. The reduction of a completely oxidised electrode would result in a microporous silver surface (Ag - Ag distance in AgO = 3.28Å- and 2.39 Å, while in silver Ag - Ag distance = 1.44 Å (See Table I)) with the silver atoms exhibiting a lower than normal (CN = 12) average coordination. Such a microporous lattice would be energetically less stable then a normal lattice and would thus oxidise at a lower potential. Such surface 'activity' would be produced to a lesser degree on etching the electrode and would slowly decay as the surface recrystallises. This is the observed behaviour (Fig. 22).

7.4 The Kinetics of the Formation of Ag_2O at Low Electrode Coverages

7.4.a. Measurements near to the Equilibrium Potential

Perturbation measurements could not be made at low overpotential (< 10mV) for reasons discussed in Ch. 7.4.b.

Measurements of the A.C. impedance of silver Electrodes in 1.0M NaOH at the $Ag_2O/Ag/OH^-$ equilibrium potential were made. It was found that the reaction rate (indicated by C_{xs} at low frequencies) increased with time, reaching a stable level after ~10 hrs (Fig. 23).

This stabilisation process is of interest. The increase in apparent reaction rate with time might be due to the slow dissolution of a film at the electrode. Studies of the double layer structure (Ch. 6) do not indicate the presence of a surface film and consequently the increase in reaction rate must be caused by a surface roughening process. Such a process could be due to the dissolution/precipitation mechanism proposed for the initial formation of Ag_2O (98).

Attempts were made to fit faradaic impedance data to the simple C.T. impedance analogue (Fig. 8) and to more complex analogues involving alternative reaction paths (Appendix 5) using computerised optimisation techniques (Appendix 6). A satisfactory solution was not obtained for the three analogues tried, and it must be concluded that the exchange reaction is complex and is not under partial linear diffusion control, but probably involves adsorption of the electroactive species at the electrode. If the change in electrode impedance with time represents a surface roughening effect an anamalous

Fig. 23 Change in Electrode Impedance with Time at the Ag_2O/Ag equilibrium Potential 1.0M NaOH, 23°C.

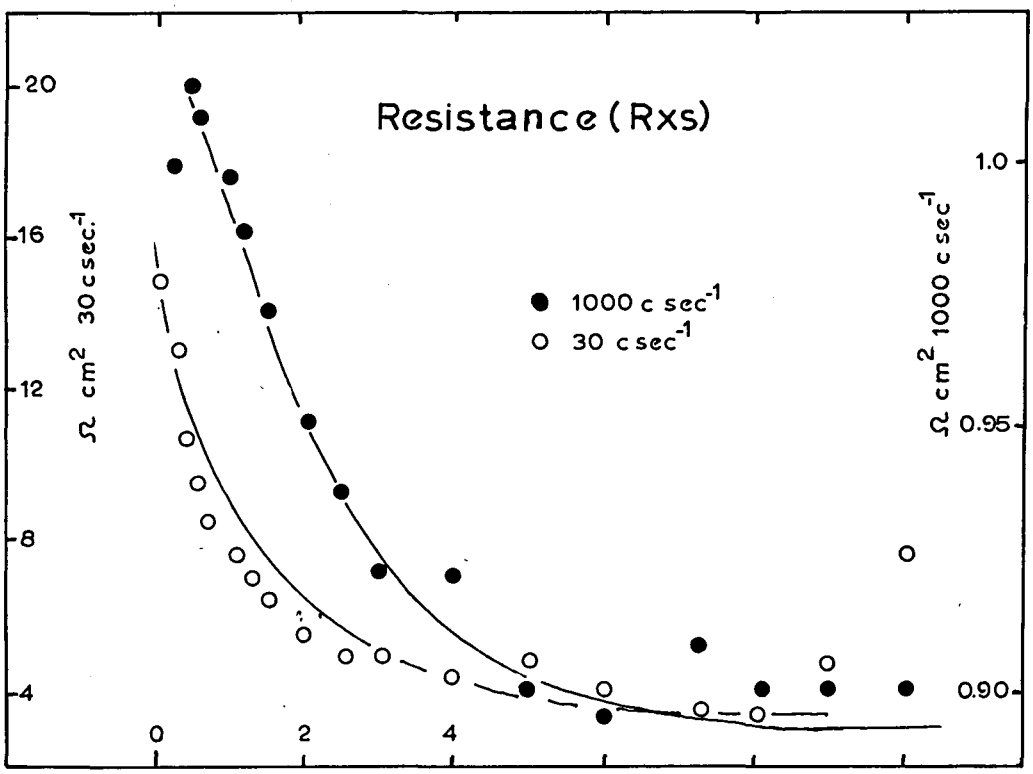
Resistance (Rxs)
20
16
12
8
4
0
2
4
1.0
0.95
0.90
Ω cm² 30 c sec⁻¹
Ω cm² 1000 c sec⁻¹
1000 c sec⁻¹
30 c sec⁻¹

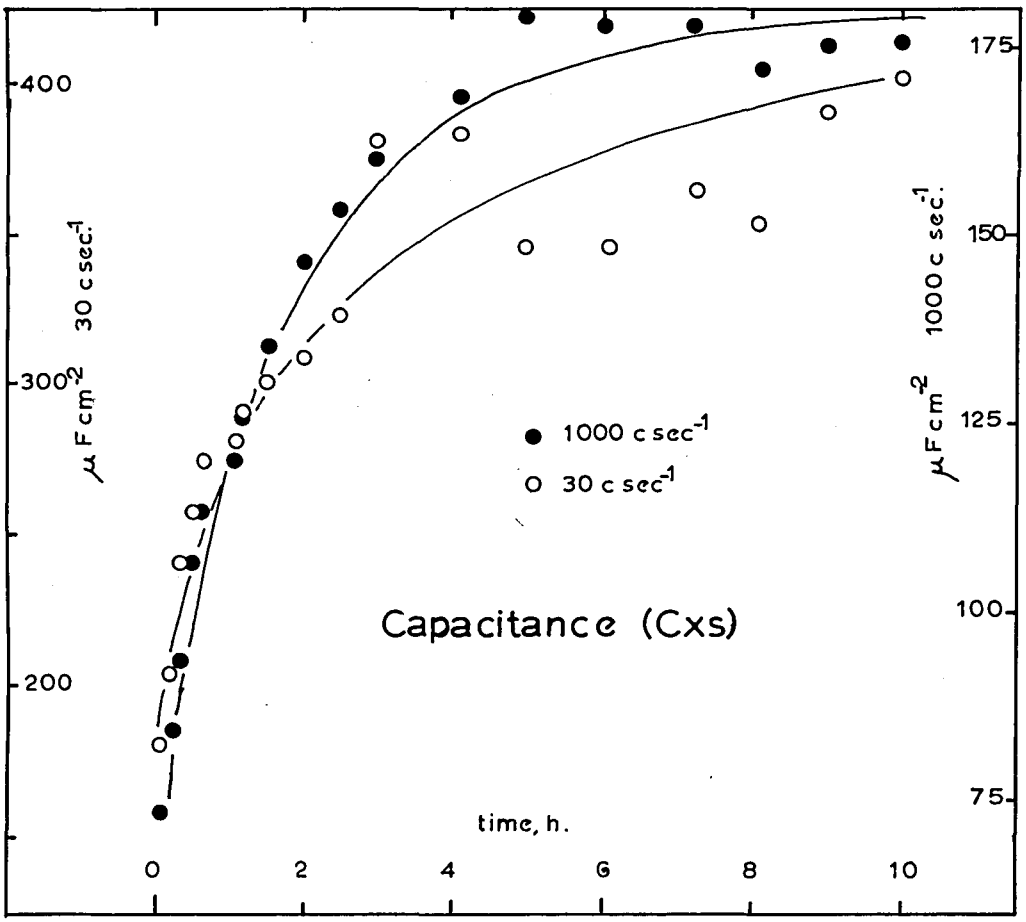
Capacitance (Cxs)
400
300
200
0
2
4
6
8
10
175
150
125
100
75
μF cm⁻² 30 c sec⁻¹
μF cm⁻² 1000 c sec⁻¹
1000 c sec⁻¹
30 c sec⁻¹
time, h.

frequency dispersion (51) will also result.

It would appear that the elucidation of kinetic parameters from faradaic impedance data for the Ag_2O/Ag exchange reaction is not possible using presently established techniques.

7.4.b. Measurements away from the equilibrium potential

The kinetics of the formation of Ag_2O in the Tafel region ($\eta > 50mV$) were studied using either galvanostatic or potentiostatic pulses applied to an equilibrated, clean (see Ch. 7.2.b.) electrode.

A typical galvanostatic potential-time curve is shown in Fig. 24. It is apparent that initially the electrode potential is at a value negative to the $Ag_2O/Ag/OH^-$ equilibrium potential (line A - B). The initial vertical gap in the trace is the pseudo-ohmic overpotential, η_Ω (Ch. 4.2.a.). The initial slope of the trace yields a value for C_L according to Equation [4.3]. Values calculated by this method ($C_L = 85 \pm 20\ \mu F\ cm^{-2}$) agree with the value ($\sim 80 \mu F cm^{-2}$) found by A.C. bridge techniques (Fig. 14). The rate of increase in potential is seen to decrease with time and does reach a constant value (Fig. 24). This linear η - t portion of the trace when extrapolated to t = 0 (see Ch. 4.2.a.) and corrected for η_Ω yields η_D, the activation overpotential. This method is applicable (at silver electrodes) only to the determination

Fig. 24 Typical Galvanostatic Potential-time Trace for the Formation of Ag_2O. Applied Current-Density = 46 $mAcm^{-2}$ 1.0M NaOH, 23°C. Line A-B represents the $Ag_2O/Ag/OH^-$ Equilibration Potential.

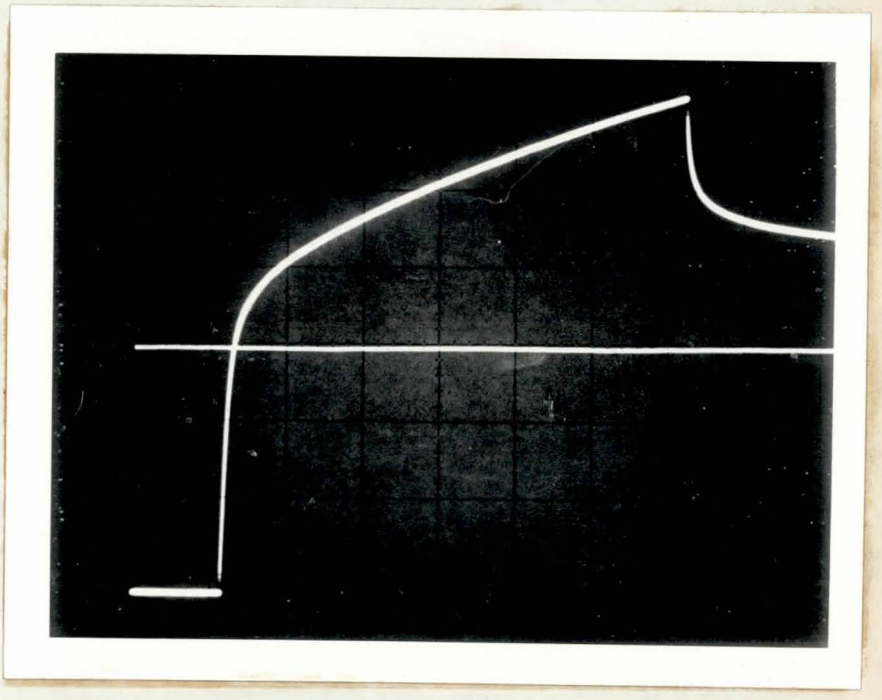

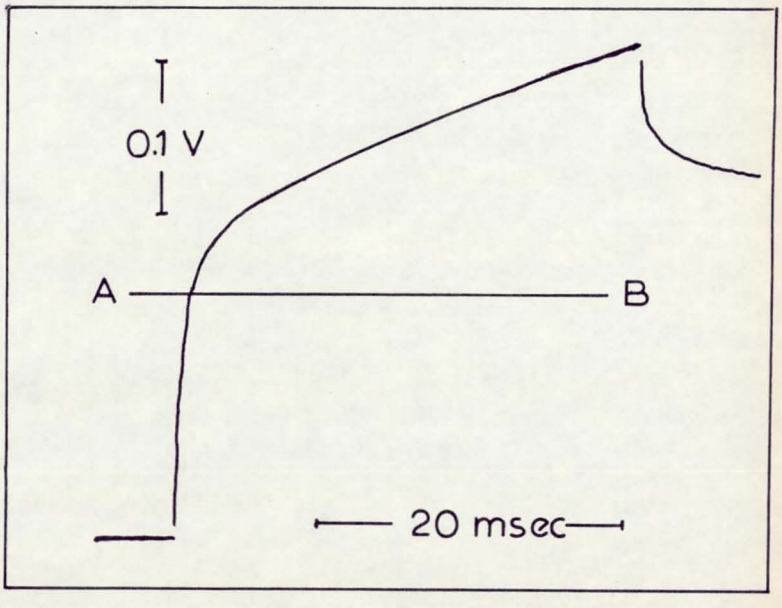
0.1 V
A
B
20 msec

of η_D - i data at high values of η_D. Low η_D values cannot be determined accurately as long times ($\gg$1 sec) elapse before the linear portion of the η - t curve is attained Data recorded over these long time intervals will be influenced by electrolyte migration and convection.

A typical potentiostatic current-time curve is shown in Fig. 25. The current varies as the reciprocal of time rather than as the expected $\sqrt{t}$ (Ch. 4.2.b.) function. Extrapolation of 1/i - t curves (Fig. 25) to t = 0 yields values for i corresponding to the applied potential. The potentiostatic technique can be used only at high overpotential due to the accuracy ($\pm$ 1 mV) of the potentiostat.

The Tafel plot comparing the potentiostatic and galvanostatic methods is shown in Fig. 26. The agreement between the two methods is good. Extrapolation of the linear portion of the curve to $\eta_D = 0$ yields the exchange current density, i_o, while its slope yields the charge transfer coefficient, α, according to Eq. [3.15]

A summary of the charge transfer parameters α and i_o obtained from a series of Tafel plots at different temperatures and $[OH^-]$ is given in Table IV.

It is immediately apparent that rational values for α, $(0<\alpha<1)$, are not obtained in every case if a value for n = 1 is used. A value for n = 2 will yield rational values for α.

Fig. 25. The oxidation of Silver to Ag_2O. Typical Potentiostatic current-time curve and derived reciprocal curve. Applied overpotential = 80mV, 23°C, 1.0M NaOH, 4.45×10^{-2} cm^2. On Photograph: Horiz. Scale = 0.2 m/sec/div. Vert. Scale = 0.165 mA/div.

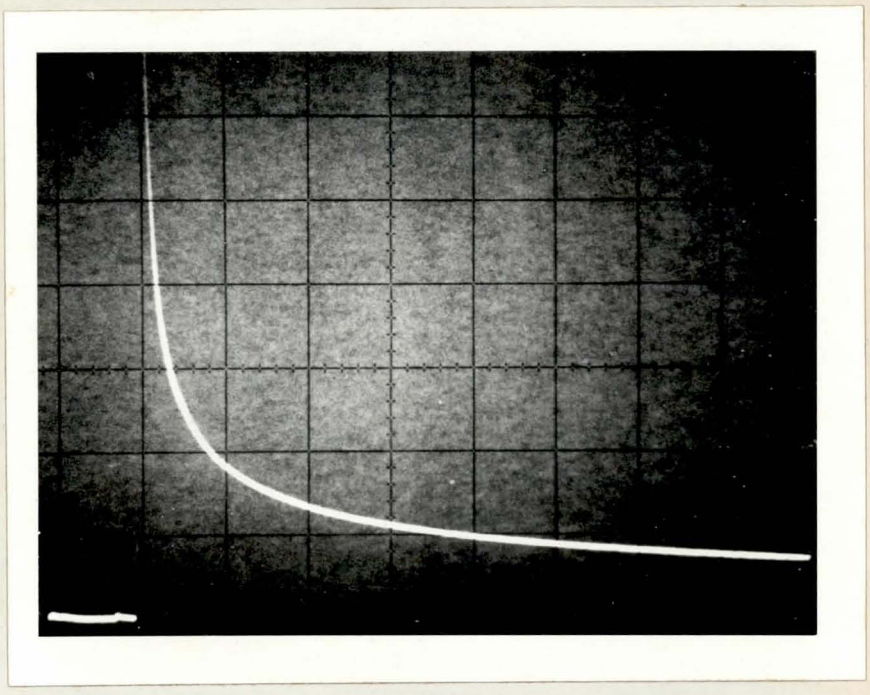

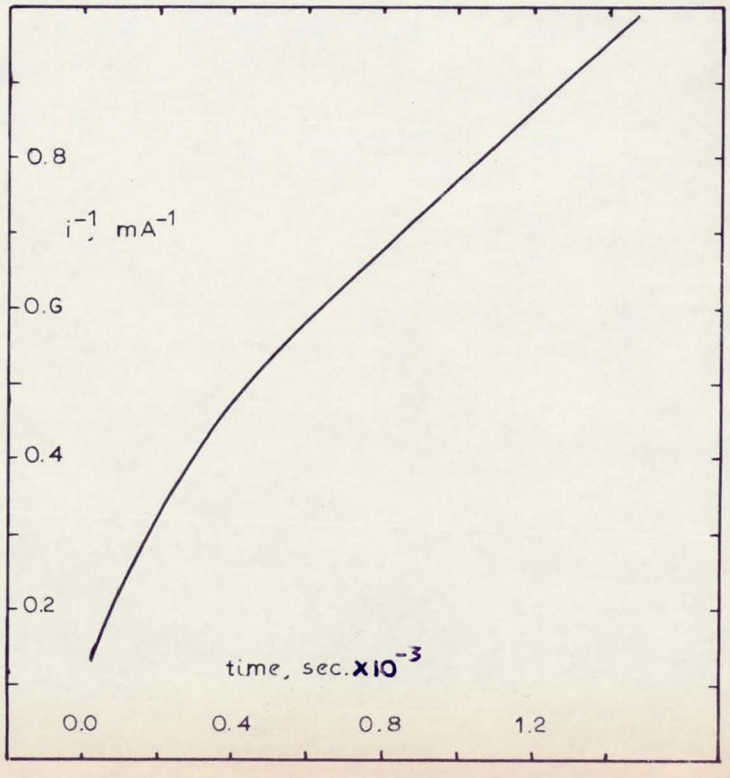
0.8
i^{-1}, mA^{-1}
0.6
0.4
0.2
time, sec. $\times 10^{-3}$
0.0
0.4
0.8
1.2

Fig. 26 Typical Tafel Plot for the Formation of Ag_2O in 1.0M NaOH at 23°C. Comparison of Potentiostatic and Galvanostatic Technique.

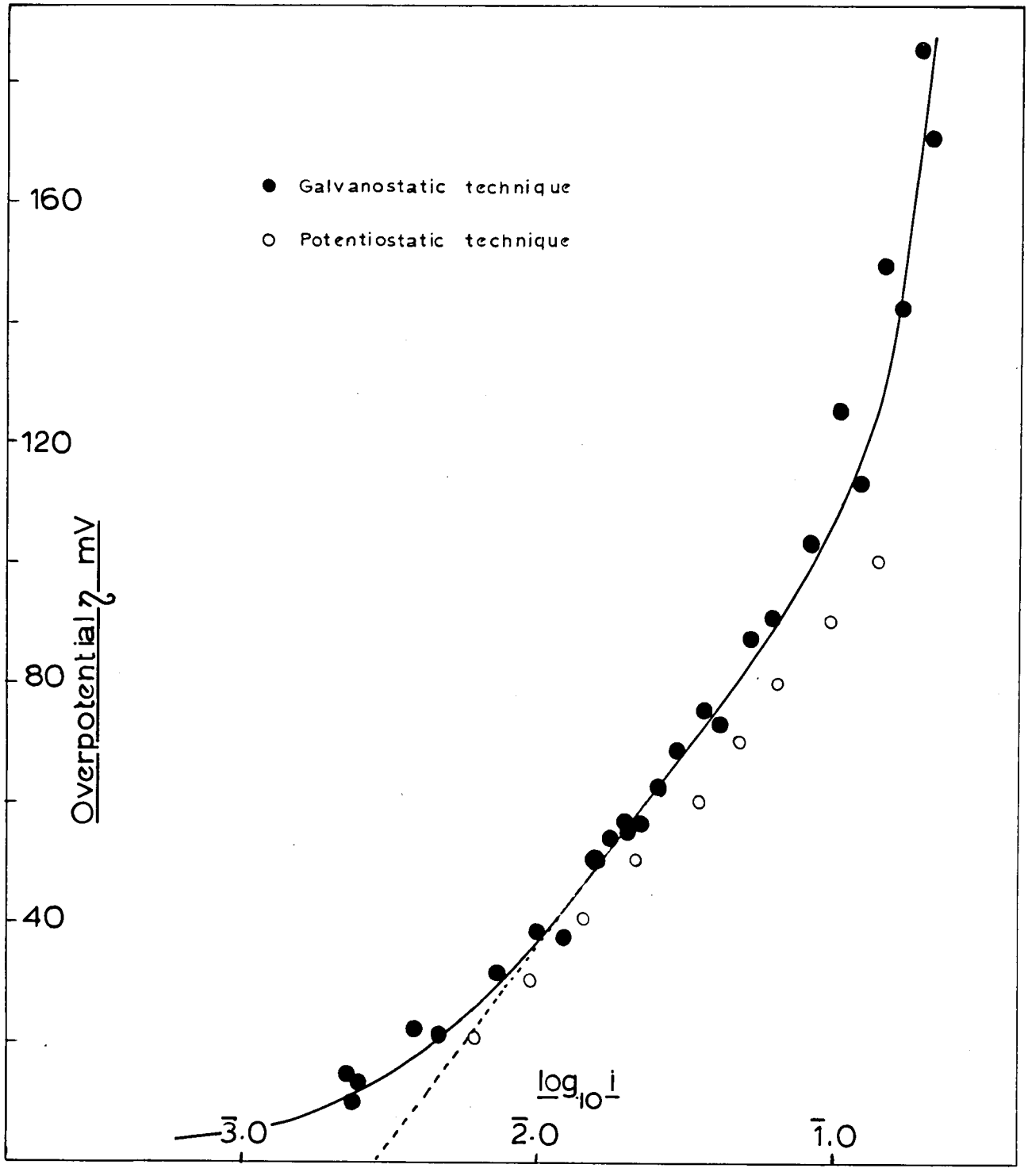
Galvanostatic technique
Potentiostatic technique
160
120
80
40
Overpotential η mV
log10 i
3̄.0
2̄.0
1̄.0

TABLE IV

The oxidation of Silver to Ag_2O. Summary of Results (36)

Temperature °K	OH^- Concentration* M	i_o mAcm^{-2}	$n(1-\alpha)$ (from Tafel slope)	α if n=1	α if n=2
273	1.0	1.0	0.74	0.26	0.63
296	1.0	2.8	0.90	0.10	0.55
313	1.0	3.0	1.2	-0.2	0.40
333	1.0	6.5	~1.2	-0.2	~0.4
296	0.10	0.95	0.50	0.50	0.75
296	0.28	1.41	0.69	0.31	0.66
296	1.0	2.8	0.90	0.10	0.55
296	4.86**	7.3	1.3	-0.3	0.35

*Total $[Na^+]$ = 1.0M (Except for **)

As n is the number of electrons transferred per unit rate determining reaction, a value for n = 2 means that the reaction process must be second order w.r.t. silver. (Silver exists as Ag^{I} in Ag_2O). This is in agreement with STONEHART (144) who used a P.S.V. technique.

For the formation of Ag_2O Eq. [3.16] now becomes:-

$$i_o = 2Fk^o \, C_{Ag}^{2\alpha} \cdot C_{OH^-}^{2\alpha} \cdot C_{Ag_2O}^{1-\alpha} \qquad [7.5]$$

Correlation of the dependence of i_o on $[OH^-]$ (Fig. 27) yields a value for α of 0.3. Clearly this inconsistent with the values for α calculated from the Tafel slope (see Table IV).

This inconsistency of the two methods (Tafel slope and concentration dependence) for the determination of α can be explained in terms of specific adsorption of OH^- at the electrode (134). If the concentration of OH^- at the electrode obeys a Freundlich isotherm (73):-

$$C_{OH^-}(ads) = C_{OH^-}^{1/P}(soln.) \qquad [7.6]$$

Equation 7.5 becomes (assuming $C_{Ag} = C_{Ag_2O} = 1$):-

$$i_o = k_1^o \cdot C_{OH^-}^{2\alpha/P} \qquad [7.7]$$

A value for the Freundlich exponent, P = 2 would give self consistent values for α. Specific adsorption of

Fig. 27. Dependence of i_o on $[OH^-]$ from Tafel Plot. data for the Oxidation of Silver to Ag_2O in 1.0M NaOH at 23°C.

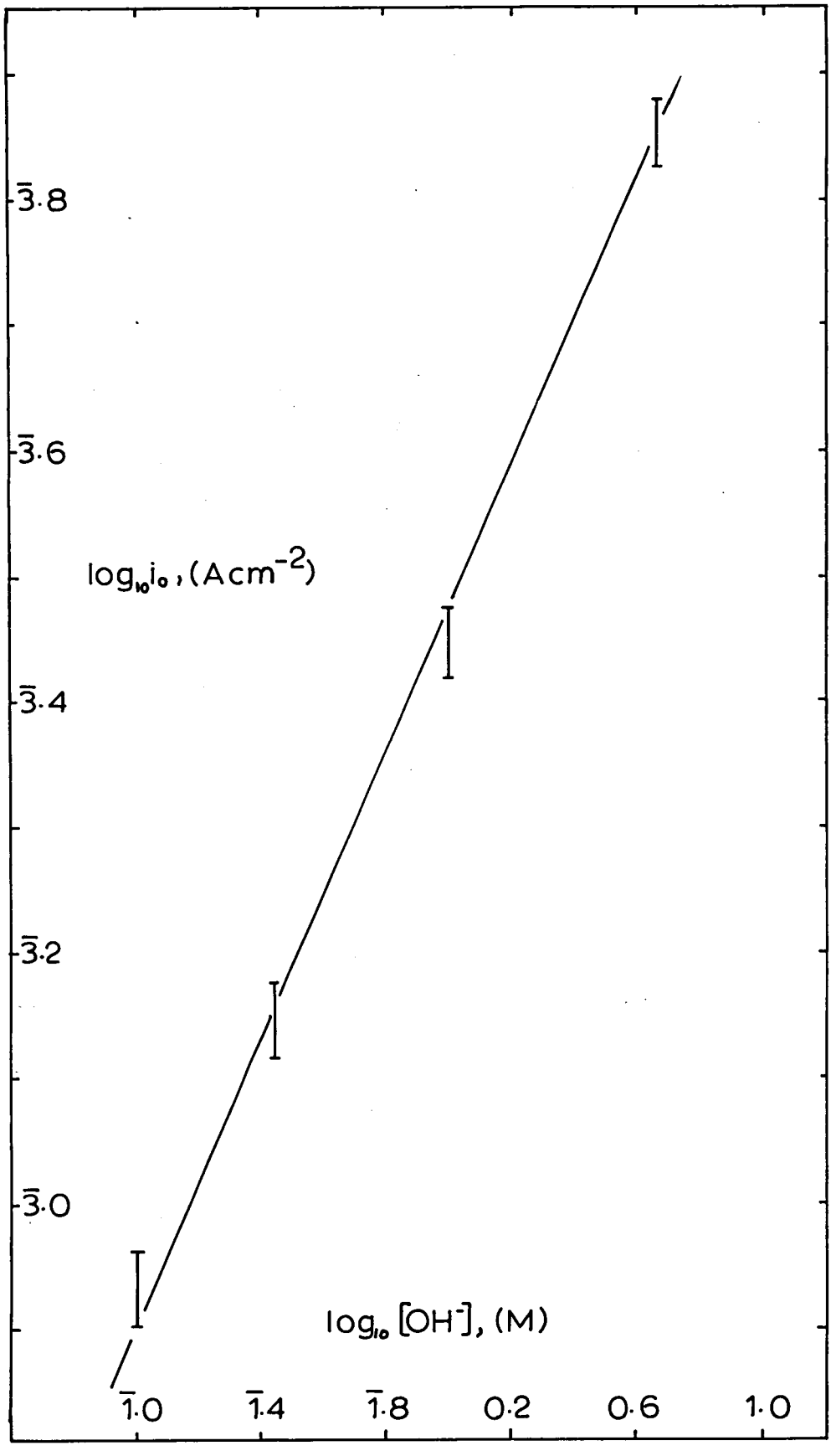
$\bar{3}.8$
$\bar{3}.6$
$\log_{10} i_o$, ($A cm^{-2}$)
$\bar{3}.4$
$\bar{3}.2$
$\bar{3}.0$
$\log_{10}[OH^-]$, (M)
$\bar{1}.0$
$\bar{1}.4$
$\bar{1}.8$
0.2
0.6
1.0

OH^- at the electrode would account for the variations of α with $[OH^-]$ and temperature (Table IV), and also the anomalous potentiostatic current-time dependence.

The dependence of i_o on temperature (Fig. 28) enables a value for ΔH^*, the enthalpy of activation, to be derived, according to the Arrhenius equation (1). From Fig. 28 a value is derived for the activation enthalpy, $\Delta H^* = 5.5 \pm 1$ kcal $mole^{-1}$. This value is lower than the accepted value for charge transfer reactions ($\sim$10 kcal $mole^{-1}$). Low values for the enthalpy of activation are a further indication of the adsorption of electroactive species at the electrode (59).

7.5 The Mechanism and Kinetics for the Formation of Thick Films of Ag_2O

Neither A.C. or perturbation methods can be used for the study of thick films of Ag_2O because of the high film resistance (103). P.S.V. techniques can be used under these conditions and have been applied to the study of silver oxide electrodes (38, 144, 145)

A typical potentiodynamic current curve for an equilibrated electrode is shown in Fig. 22B. The trace is in the form of a current peak which indicates that the reaction is self limiting. The potential, E_m, at which the maximum current flow is observed is ($>$50mV) more positive than the $Ag_2O/Ag/OH^-$ equilibrium potential and the charge transfer reaction is, under these conditions, irreversible.

For P.S.V. experiments under partial diffusion and

Fig. 28 Arrhenius Plot for the Formation of Ag_2O in 1.0M NaOH

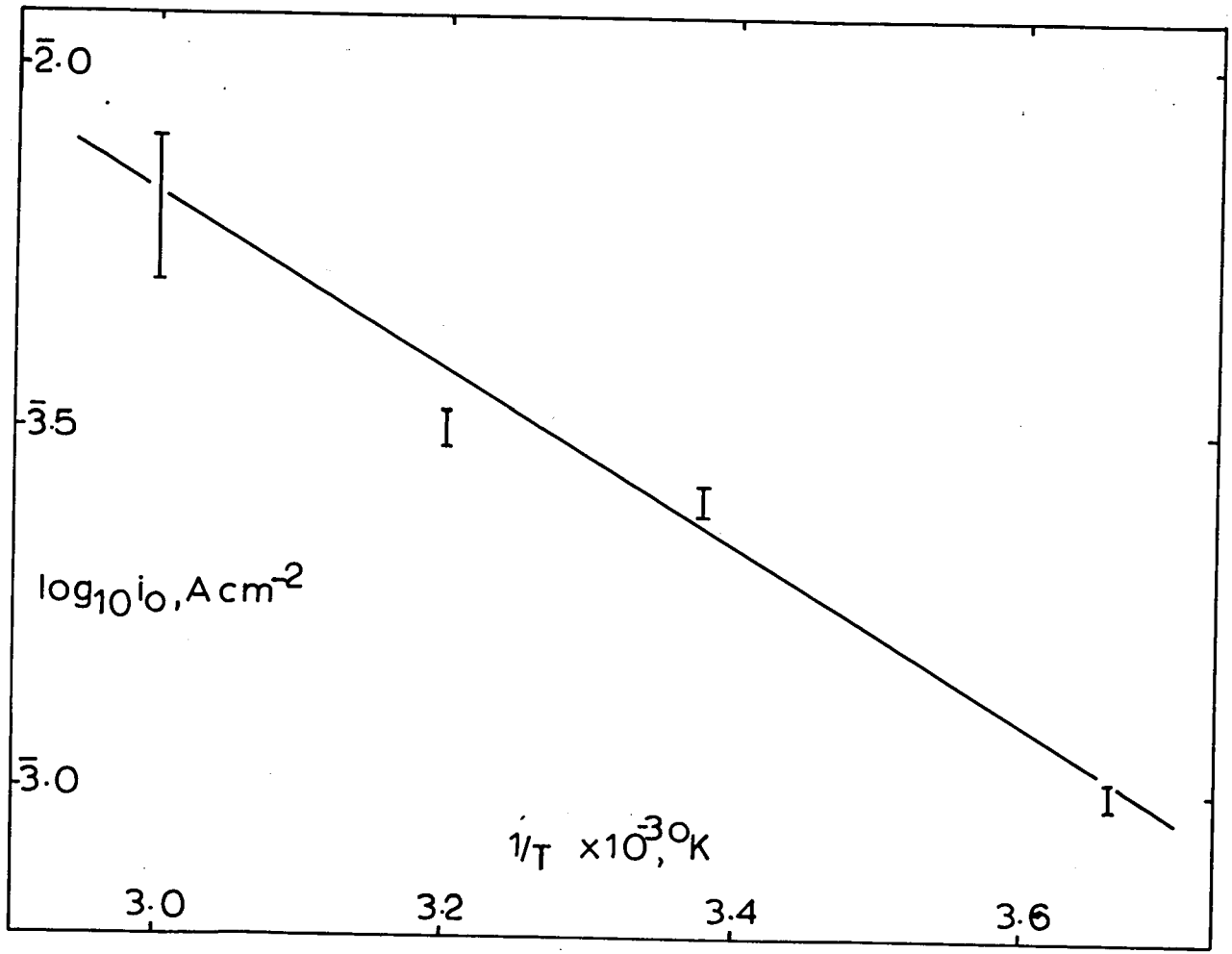
$\bar{2}.0$
$\bar{3}.5$
$\bar{3}.0$
$\log_{10} i_o$, A cm^{-2}
$1/T \times 10^{-3}$ °K
3.0
3.2
3.4
3.6

irreversible charge transfer conditions the parameters I_m and E_m obey Equations of the form (48, 122):-

$$I_m = K\, C_i n (\alpha n_a)^{\frac{1}{2}} \cdot v^{\frac{1}{2}} \qquad [7.8]$$

$$E'_m - E''_m = \frac{RT}{(1-\alpha)n_a F} \cdot \ln \sqrt{\frac{v''}{v'}} \qquad [7.9]$$

For the formation of Ag_2O, I_m varies linearly with $\sqrt{\text{potential sweep rate}}$ (Fig. 29), however, the slopes of these $I_m - \sqrt{v}$ plots are virtually independent of $[OH^-]$ (Table V). Thus although the reaction is under partial diffusion control it is not OH^- diffusion in the electrolyte. The diffusion reaction must be either Ag^+ or OH^-(or $O^=$) diffusing in the solid phase to either the Ag_2O/electrolyte interphase or the Ag/Ag_2O interphase. Such mechanisms have been proposed by FLEISCHMANN et al.(63), CROFT (46), TAKEHARA et al.(148) and KUKOZ et al.(100). P.S.V. experiments do not distinguish between the two mechanisms indeed the true diffusion process may be a combination of both in that the diffusion of lattice vacancies is probably the rate controlling mechanism.

The correlation of E_m - v data according to Eq. [7.9] is difficult due to the large error ($\pm$ 10mV) inherent in the measurement of E_m from current-potential curves. E_m -log v plots appear to give straight lines of slope $\sim$ 24mV (Fig.30) which gives a value for $(1-\alpha)n_a = 0.83$. If n_a is assumed

Fig. 29 Dependence of Peak Current, Im, on Potential Sweep Rate, v, (upper plot) and on $\sqrt{v}$ (lower plot). Silver in $NaOH/NaClO_4$ at 1.0M Na^+, 23°C. Electrode Area = 4.45×10^{-2} cm^2.

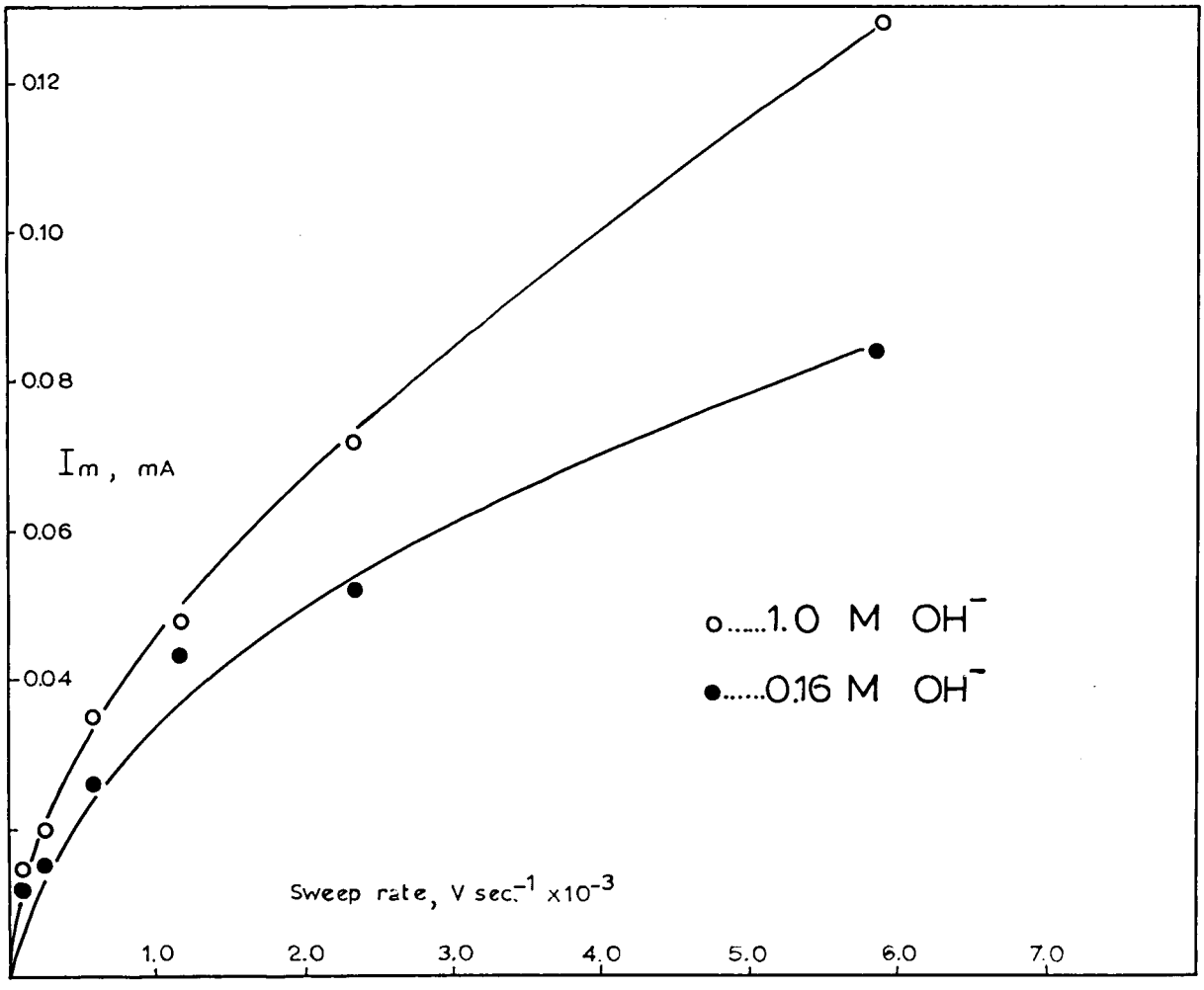
0.12
0.10
0.08
Im , mA
0.06
0.04
o.....1.0 M OH⁻
●.....0.16 M OH⁻
Sweep rate, V sec.⁻¹ x10⁻³
1.0
2.0
3.0
4.0
5.0
6.0
7.0

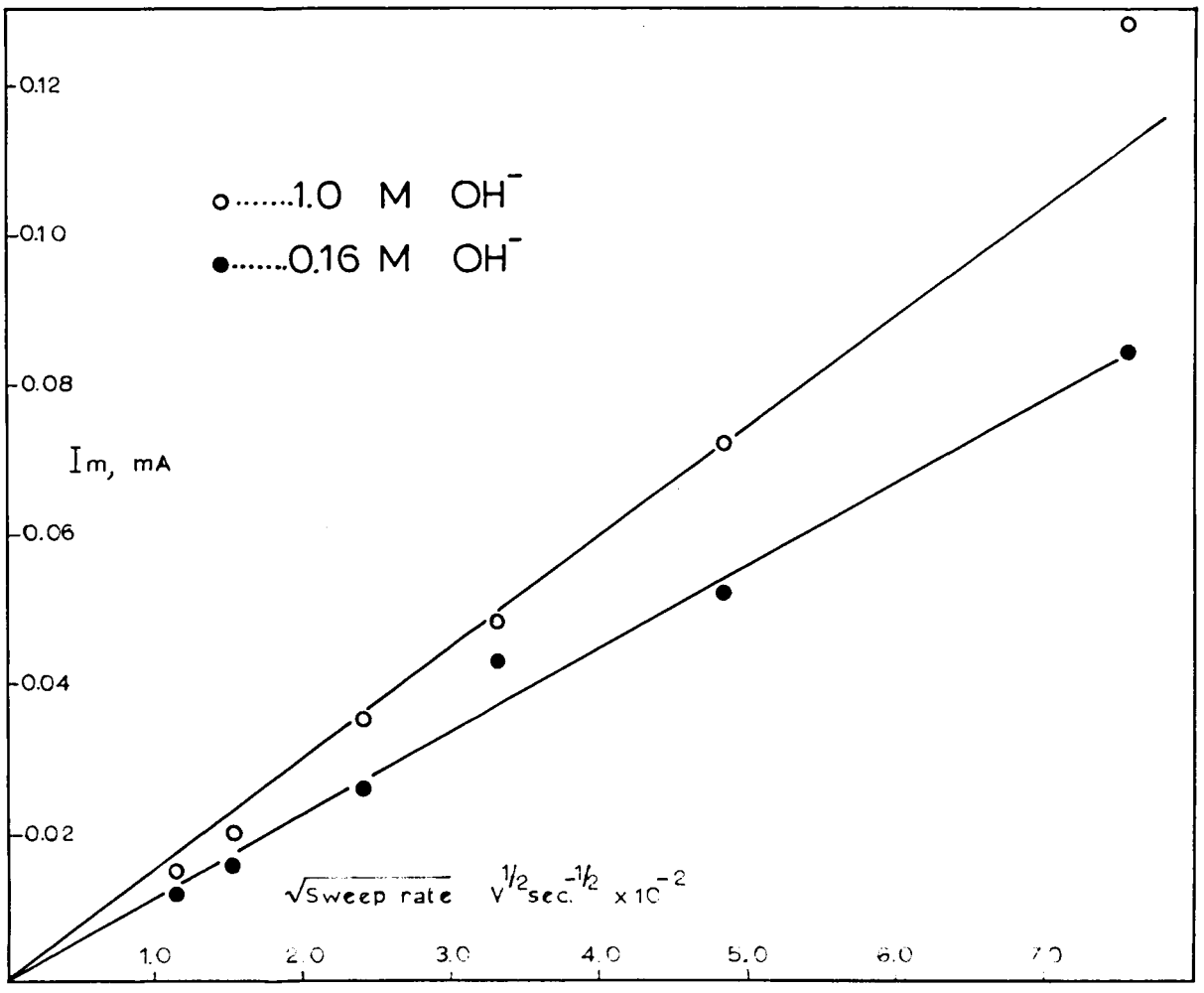
0.12
o.....1.0 M OH⁻
0.10
●.....0.16 M OH⁻
0.08
Im, mA
0.06
0.04
0.02
√Sweep rate V^1/2 sec.^-1/2 x10⁻²
1.0
2.0
3.0
4.0
5.0
6.0
7.0

Fig. 30 The Dependence of the Potential of the Current Maximum for Silver on Sweep Rate and $[OH^-]$ 23°C, Electrode Area = 4.45×10^{-2} cm^2.

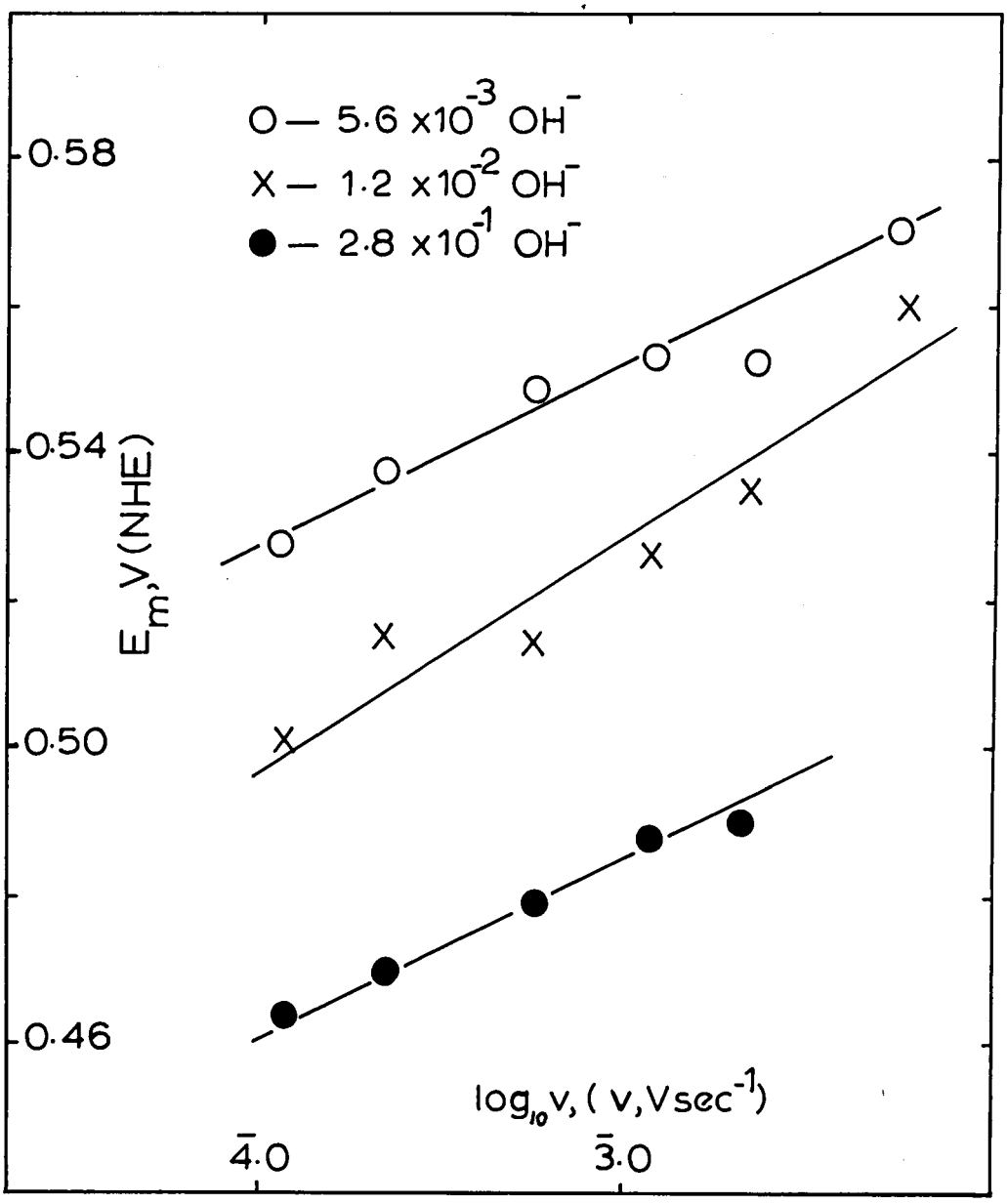
O — 5.6 x10^-3 OH^-
X — 1.2 x10^-2 OH^-
● — 2.8 x10^-1 OH^-
0.58
0.54
0.50
0.46
E_m, V (NHE)
log_10 v, (v, V sec^-1)
4̄.0
3̄.0

TABLE V

The Dependence of the Slope of I_m vs $\sqrt{v}$ curves on OH^- Concentration. Electrode area = 4.45×10^{-2} cm^2. 23°C Total $[Na^+]$ = 1.0M.

OH Concentration	$\frac{\partial I_m}{\partial \sqrt{v}}$
M	mA $sec^{\frac{1}{2}}$ $V^{-\frac{1}{2}}$
5.6×10^{-3}	0.96
1.0×10^{-2}	0.96
1.2×10^{-2}	0.99
2.0×10^{-2}	0.98
1.2×10^{-1}	0.87
1.6×10^{-1}	1.11
2.8×10^{-1}	1.11
1.0	1.50

to be 2 (see Ch. 7.4.b.) a value for the charge transfer coeffient, α = 0.59 is deduced which agrees well with the value for α at low Ag_2O coverages (Ch 7.4.b.) and with the value (α = 0.68) reported by STONEHART (144).

The area of the current-potential (time) peak indicates that the reaction ceases ofter the oxidation of ~100 atomic layers of silver. CAHAN et al (34) deduced a similar value (50 - 100 atomic layers). Such a thick film would have considerable electrical resistance ($> 10^2 \Omega cm^{-2}$ when dry) even when moist. This resistance represents, under galvanostatic conditions, a potential drop sufficient to cause the oxidation of Ag_2O to AgO to start at the Ag_2O/electrolyte interphase and this reaction then proceeds to completion.

7.6 The Mechanism and Kinetics for the Oxidation of Ag_2O to AgO

The study of the oxidation of Ag_2O using galvanostatic techniques is difficult since the potential-time curve (see Fig. 18) is very complex. Potential measurements are not reliable until effects due to the "superpolarisation" peak have subsided (~ 1-5 sec) and as a consequence, transient responses are of little value.

Rising potentiostatic current-time curves show that the electrode reaction is controlled by an electrocrystallisation process. These transients rise in accordance with a

time cubed law (Fig. 31). If a carefully controlled 'L' double potential pulse is applied to the electrode current-time curves which obey an $i \propto t^2$ law are given (Fig. 32). Comparison with Eqs. [3.20] to [3.25] shows that the reaction mechanism is controlled by slow nucleation and 3-D growth. The slopes of the $i-t^3$ and $i-t^2$ curves at 130mV overpotential (Figs. 31 and 32) yield a value for A, the nucleation exponent, of $\backsim 2 \times 10^{-3}$ sec^{-1} at this potential. Reproducible $i - t^2$ plots are relatively difficult to obtain possibly because of the difficulties inherent in producing a reproducible Ag_2O surface.

The slopes of $i-t^3$ curves are very dependent on electrode potential, obeying a Tafel type law at low (<200mV) overpotential (Fig. 33). A 'Tafel' slope of $\backsim$ 15mV is observed.

These results agree substantially with those of FLEISCHMANN, LAX and THIRSK (64) who have studied this reaction in detail.

7.7 Kinetic Consideration Concerning the Use of Silver Oxide Electrodes in Electrosynthesis

Two types of electrosynthesis process have to be considered.

7.7.a. Chemical Processes

If the organic oxidation rate is controlled by a chemical process the electrode reaction will be a chemical

Fig. 31 The Potentiostatic Oxidation of Ag_2O to AgO using a Single Potential Pulse. Rest Potential = 0.550 V (vs. $Ag_2O/Ag/OH^-$(1M), 23°C, 1.0M NaOH

Fig. 32 The Potentiostatic oxidation of Ag_2O to AgO Using a Double Potential Pulse. Conditions as in Fig. 31.

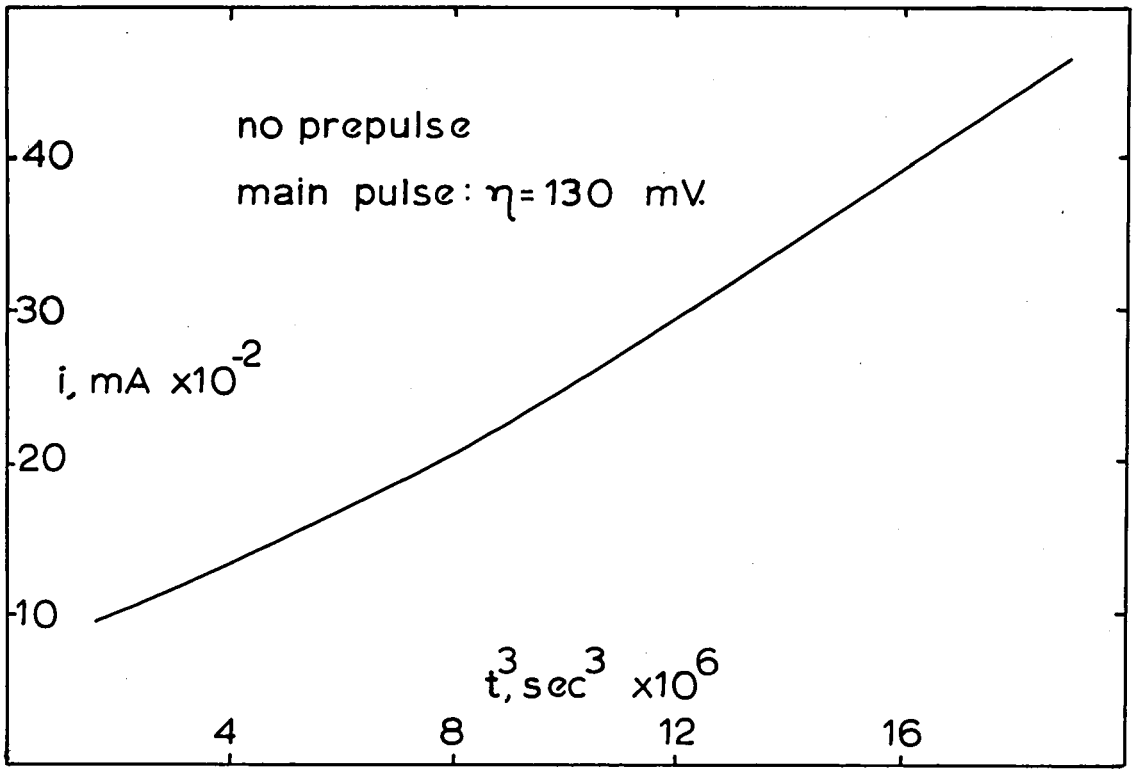
no prepulse
main pulse: η = 130 mV.
40
30
20
10
i, mA x10^-2
t^3, sec^3 x10^6
4
8
12
16

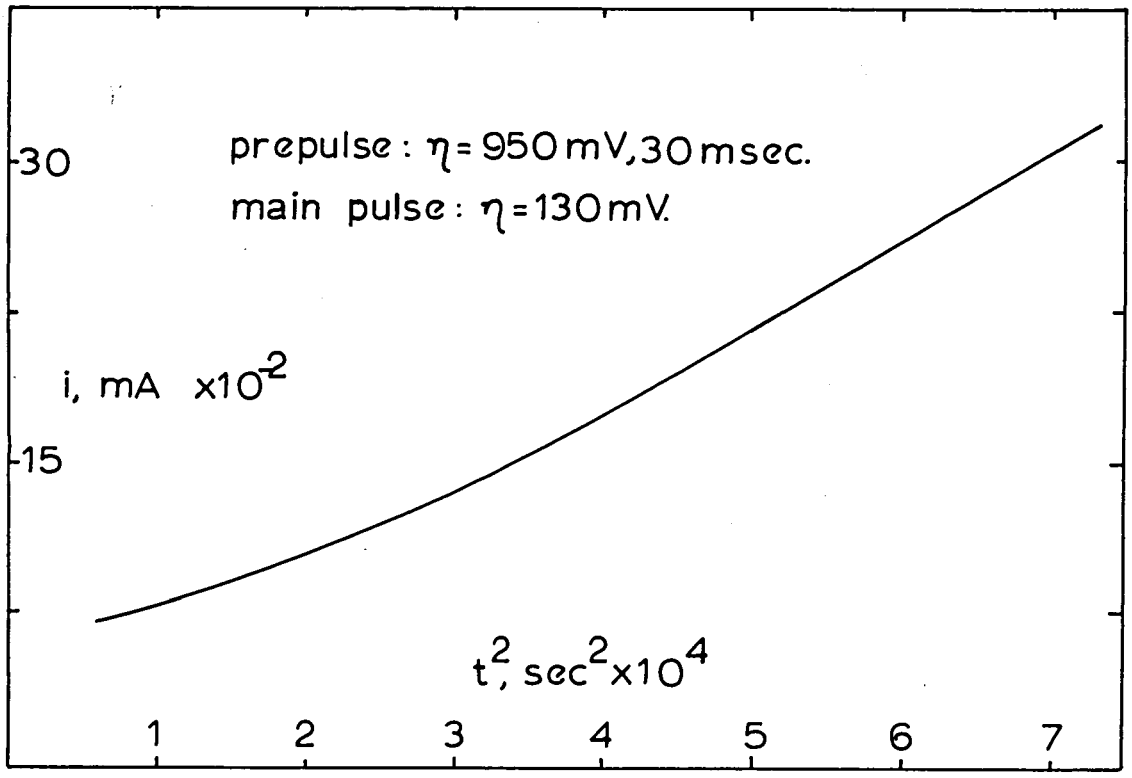
prepulse: η = 950 mV, 30 msec.
main pulse: η = 130 mV.
30
15
i, mA x10^-2
t^2, sec^2 x10^4
1
2
3
4
5
6
7

Fig. 33 The Oxidation of Ag_2O to AgO. Dependence of the Parameter di/dt^3 on the applied Overpotential.

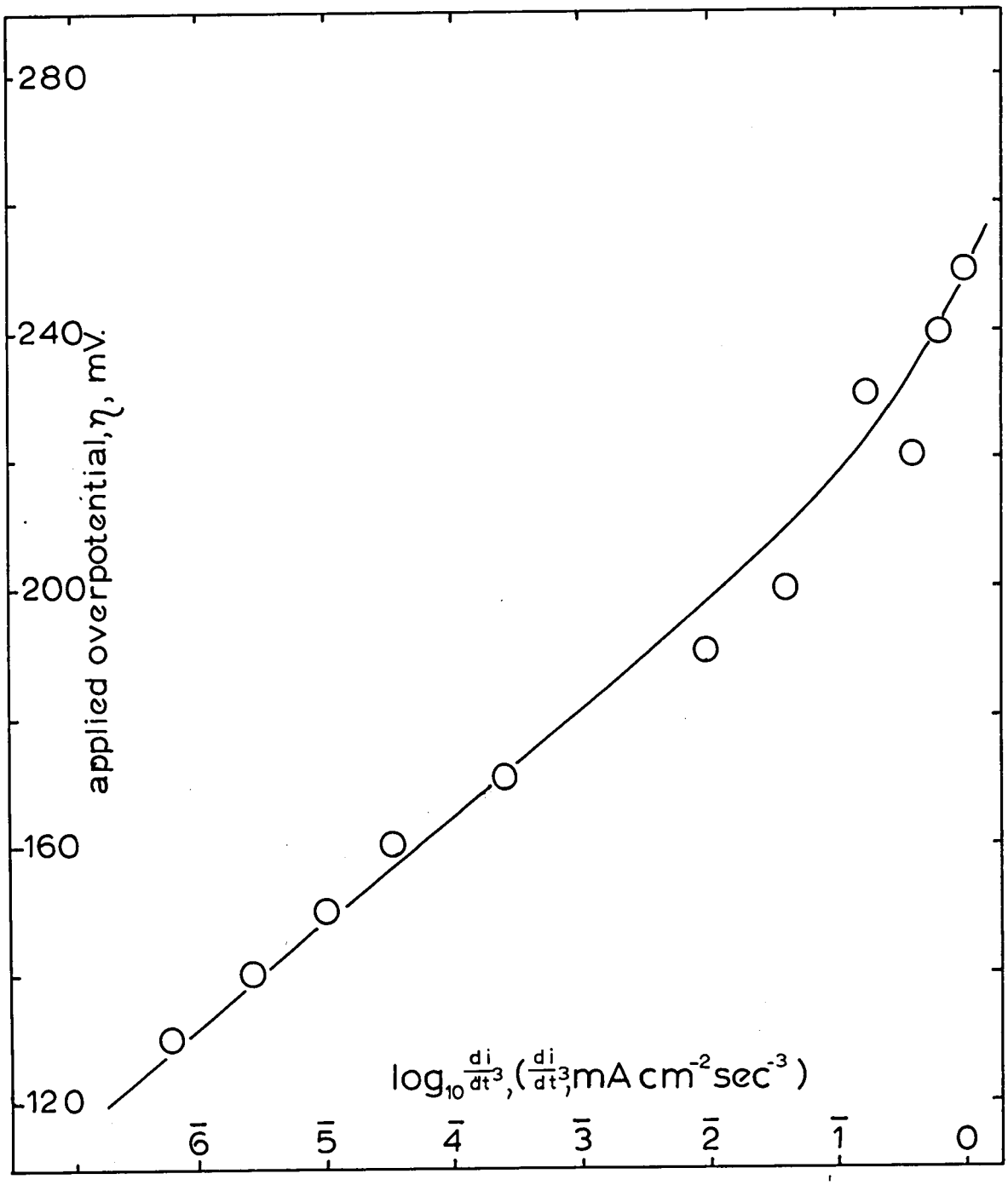
280
240
200
160
120
applied overpotential, η, mV.
$\log_{10}\frac{di}{dt^3}$, ($\frac{di}{dt^3}$; mA cm^{-2} sec^{-3})
6̄
5̄
4̄
3̄
2̄
1̄
0

reaction involving electrochemical regeneration of one of the reactants. The reaction is thus likely to change mechanism abruptly as the electrode potential is moved to higher anodic values and the basic electrode reaction changes from the formation of Ag_2O to the formation of AgO. However the organic oxidation mechanism will not change with potential within a potential region.

Whether the reaction involves Ag_2O or AgO the kinetics will be very difficult to interpret using electrochemical measurements since both the Ag_2O and AgO formation reactions are potential and time dependent.

7.6.b. Electrochemical Processes

If the organic oxidation rate is controlled by an electrochemical process the reaction mechanism might change at the Ag_2O/AgO transition potential due to a catalytic effect: but within each potential region the reaction rate will vary with potential in the classical manner. The overall mechanism might also change. If the organic oxidation rate is slower than the oxidation of silver the kinetics will be amenable to elucidation by electrochemical methods, although at Ag_2O electrodes the resistive properties of Ag_2O will cause difficulties. (See Ch. 5).

CHAPTER 8

The Oxidation of Organic Compounds at Silver Oxide Electrodes

8.1. Introduction

The electrochemical oxidation of organic compounds, of interest as a source of electrical power (8) and of potential commerical significance as a synthetic process, has been studied mainly at platinum electrodes. (127).

At present, the only anodic syntheses of probable commercial significance are coupling reactions (95). Synthetic oxidations of aromatic compounds are generally non specific (156) and yield polymers, while the oxidation of aliphatic alcohols yields oxides of carbon. Anodic oxidation of aliphatic amines at platinum yields compounds resulting from the cleavage of the C-N bond, although at very low reaction rates (13).

Commercially significant oxidations will probably involve the formation of C to X bonds (where X is an electronegative species e.g. oxygen) and thus aqueous solvents might be a requirement, together with catalytically active electrodes to ensure rapid reaction rates.

Silver in its high valency states is useful reagent for the oxidation of organic functional groups (9, 10, 104, 147) and is a catalyst in synthetic chemical processes (61) and in fuel cell electrodes. It would seem that a silver oxide anode might posess specific electroactivity.

8.2 Experimental

8.2.a. Electrochemical Oxidations

Fig. 34 Repetitive Potential Pulse Characteristics.

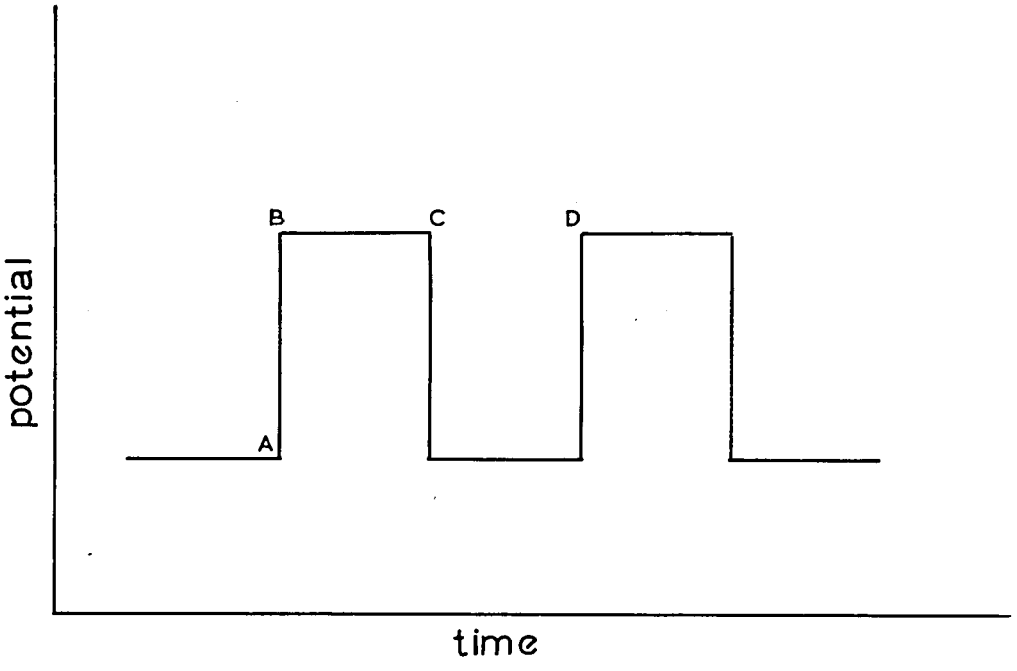

Step Height = AB

$$\text{Frequency} = \frac{1}{BD}$$

$$\text{Duty Ratio} = \frac{BC}{BD} \times 100\,\%$$

All experiments were carried out under conditions of controlled potential. For certain mechanistic studies a repetitive potential pulse sequence (Fig. 34) was applied to the electrode but the majority of experiments were at constant potential (usually between 0.6 and 0.8 V N.H.E.)

Cells of Type III (Appendix I) were used in conjunction with a working electrode of area ~ 2 cm^2 (Appendix 3). Reference electrodes were either $Ag_2O/Ag/OH^-$ (1.0M) (Appendix 2) or standard Sat. Cal. reference electrodes.

Electrolytes were generally 1.0M NaOH with known concentrations of the organic compound. Organic compounds (B.D.H. Ltd.) were distilled immediately before use. The electrolytes were saturated with and under an atmosphere of nitrogen.

Experiments were run until 50 -100 coulombs had passed to obtain sufficient product for reliable analysis.

8.2.b. Analysis

Organic components of the electrolytes were extracted into diethyl ether at the finish of each experiment. Volatile products were purged from the cell with nitrogen and trapped in either Br_2/CCl_4 (for alkenes) or 2.4 di-nitrophenylhydrazine (for aldehydes and ketones).

Analyses were carried out using g.l.c. (Pye 104). Unknown compounds were identified by comparison with authentic samples on at least two different stationary phases. Quantitative determinations were made from

comparison of integrated peak areas with that for a suitable internal standard. Quantitative results were accurate to within $\pm$ 5% except for the more volatile reaction products.

8.3 The Oxidation of Alcohols

The oxidation of alcohols proceeded very slowly at an AgO electrode at Potentials below that at which evolution of oxygen becomes the dominant reaction (+ 0.8 V N.H.E.)

Oxidation of isopropanol (1.0M in 1.0M NaOH) proceeded at a current density $\ll 1 mAcm^{-2}$ at 0.70 V(N.H.E.), and was not significantly affected by electrolyte agitation. The unique product was acetone, produced in ~100% coulombic yield. Other alcohols behaved in a similar manner.

8.5 Results and Discussions:- The Oxidation of Aliphatic Amines

8.4.a. Primary Amines

Only amines up to C_4 could be studied since higher molecular weight amines had very low solubility in the supporting electrolyte solution.

The amines were oxidised rapidly at a rate apparently controlled by diffusion. (Agitation of the electrode increased the current considerably). It was difficult to control the agitation and, as a consequence reaction rates and relative product yields were not very reproducible. There was, in addition, a continuous background reaction, namely the formation of a silver^{I} - amine complex (see Ch. 9.4.a.), and valid kinetic data could not therefore be made.

TABLE VI

The Oxidation of Primary Aliphatic Amines in 1M NaOH at an AgO Electrode at 23°C. 0.74 V N.H.E.

Amine	Products
n-Propylamine	n-Propionitrile
n-Butylamine	n-Butyronitrile, n-Butyraldehyde
iso-Butylamine	iso-Butyronitrile, iso-Butraldehyde
iso-Propylamine	Acetone
sec-Butylamine	Methyl-Ethyl-Ketone
tert-Butylamine	t-Butanol, 2 methyl-Prop-1-ene, 2-methyl-2-nitro-Propane

TABLE VII

The Effect of Chemical Parameters on the Oxidation of n-Butylamine in NaOH at an AgO electrode at 23°C 0.74 V N.H.E.

Concentration		Aldehyde: Nitrile ratio
Amine	$[OH^-]$	
$4x10^{-1}M$	0.5M	0.01
$4x10^{-1}$	1.0M	0.02
$4x10^{-1}M$	2.0M	0.55
$4x10^{-1}M$	4.0M	8.00
$2x10^{-1}M$	1.0M	0.05
$4x10^{-1}M$	1.0M	0.02
$8x10^{-1}M$	1.0M	0.01

TABLE VIII

The effect of Electrode Potential on the Oxidation of n-Butylamine at AgO electrodes 5.0M $[OH^-]$, 4×10^{-1}M amine 23°C

Potential V N.H.E.	Ratio of Aldehyde:Nitrile
0.64	9.0
0.74	0.1

The products of the oxidation of primary amines are given in Table VI. It is immediately apparent that the oxidation products are dependent on the substitution of the α carbon atom. The oxidations of n-butylamine and n-propylamine are of particular interest as the major product in each case is the nitrile which contrasts with the processes occurring at a platinum anode (13). Aldehyde can be produced, at AgO electrodes, from amines having 2α-Hydrogen atoms, only under carefully controlled chemical (Table VII) and electrochemical (Table VIII, Fig. 35) conditions. The ratio of aldehyde: nitrile in the oxidation products was found to increase with increasing $[OH^-]$ and to decrease with increasing [amine] and electrode potential (Table VII and VIII).

The dependence of the aldehyde:nitrile ratio on the chemical and electrochemical parameters suggests that the overall oxidation mechanism (for amines with 2α-H atoms) is branched, with only one branch involving further electrochemical reaction. Comparison with the products formed from amines with alkyl substitution at the α-C atom suggests that the overall reaction scheme is of the form depicted in Fig. 36. It is postulated that the branch in the (primary) reaction mechanism occurs at an imine species (III), which can be hydrolysed (giving aldehyde) or further oxidised (giving nitrile). Such a species would possibly have a longer life than one of the charged intermediates shown (e.g. II or IV) and thus

Fig. 35 Repetitive Potential Pulse Oxidation of n-Butylamine. Effect of Pulse Parameters on the Relative Yields of Aldehyde and Nitrile. 1.0M NaOH, 4×10^{-1}M amine, 23°C. Pulses rise from +0·600V N.H.E.

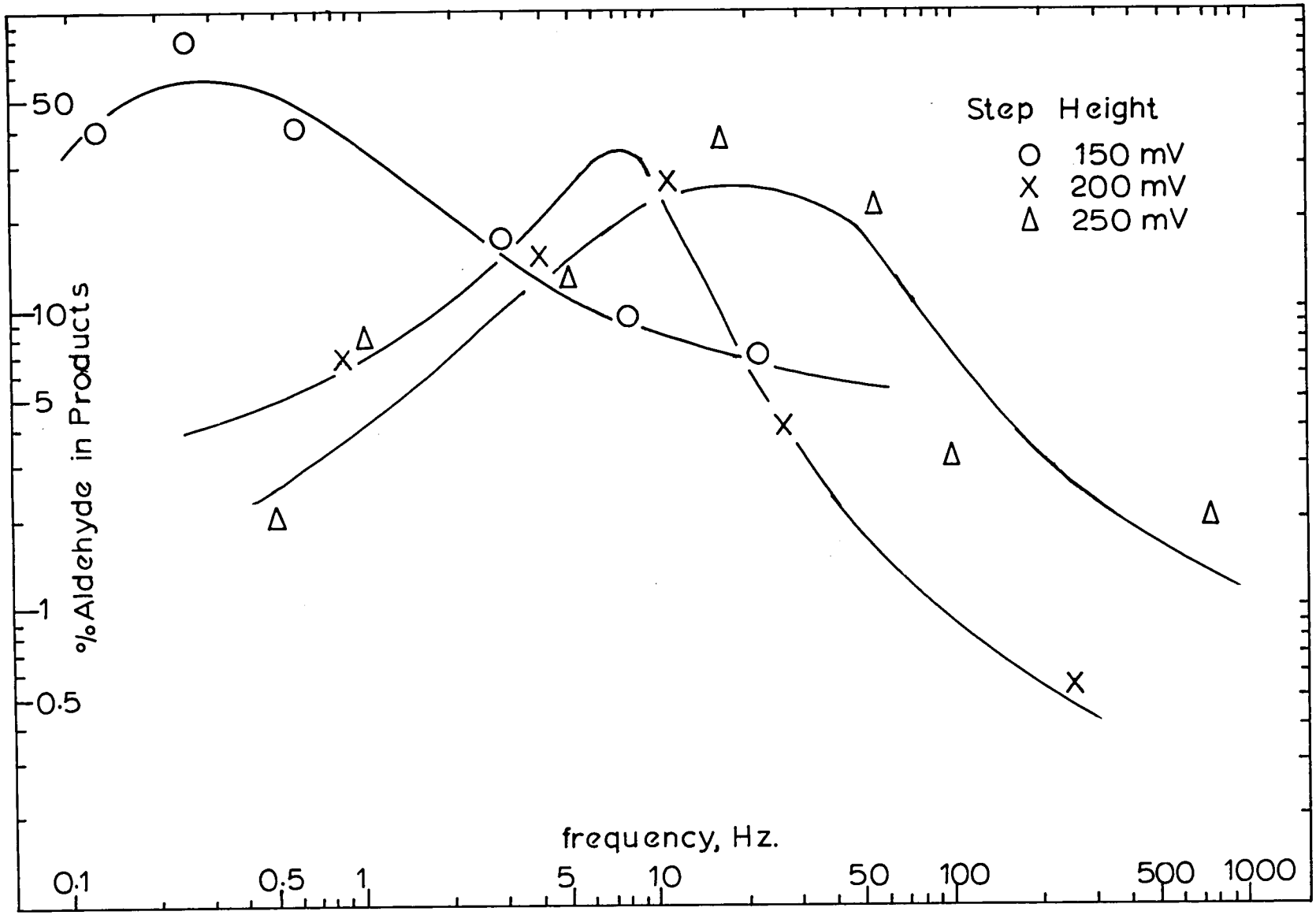
Step Height
O 150 mV
X 200 mV
Δ 250 mV
% Aldehyde in Products
50
10
5
1
0.5
frequency, Hz.
0.1
0.5
1
5
10
50
100
500
1000

Fig. 36 Proposed Reaction Mechanisms for the Oxidation of Aliphatic Primary Amines at AgO. Effect of Aliphatic Substitution at the ∝-C Atom

Primary

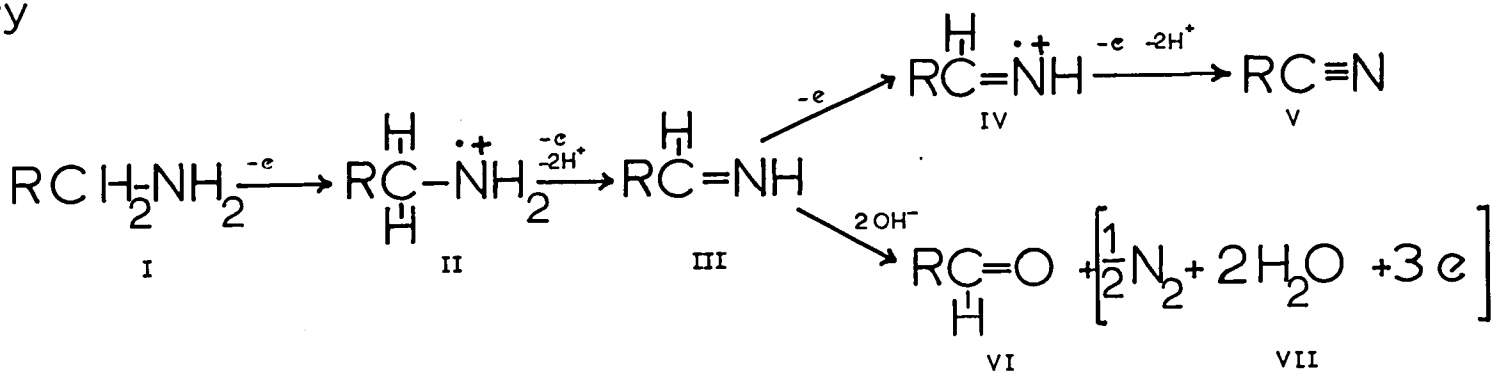

Secondary

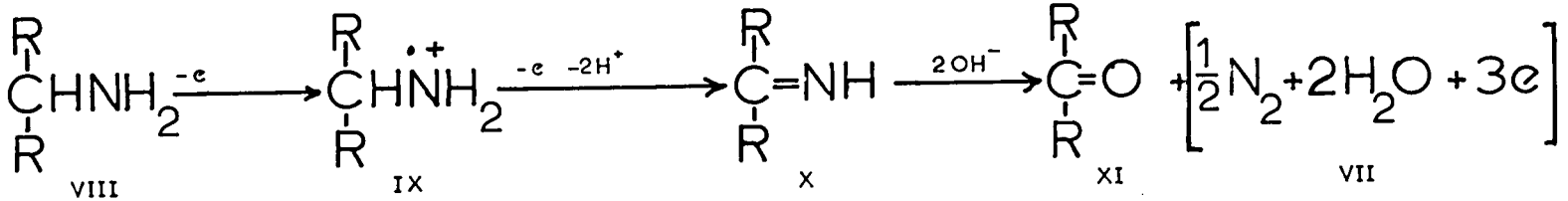

Tertiary

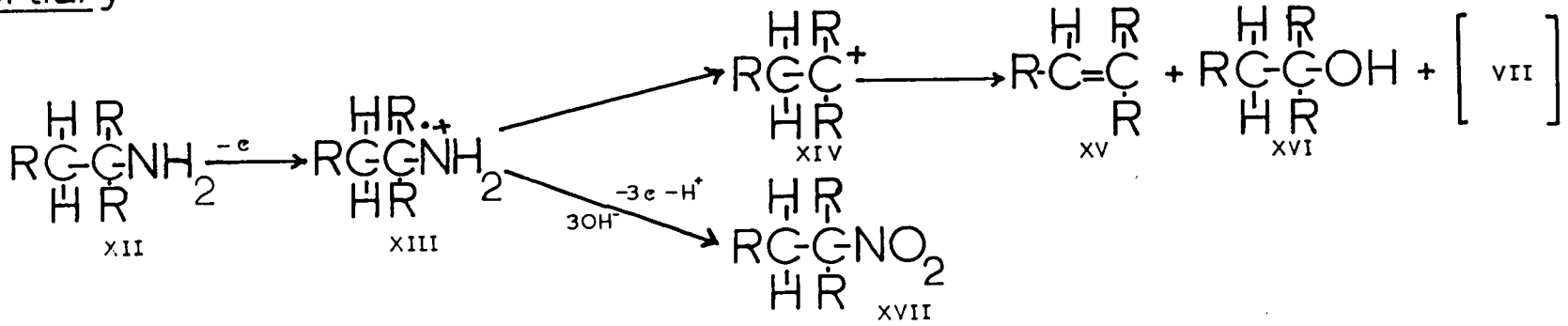

be more likely to react in two different ways. The electrochemical oxidation of the imine implies that it reacts at the electrode surface, and thus the experimental results (Tables VII, VIII and Fig. 35) can be explained in terms of competitive adsorption of amine and OH^-. For each relative surface concentration a steady state concentration of imine is produced. The hydrolysis of imine to aldehyde (species VI) proceeds rapidly if the ratio of $[Imine]$ to $[OH^-]$ is low. If $[imine] : [OH^-]$ is high the electrochemical reaction yielding nitrile (species V) proceeds more rapidly than the hydrolsis. These steady state concentrations are potential dependent (Table VIII). The potential pulse experiments show that the $[Imine] : [OH^-]$ ratio is time dependent. There is an optimum time for the production of aldehyde which is potential dependent (Fig. 35). If this time is exceeded (low frequency) there is an increase in the relative yield of nitrile, while at high frequencies the electrode reaction cannot follow the potential relaxations and the potential is effectively constant at an average value.

It is difficult to derive the nature of the intermediate species II (IX and XIII) and IV in the postulated reaction scheme (Fig. 36). It seems likely that an electron will be removed most readily from the lone pair on the nitrogen atom to yield a species of the type proposed. Such a species has also been postulated by BARNES and MANN (13). Successive processes are likely to be:

de-protonation and successive charge transfer and deprotonation (or possibly loss, and subsequent oxidation, of a hydrogen atom) to yield species III (or X).

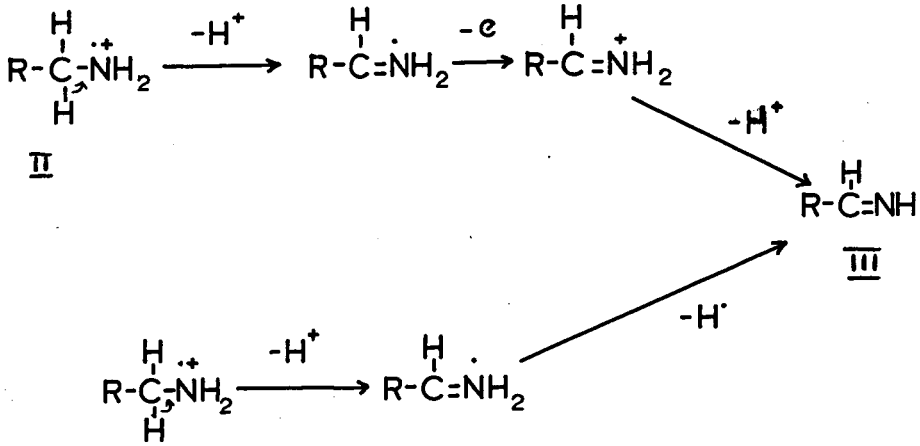

[8.1]

[8.1.a]

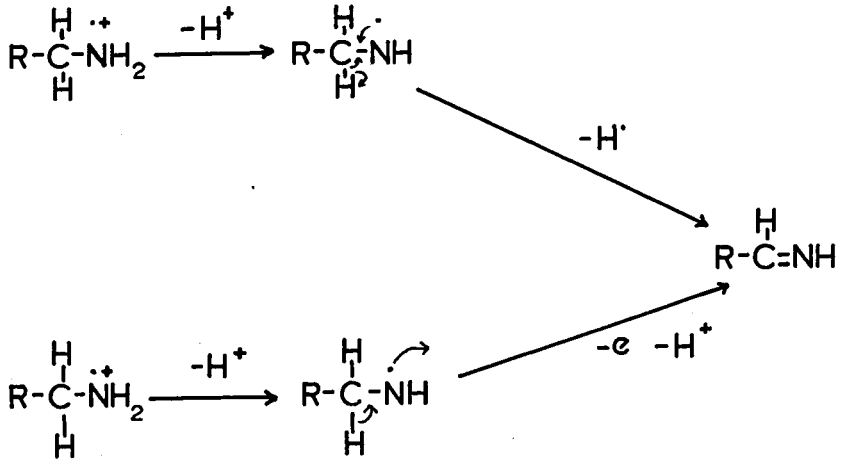

[8.2]

[8.2.a]

Of these reactions the most probable is either [8.2] or [8.2(a)] in which homolytic fission of a C-H bond occurs. Mechanisms [8.1] and [8.1.(a)] predict a heterolytic fission of a C-H bond in preference to the loss of a proton from a quaternary nitrogen atom. The species involving pentavalent nitrogen in mechanisms [8.1] and [8.1.(a)] would be very short lived if formed at all.

Similar reaction schemes can be drawn for the oxidation of imine to nitrile.

The postulated base catalysed hydrolysis of imine to yield aldehyde can proceed by several mechanisms e.g.:-

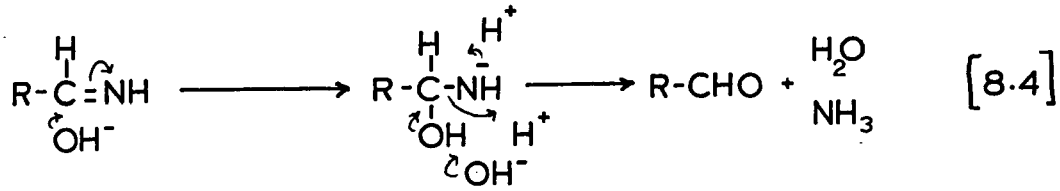

[8.4]

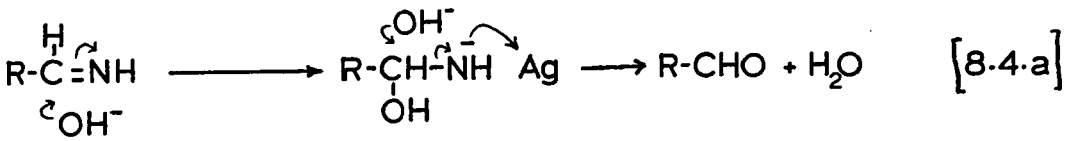

[8.4.a]

A further group of mechanisms is possible in which the hydrolysis yields amide:-

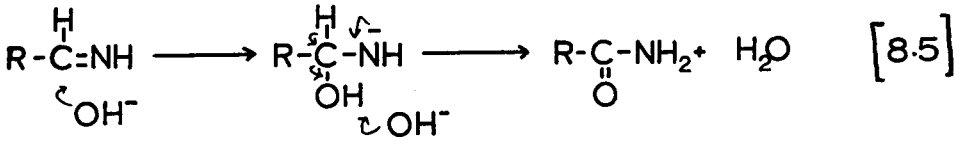

[8.5]

No trace of free amide was found in any exppriment, and, although carboxlylic acid was detected in a few experiments this is probably the product of oxidation of the aldyhyde by AgO (37) and not due to hydrolysis of amide formed according to [8.5]

The oxidation of tert-butylamine, a primary amine with no α-H atoms, yielded tert-Butanol, 2-methyl-2nitro-propane and iso-butene in roughly equivalent yields. The alcohol and alkenes are probably derived from the tertiary carbonium ion (R_3C^+) which is relatively stable (in comparison with primary and secondary carbonium ions). The formation of nitro alkane is of interest as this must involve direct attack of OH^- at the N atom in a mechanism of the form:-

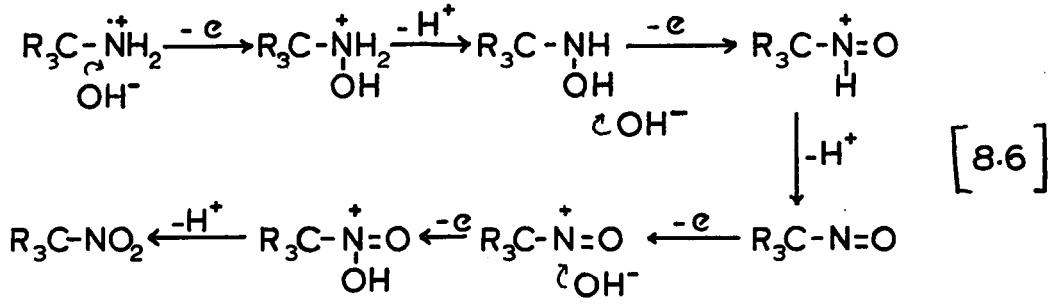

[8.6]

The products obtained from the oxidation of primary and secondary substituted alkyl amines do not arise from either the above mechanism, [8.6], or from reactions of carbonium ions and thus these reactions must be

energetically less favourable than the cleavage of the α C-H bond. The oxidation of n-butyraldoxime (CH_3 $(CH_2)_2$ CH=N-OH) under similar conditions yields nitro-n-butane in addition to n-butyronitrile (40) which indicates that the R-N^{OH} group is perhaps a precursor to the nitro-alkane, rather than the oxidation of NH_3 to NO_2^- with subsequent reaction with R_3C^+.

8.4.b. Secondary Amines

Due to the low solubility of many secondary amines in the electrolyte only di-ethylamine and di-isopropylamine were studied.

These amines behaved in a different manner than aliphatic primary amines at an AgO electrode. The electrode reaction was generally much slower, although it could be made appreciably faster by applying a repetitive potential pulse sequence to the electrode . This suggests that the electrode is being 'blocked' by a reaction product, which is also indicated by potential sweep studies (Ch. 9.3.c)

The oxidation of di-ethylamine yielded:- Ethanol, Ethylene and a trace of Acetonitrile. Ethylamine and nitro-ethane were not present in detectable concentrations. The oxidation of di-isopropylamine yielded isopropanol and prop-1-ene only.

It is possible that the alcohol produced in these oxidations is the species responsible for 'blocking' the electrode. Alcohols are only oxidised slowly at AgO

electrodes (Ch. 8.3) and thus, if they were adsorbed more strongly than amine, would passivate the electrode. An alternative 'blocking' species could be the nitrogen residues from the amines. However, ammonia is oxidised rapidly at platinum (125) and at AgO at these potentials and moreover no 'blocking' effect is observed in the oxidation of sec-butylamine or of n-butylamine under conditions where aldehyde is the major product.

The mechanism for oxidation of secondary amines is complex. It is apparent that no primary amine is produced as an intermediate (no acetaldyhyde detected in the oxidation of Et_2NH or Acetone in the oxidation of $(i\text{-}Pr)_2NH$) although traces of MeCN were found in the oxidation products of Et_2NH. The oxidation probably involves the (nearly) simultaneous cleavage of both C-N bonds with the formation of carbonium ions which either eliminate H^+ or react with OH^-

The oxidation of secondary amines at AgO electrodes is possibly similar to the oxidation of primary amines at platinum (13)

8.4.c Tertiary Amines

Tertiary amines (with the exception of tri-methylamine) are virtually insoluble in 1.0M NaOH. Any possible reaction products of tri-methylamine would be very difficult to separate and analyse and therefore the oxidation of tri-ethylamine was studied.

A saturated solution of tri-ethlyamine (~ 0.15M) was oxidised at a potential of 0.75V N.H.E. The reaction rate was very slow ($< 0.2 mAcm^{-2}$) and was not affected by either agitation or repetitive potential pulses. Analysis of the electrode after ~70 hrs did now show any organic compound other than tri-ethylamine.

8.5 General Features of the Oxidations of Simple Aliphatic Compounds at Silver Oxide Electrodes

8.5.a. Comparisons Between the Behaviour of Alcohols and Amines.

Considerable differences are observed in the rates of oxidation of primary amines and alcohols at both silver oxide electrodes and bulk AgO (37). These differences are much greater than would be expected from a study of the rates of oxidation using $silver^{II}$ picolinate (39), and may be a measure of large differences in the mode of adsorption of amines and alcohols at AgO.

Amines would be expected to be adsorbed strongly at AgO in view of the known $silver^{I}$ and $silver^{II}$ complexes (118). AgO can be considered as having an outer surface of close packed oyxgen atoms which can be displaced by amine molecules to form 'surface complexes' which are readily oxidised. Alcohol molecules are not so readily oxidised as they are probably bound to the surface by hydrogen bonds and do not penetrate the oxygen 'shell' to the extent that amines do, and thus are not so easily involved in electron transfer reactions.

8.5.b. Comparisons between the Oxidation of Primary, Secondary and Tertiary Amines

There are significant differences in the mechanism and rate of oxidation of the three classes of amines.

Primary amines are oxidised rapidly and the overall mechanism can be controlled by chemical and electrochemical methods (for amines which can exhibit alternative reaction paths i.e. have 2α hydrogen atoms).

Secondary amines react to give products resulting from reactions of carbonium ions. These products can 'passivate' the electrode thus stopping the reaction.

Tertiary amines appear to react only very slowly - if at all.

These differences in reactivity are probably not steric effects as amines are 'umbrella' shaped at the nitrogen atom with the lone pair (which would be involved in complex bonding) pointing outwards. It would appear that the significant factor affecting reactivity is the number of hydrogen atoms at the nitrogen atom. This suggests that the loss of one of these protons is the rate controlling process and that reaction [8.2] is the most likely (of reactions [8.3], [8.2] and [8.1]) in the oxidation of primary amines.

CHAPTER 9

The Effect of Organic Compounds on the Electrochemical Behaviour of Silver in Alkali

9.1 Introduction

The electrochemical oxidation of organic compounds at AgO electrodes has been discussed in Ch. 8. It is apparent that electrochemically 'active' organic compounds will affect the behaviour of silver oxide electrodes.

Of the methods available for the study of electrochemical reactions (see Ch. 4) perhaps best general diagnostic technique is potential sweep voltammetry (P.S.V.) (158). Comparison of the dynamic current-potential curves readily shows any effects due to adsorption or reaction pseudo-capacitances (80) of the organic compound.

There have been many studies, using P.S.V. of the electrochemical behaviour of alcohols at platinum electrodes (29, 30). The current-potential curves have been interpreted in terms of the potential dependent adsorption and oxidation of the alcohol and its oxidation intermediates.

MANN (112) has studied the oxidation, at platinum, of aliphatic amines in acetonitrile. The current-peak potential (E_m) was correlated with the aliphatic substitutes according to a Hammet-Taft (139) relationship. Primary amines gave different correlations than secondary and tertiary amines. MASUI, SAYO and TSUDA (114) studied

the P.S.V. behaviour of aliphatic amines at vitreous carbon electrodes in alkaline electrolytes. Differences in behaviour between primary, secondary and tertiary amines were observed, although all were oxidised irreversibly.

9.2 Experimental Methods

Potential sweep experiments were carried out in a cell of Type III (see Appendix I) using a micro-electrode (see Appendix 3) of area 4.45×10^{-2} cm^2.

The electrolyte (1M NaOH) was not circulated through charcoal. All organic compounds (obtained commercially) were purified by distillation immediately before use and checked for purity using g.l.c. Aliquots were added to the electrolyte by means of a graduated pipette.

Galvanostatic experiments were carried out as described in Ch. 7. Electrolytes were saturated with nitrogen, but not circulated through charcoal.

Cell temperatures were controlled to within $\pm$ 0.1°C by means of a water bath thermostat.

9.3 The effects due to Alcohols

The addition of iso-propanol to the electrolyte had no detectable effect on the current-potential curves for the oxidation of silver to AgO, followed by oxygen evolution. These experiments were repeated at temperatures up to 60°C without any effect (attributable to the alcohol) becoming apparent.

This behaviour is to be expected in view of the very

slow electrochemical rate of oxidation of iso-propanol at AgO electrodes (Ch. 8)

9.4 The Effects due to Primary Aliphatic Amines

The addition of primary amines to the electrolyte had a significant effect on the current potential curve (Fig. 37). This effect was dependent on the concentration of the amine (Fig. 38) and on the potential region.

9.4.a. The Ag_2O formation of Potential Region

On addition of primary amine to the electrolyte the peak due to the formation of Ag_2O becomes a wave. This behaviour suggests that the electrode reaction is controlled by a non-electrochemical process, and that the products of the rection do not passivate the electrode. Such a process could be the formation of a soluble Ag_2O (or Ag^+)-amine complex; the rate determining step being the diffusion of the complex from the electrode, or of amine to the electrode. In the case of the four isomeric butylamines a linear current-concentration dependence was observed only for the n- and iso- isomers (the two isomers with one aliphatic substituent at the α-carbon atom); while the sec-isomer obeys an $i \propto C_{amine}^{1.5}$ law and the tert-isomer an $i \propto C_{amine}^{2}$ law (Fig. 39). The temperature dependences of the wave heights (Fig. 40) show that the enthalpy of activation (ΔH^*) is $\sim$1 kcal mole^{-1} for both n- and tert-butylamine suggesting that the overall rate determining process is diffusion. The anamalous concentration

Fig. 37 Potentiodynamic Current Curves for the Isomeric Butylamines (iso-Butylamine yields very similar curves to n-Butylamine). 1.0M NaOH, 0.13M amine, 6×10^{-4} V sec^{-1}. Electrode Area = $4.45 \times 10^{-2} cm^2$.

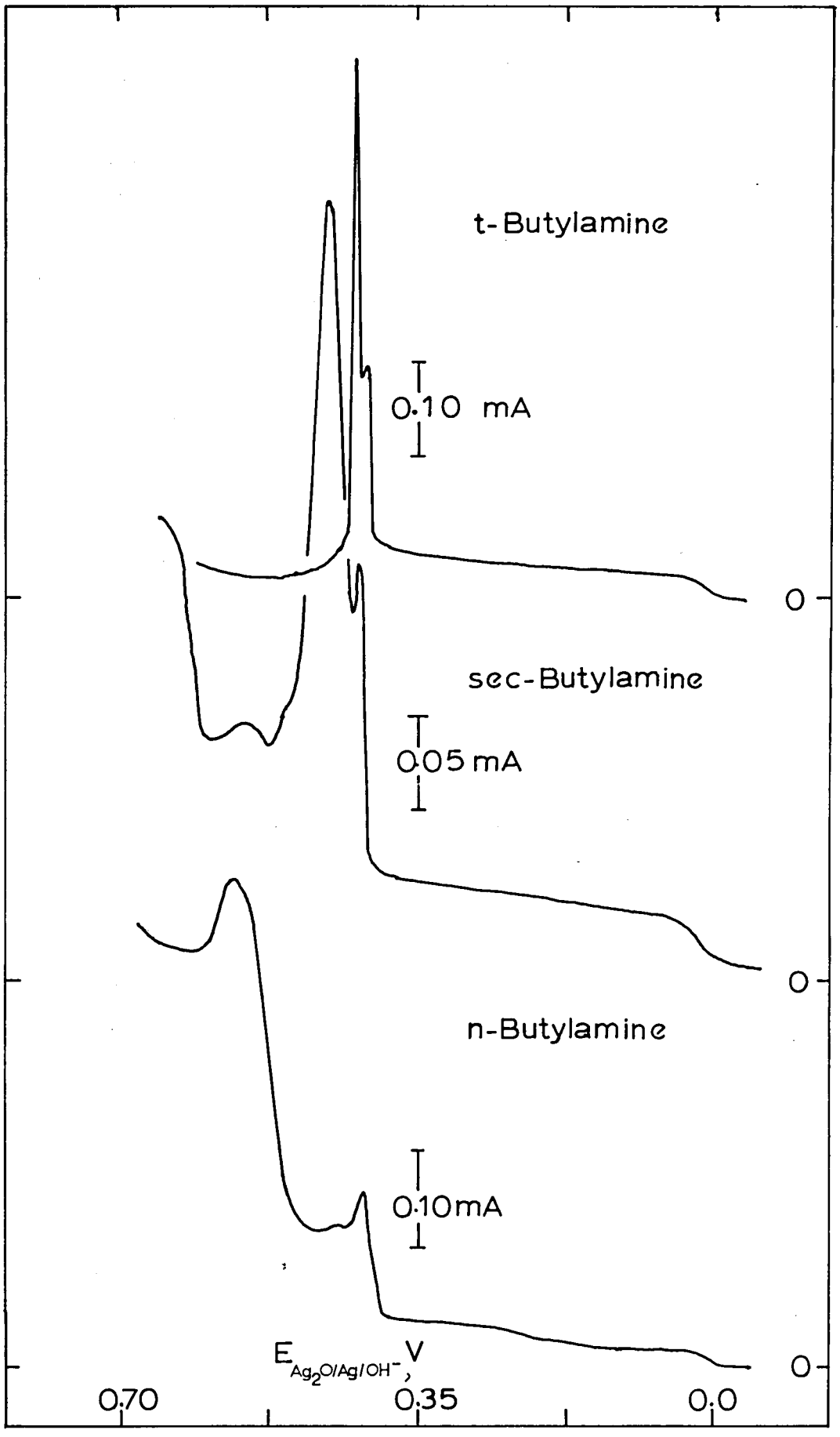
t-Butylamine
0.10 mA
0
sec-Butylamine
0.05 mA
0
n-Butylamine
0.10mA
0
$E_{Ag_2O/Ag/OH^-}$, V
0.70
0.35
0.0

Fig. 38 The Effect of n-Butylamine on the Potentiodynamic Current Curve of Silver in 1.0M NaOH at 23oC 6×10^{-4} V sec^{-1}. A- 0.0M, B- 33×10^{-2}M, C- 1.3×10^{-1}M, D- 2.0×10^{-1}M. Electrode Area = $4.45 \times 10^{-2} cm^2$

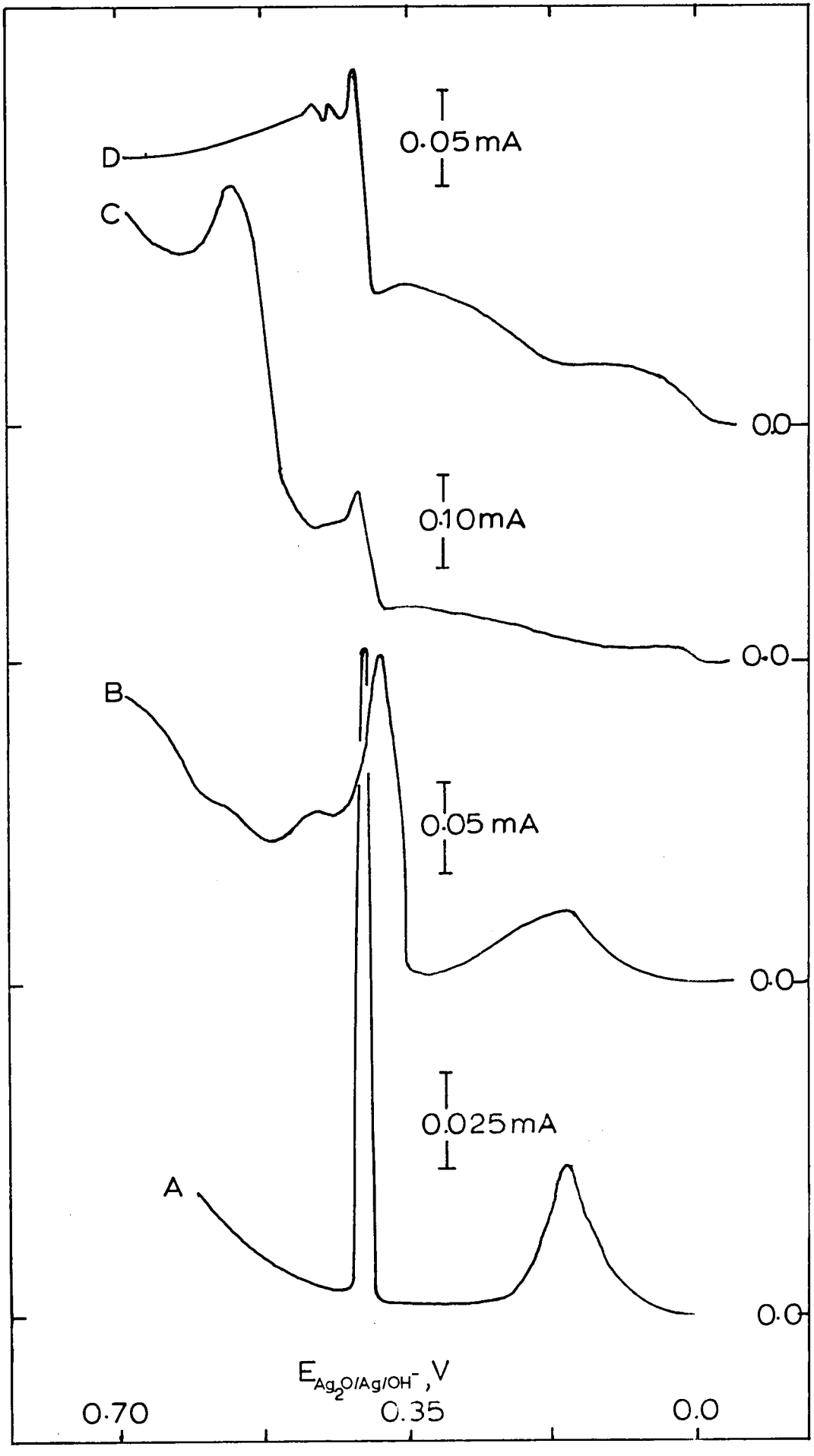
D
0·05 mA
C
0·0
0·10 mA
0·0
B
0·05 mA
0·0
0·025 mA
A
0·0
$E_{Ag_2O/Ag/OH^-}$, V
0·70
0·35
0·0

Fig. 39. The Concentration Dependence of the Ag_2O Wave for Different Amines. 1.0M NaOH, 23°C, 6×10^{-4} V sec^{-1}.

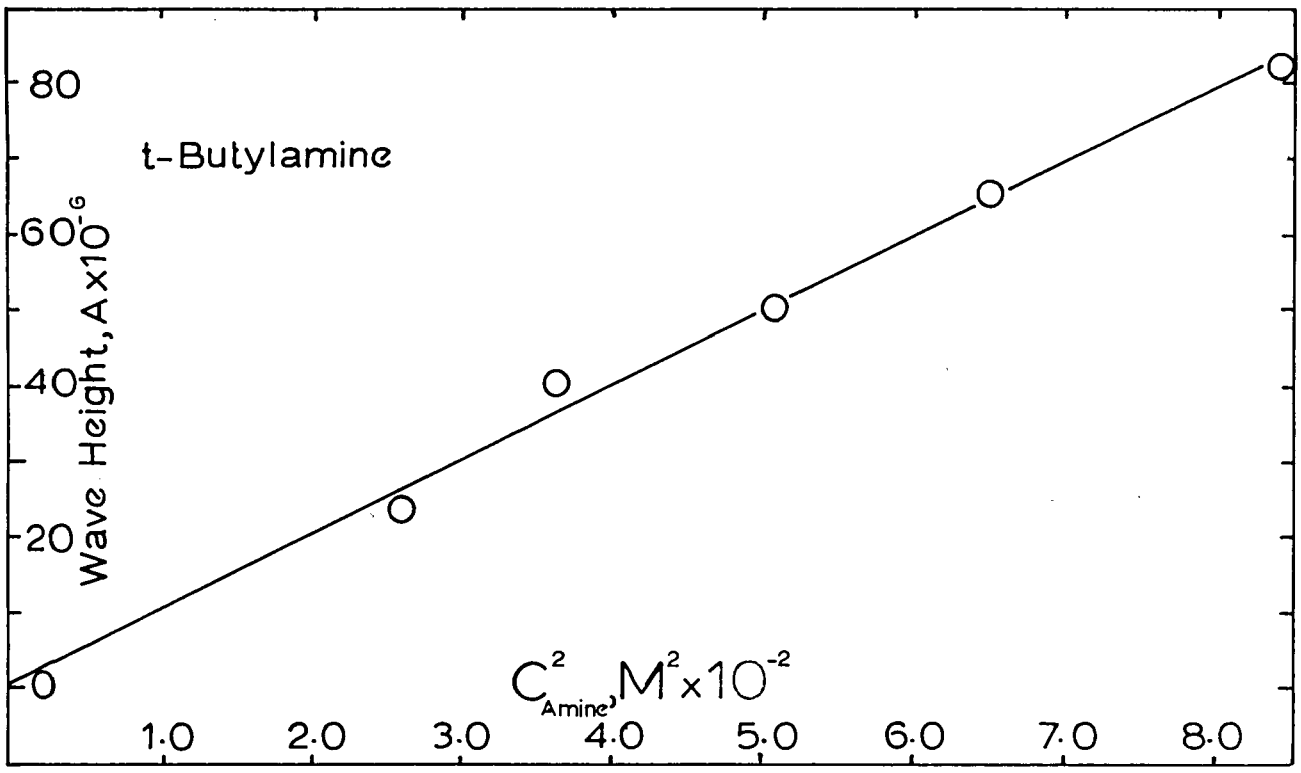
80
t-Butylamine
60
40
20
0
Wave Height, A x10^-6
C^2 Amine, M^2 x10^-2
1.0
2.0
3.0
4.0
5.0
6.0
7.0
8.0

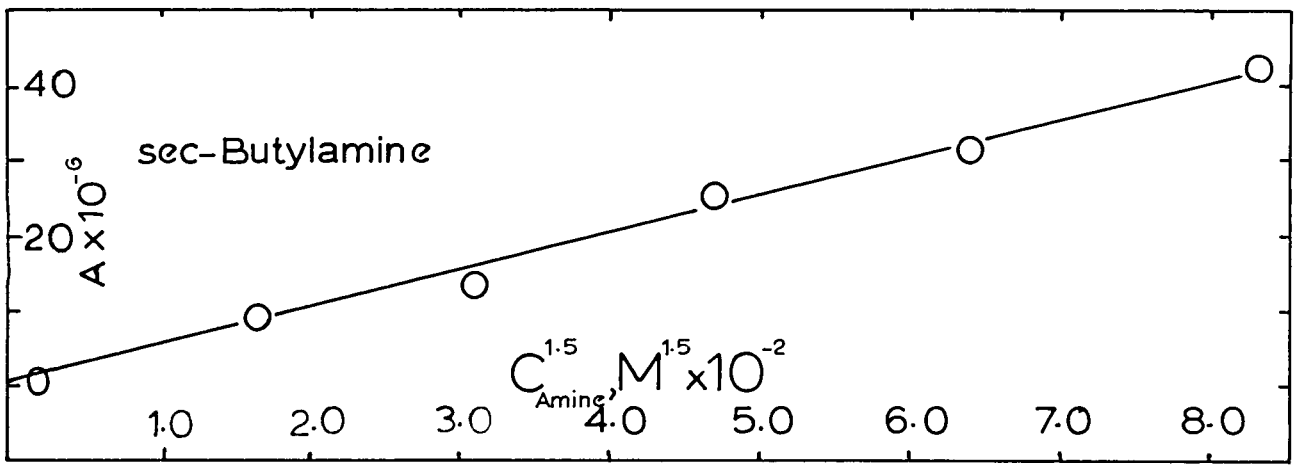
40
sec-Butylamine
20
0
A x10^-6
C^1.5 Amine, M^1.5 x10^-2
1.0
2.0
3.0
4.0
5.0
6.0
7.0
8.0

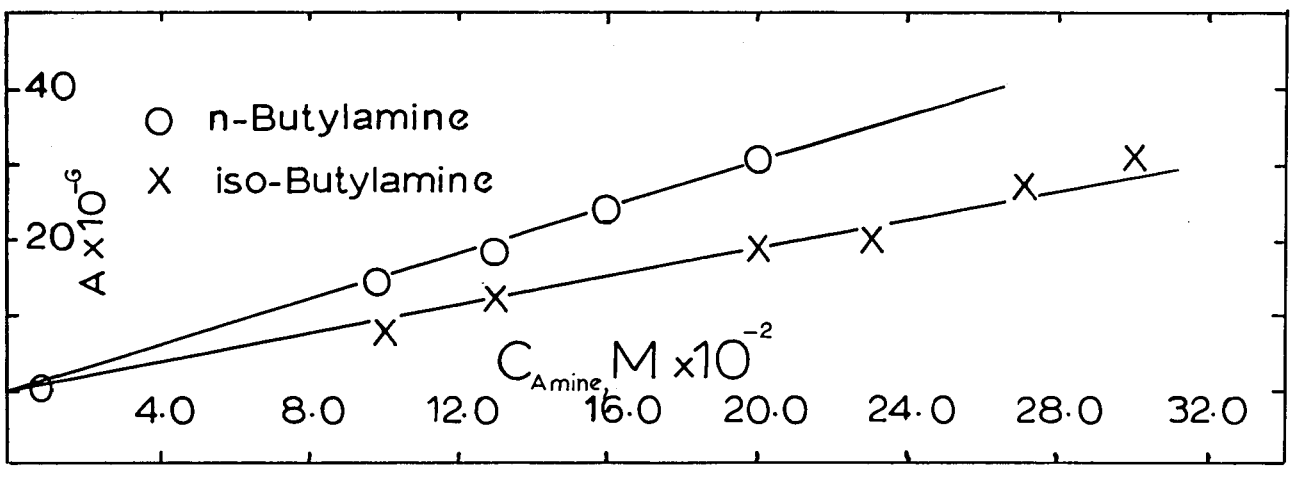
40
O n-Butylamine
X iso-Butylamine
20
A x10^-6
C Amine, M x10^-2
4.0
8.0
12.0
16.0
20.0
24.0
28.0
32.0

Fig. 40 Arrhenius Plots of the Rate of Formation of Ag^{I}-Amine Complexes from P.S.V. Data. 1.0M NaOH, 23°C, 6×10^{-4} V sec^{-1}, Electrode Area = 4.45×10^{-2} cm^2.

Fig. 41 Dependence of the Ag_2O Exchange Current on [n-Butylamine] (from Tafel Plots). 1.0M NaOH, 23°C.

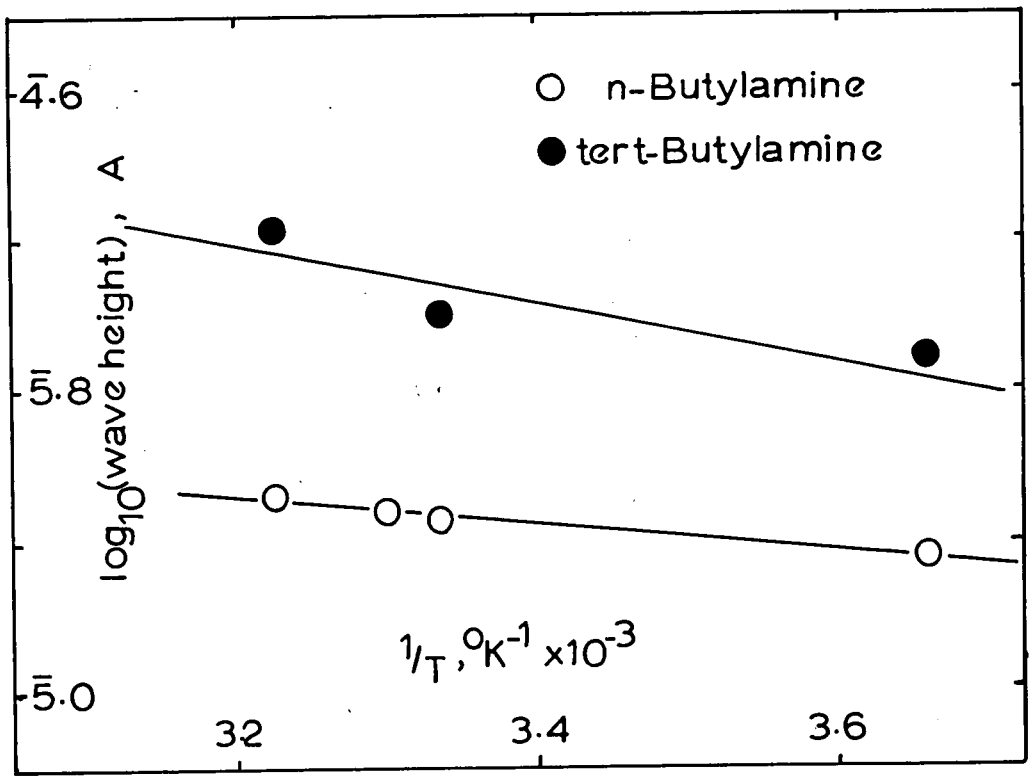
n-Butylamine
tert-Butylamine
$\log_{10}$(wave height), A
$1/T$, $^{o}K^{-1}$ x10^{-3}
$\bar{4}.6$
$\bar{5}.8$
$\bar{5}.0$
3.2
3.4
3.6

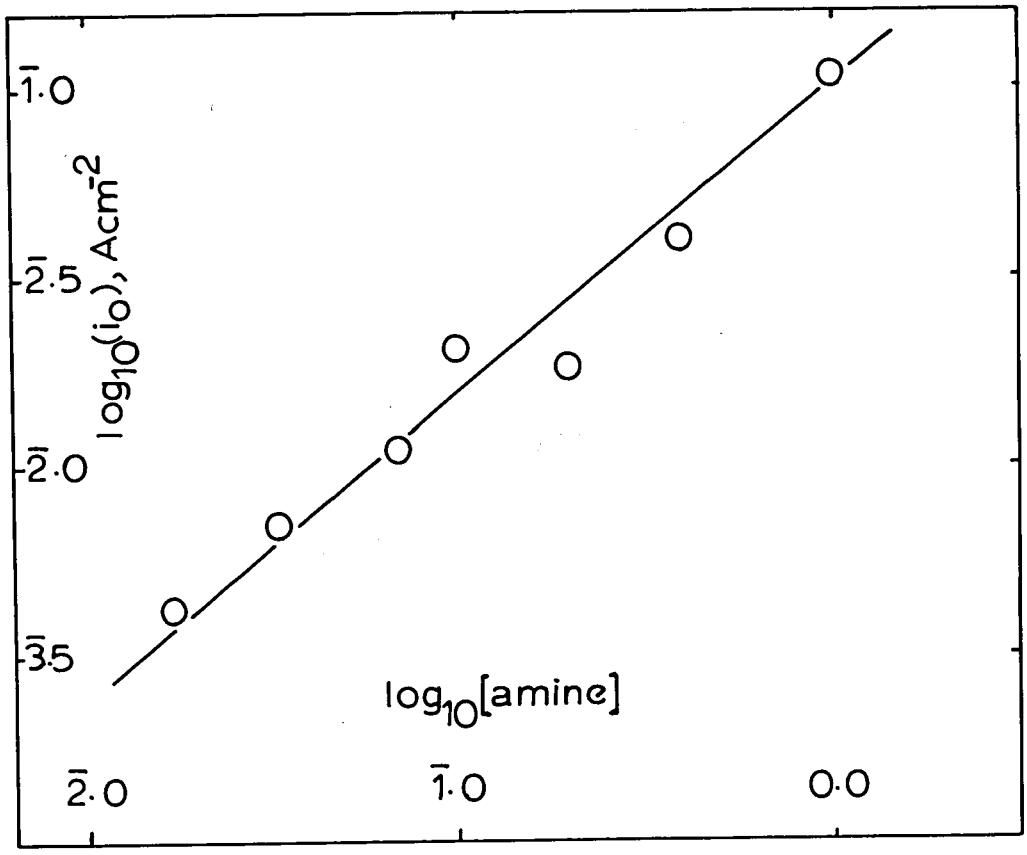
$\log_{10}(i_o)$, Acm^{-2}
$\log_{10}$[amine]
$\bar{1}.0$
$\bar{2}.5$
$\bar{2}.0$
$\bar{3}.5$
$\bar{2}.0$
$\bar{1}.0$
0.0

dependence for the sec- and tert-isomers is probably due to lower stability constants for their complexes than for the n- and sec- butylamine - Ag^{I} complexes.

To determine the composition of these complexes excess Ag_2O was added to known concentrations of amine in 1.0M NaOH, the system allowed to reach equilibrium ($\sim$4 hrs) and the complexed silver in solution determined by Volhard's Method (153). The results for n-butylamine and tert-butylamine are shown in Fig. 42. The concentration of dissolved silver varies directly with the concentration of n-butylamine. This indicates that the n-$BuNH_2$-Ag^{I} complex has a high stability constant and the slope, $\frac{d[\text{amine}]}{d[\text{silver}^{1}]} = 4$, suggests that the ratio of n-butylamine-$silver^{I}$ in the complex is 4. This is higher than the usual coordination number for $silver^{I}$ (1-3 (44)). In the case of tert-butylamine the 'dissolved' silver concentration does not vary linearly with the concentration of amine indicating that the stability constant is low and hence explaining the anomalous potential sweep results. Attempts to determine the Ag^{I}:amine ratio in the complexes by direct titration of Ag_2O with amine using potentiometric and R.F. impedance effects to determine the end point did not yield conclusive results.

As the concentration of amine was increased in P.S.V. experiments the half wave potential ($E_{\frac{1}{2}}$) decreased (Fig. 38).

Fig. 42 The Nature of Ag^{I}-Amine Complexes. The Dependence of ['Soluble Ag^{+}'] on [Amine]

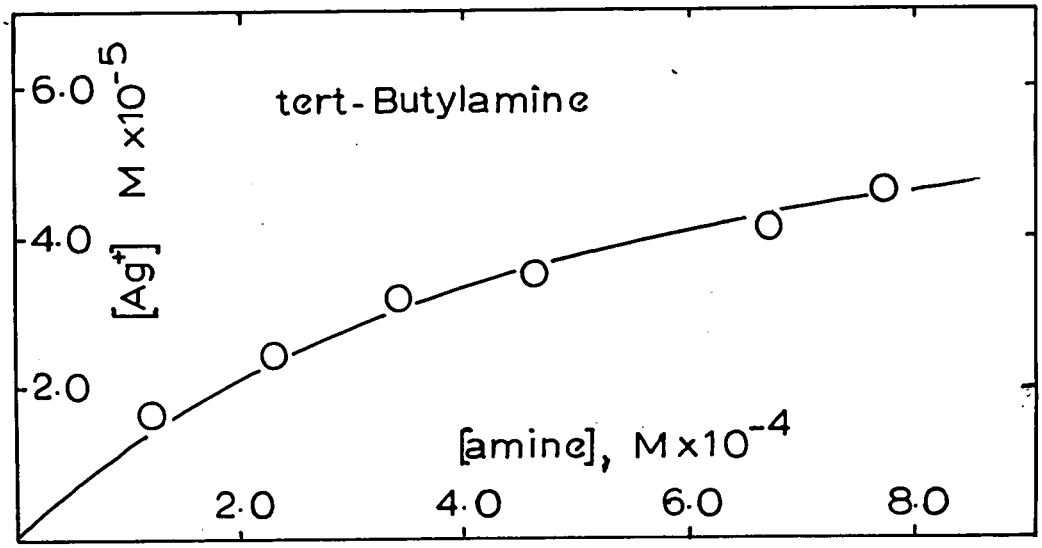
tert-Butylamine
6.0
4.0
2.0
[Ag+] M x10-5
[amine], M x10-4
2.0
4.0
6.0
8.0

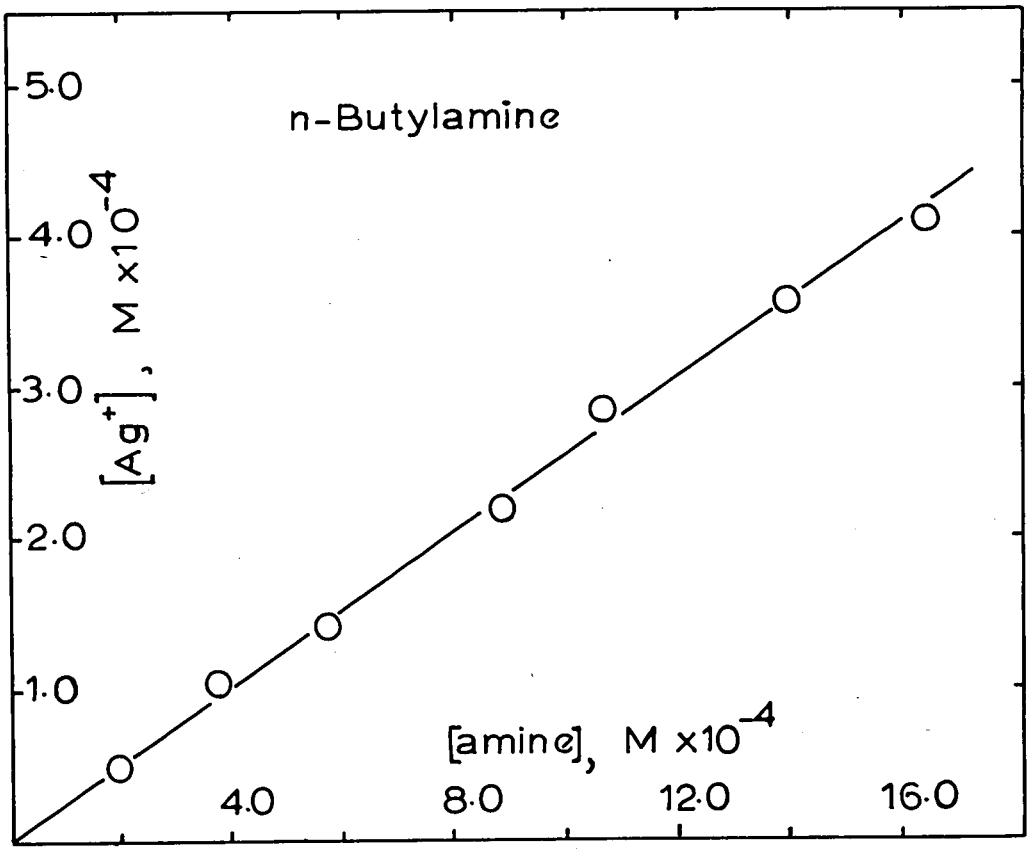
n-Butylamine
5.0
4.0
3.0
2.0
1.0
[Ag+], M x10-4
[amine], M x10-4
4.0
8.0
12.0
16.0

This effect could not be measured accurately due (inter alia) to the non symmetrical shape of the waves. This effect indicates that the exchange current, i_o, for the Ag_2O/Ag equilibrium increases with amine concentration. The determination of Tafel plots (see Ch. 7.4) for the formation of Ag_2O (Fig. 43) show that this effect is real and does represent an increase in i_o with increasing [amine] . Determination of α from dependence of i_o on [n-Butylamine] (c.f. Eq. [3.16]) yields a value of ~0.6 (Fig. 41). This indicates that n=1 i.e. a 1:1 reaction netween silver and n-butylamine is the rate determining process. Further complexing probably occurs in the diffusion layer, the most stable complex ($[Ag(nBuNH_2)_4]^+$) being formed. If the equilibrium (within the diffusion layer) does not lie on the side of the complex anomalous concentration effects will be apparent (c.f. sec- and tert-butylamine).

9.4.b. <u>The AgO Formation Region</u>

The effect of primary amines on the current-potential curves is most pronounced in this region. Further current 'humps' appear which are dependent on the concentration of amine (Fig. 38) and on the substitution at the α- carbon atom (Fig. 37). The formation of AgO appears to be unaffected by the presence of amine - the AgO peak always occurs at the same potential and is approximately constant in magnitude.

Fig. 43 Tafel Plots showing the effect of Added Amines on the Rate of Formation of Ag_2O.

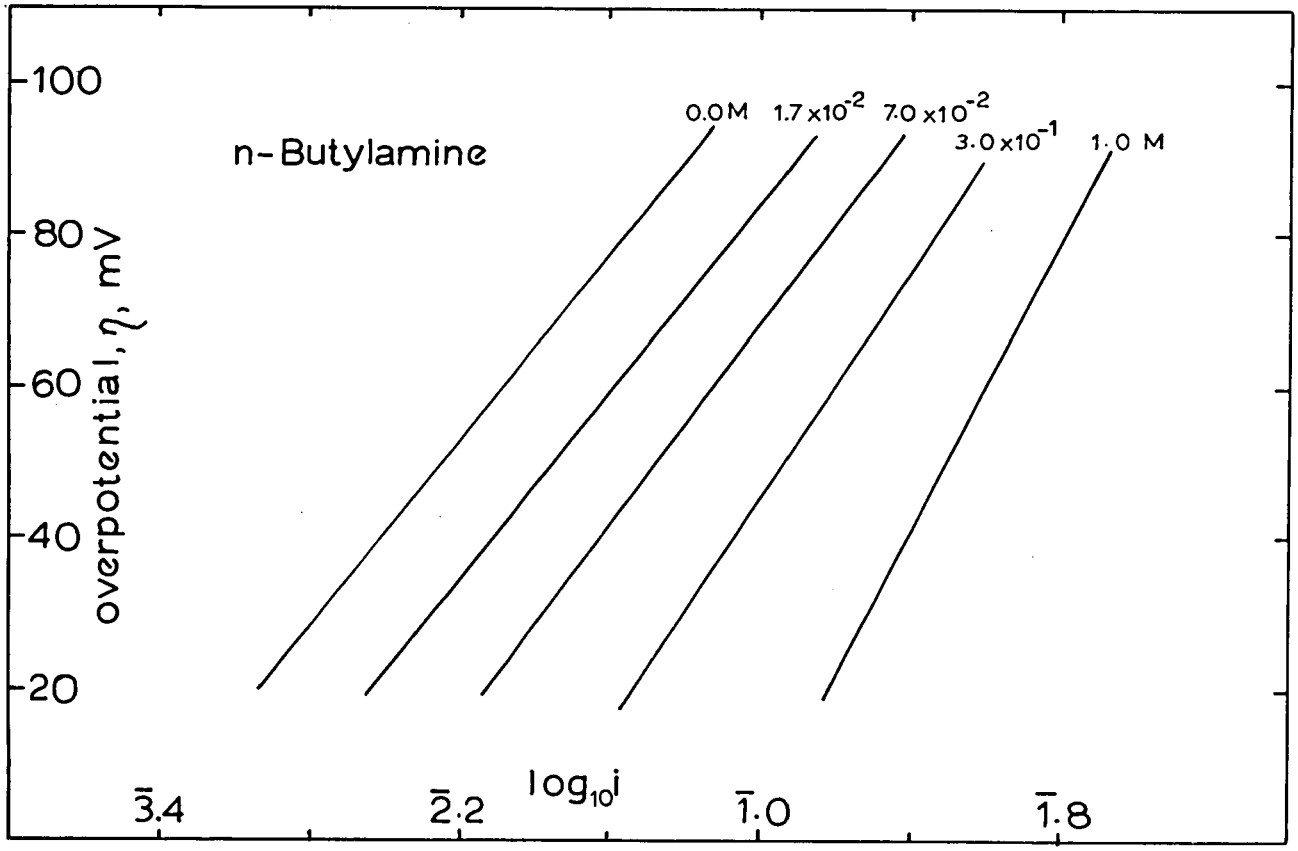
n-Butylamine
0.0 M
1.7 x10^-2
7.0 x10^-2
3.0 x10^-1
1.0 M
100
80
60
40
20
overpotential, η, mV
3̄.4
2̄.2
log10 i
1̄.0
1̄.8

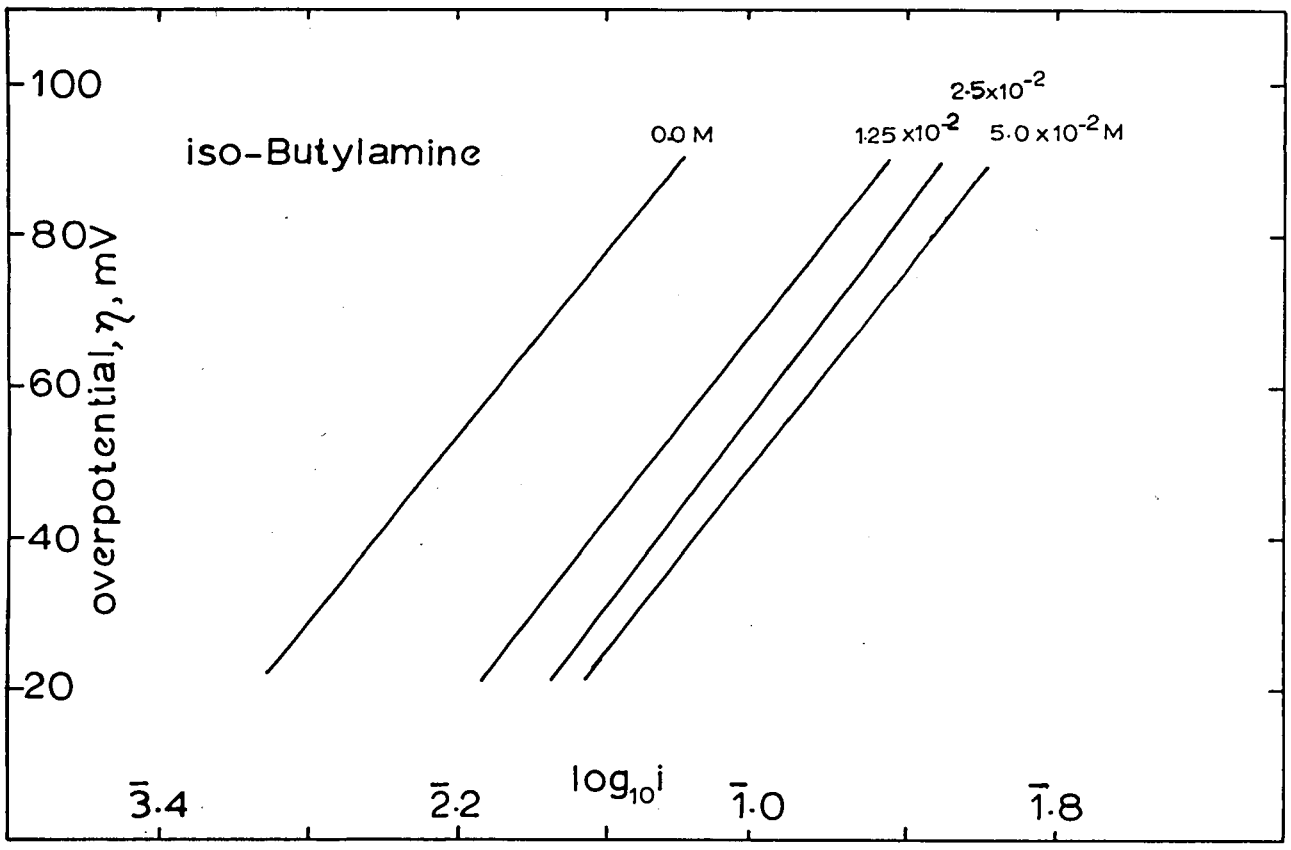
iso-Butylamine
0.0 M
1.25 x10^-2
2.5x10^-2
5.0 x10^-2 M
100
80
60
40
20
overpotential, η, mV
3̄.4
2̄.2
log10 i
1̄.0
1̄.8

(In certain cases the peak is swamped by one of the new current humps). These further humps correspond, therefore, to electrode reactions dependent on the presence of AgO.

It is difficult to correlate the appearance of the current-potential curve accurately in terms of the electrochemical reactions occurring at the electrode. The form of the tert-butylamine curve (Fig. 37) is indicative of an electrode reaction which is self inhibiting. The passivating species could be iso-butene (which is likely to form a π complex with silver^{I}) or, more likely tert-butanol (see Ch. 9.3). The sec-butylamine current potential curve also shows a large peak, much broader than the tert-butylamine peak due to the greater number of charge transfer steps occurring (Fig. 36). The n-Butylamine curve is more complex. The initial hump (after AgO formation) increases with [amine] and moves to higher potentials (Fig. 38) up to [amine] $\sim$ 0.15M after which it decreases in magnitude. This would appear to parallel the decrease in rate of formation of n-butyraldehyde with increasing [amine] (See Ch. 8.4.a. n.b. determinations of product yield were not made at [amine] >0.2M). This hump is probably due to the electrochemical reactions leading to the formation of aldehyde i.e. the formation of Imine and oxidation of ammine residues to nitrogen (step VII Fig. 36).

9.5 The Effects Due to Secondary Amines

The addition of diethylamine and di-isopropylamine to the electrode does not affect the shape of the current potential curve for the oxidation of silver, however the heights (and areas) of the peaks corresponding to the formation of Ag_2O and AgO increase as a linear function of the amine concentration (Fig. 44). These processes do not appear to be controlled by electrolyte diffusion as the current drops to ~ zero in the potential region between the peaks. The amine must, therefore, be involved in the electrode process only during the formation of the massive Ag_2O and AgO deposits. It seems that the organic reaction is self passivating and thus occurs only at growing crystallites. The inhibiting species is not soluble in amine (or electrolyte) and appears to be formed more slowly at high amine concentrations. (If the inhibiting species were soluble a current-wave would be observed). This would suggest that the rate of formation of inhibitor is dependent on $[OH^-]$ and thus the inhibitor is probably the alcohol which is an oxidation product (See Ch. 8.4.b.) of secondary amines. The more rapid increase in the AgO peak (than the Ag_2O peak) with amine concentration is due to the much faster organic electrochemical reaction rate at the higher (AgO) potential.

Fig. 44 Dependence of Ag_2O (upper plot) and AgO (lower plot) Peak Heights on Concentration of Secondary Amines. 1.0M NaOH, 23°C, 4.45×10^{-2} cm^2 Sweep Rate = 6×10^{-4} V sec^{-1}

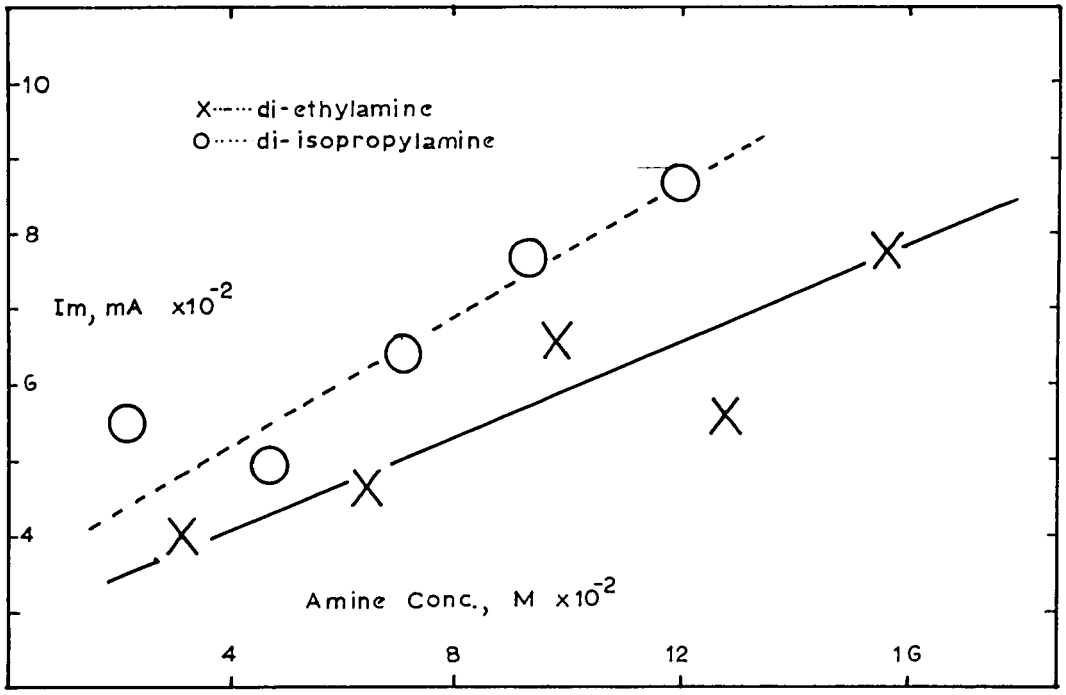
X---- di-ethylamine
O····· di-isopropylamine
Im, mA x10-2
Amine Conc., M x10-2
10
8
6
4
4
8
12
16

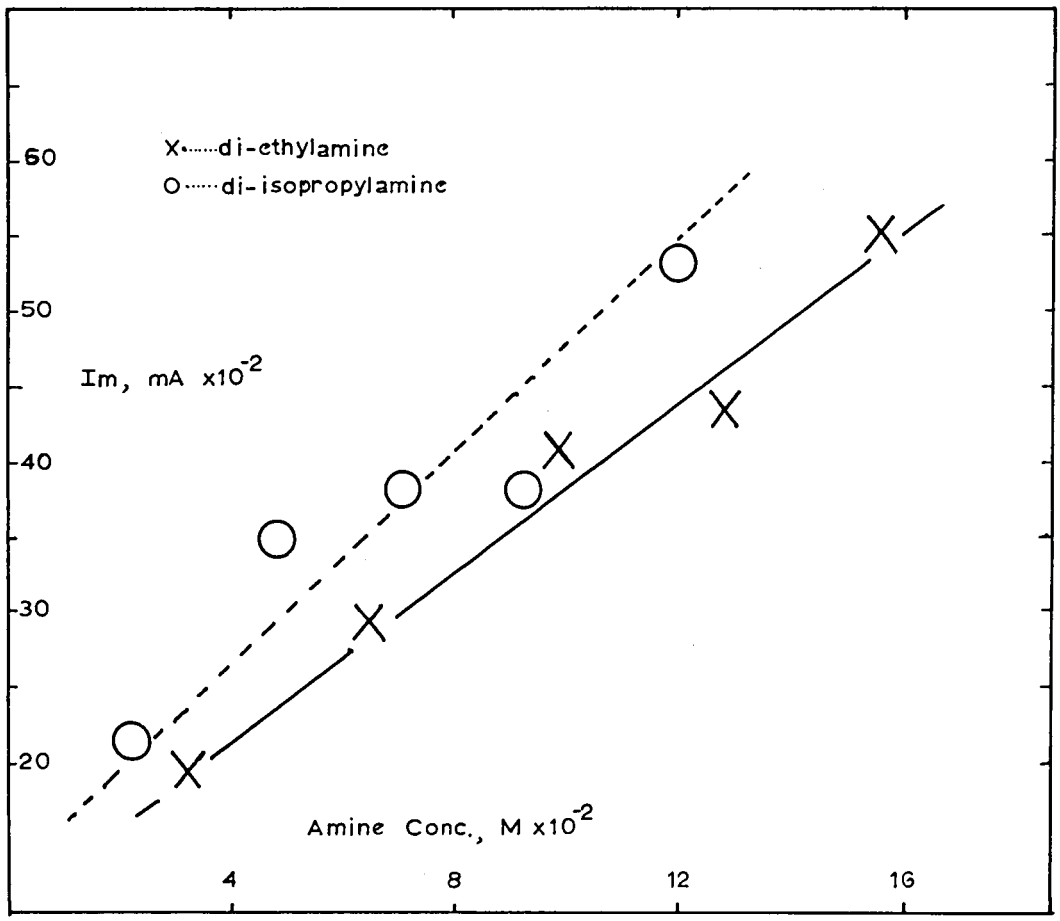
X·····di-ethylamine
O·····di-isopropylamine
Im, mA x10-2
Amine Conc., M x10-2
60
50
40
30
20
4
8
12
16

9.6 The Effects due to Tertiary Amines

Additions of tri-ethylamine to the electrolyte have no measurable effect on the current-potential curve up to the maximum solubility of the amine ($\sim 2 \times 10^{-2}$M) This is a reflection of the very slow rate of electrochemical oxidation of tertiary amines (See Ch. 8.4.c.)

SECTION 3

General Conclusions and Suggestions for Further Work

The silver electrode in alkali is of interest due to the complexity of its oxidation kinetics and also for its potential electrocatalytic activity in electrosynthesis.

Kinetic studies of the oxidation of silver in alkaline electrolytes show that the reaction mechanism and kinetics are dependent on the electrode coverage with oxide. Oxide free silver electrodes do not have a simple metal/electrolyte interphase, there is contradictory evidence for the value of E_z and indications of the presence of unusually reactive sites on the electrode which appear to be involved in a 'corrosion' type of reaction with the electrolyte. The oxidation of silverto Ag_2O is initially charge transfer controlled, being second order w.r.t. silver. Adsorption of OH^- is indicated. In thicker films of Ag_2O the reaction rate is controlled by a solid state diffusion process. The Ag_2O/AgO phase change is controlled by a classical electrocrystallisation process viz. slow nucleation with three dimensional growth of the crystallites.

Silver oxide shows a strong electrocatalytic effect in the electrosynthesisof compounds containing the R-NH-R group (R may be H). Oxidations of these compounds occur much more rapidly than at platinum electrodes (see Fig. 45) and, in certain cases (primary aliphatic primary amines)

Fig. 45 The Effect of Electrode Material on Potentiodynamic Current curve for n-Butylamine (4×10^{-1} M) in 1.0M NaOH, 23°C, 6×10^{-4} V sec^{-1}.

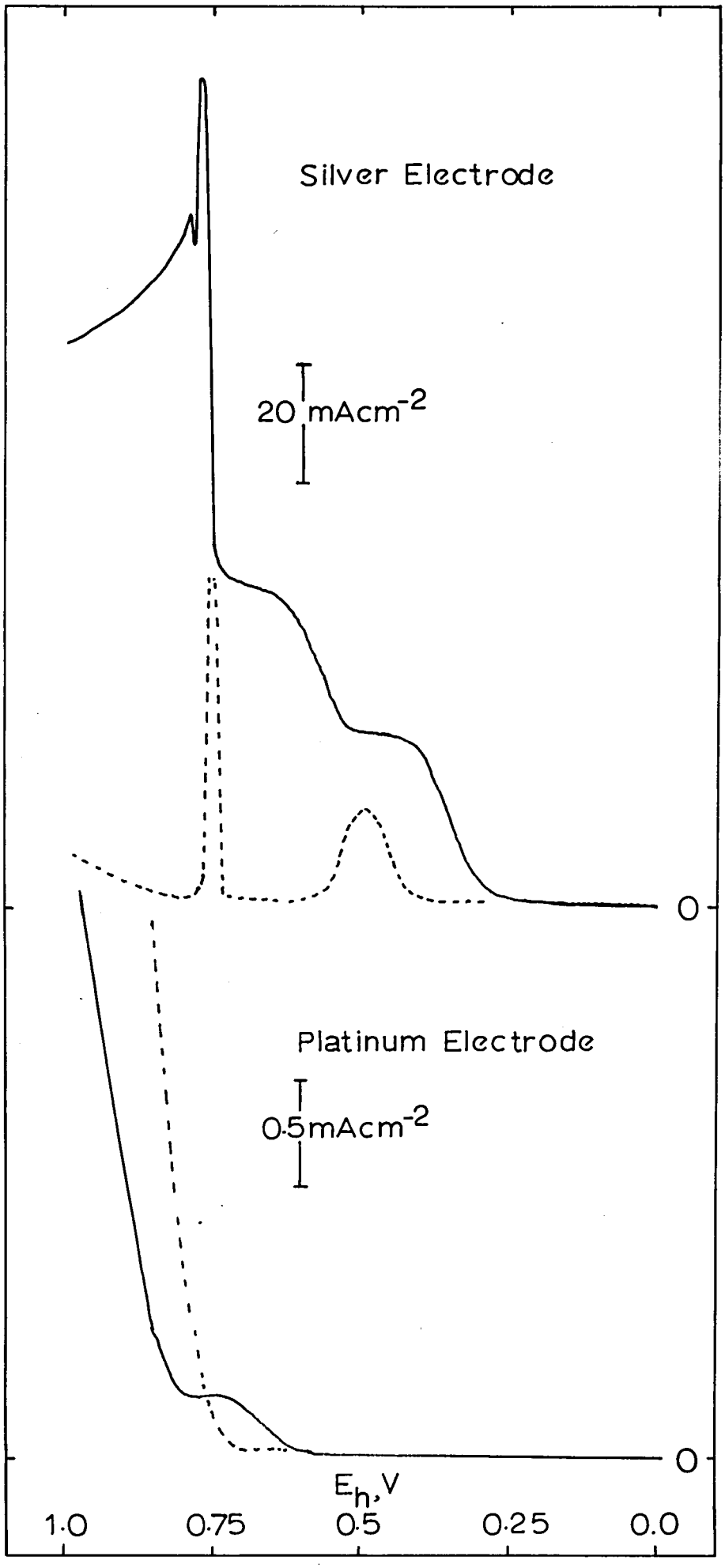
Silver Electrode
20 mAcm-2
0
Platinum Electrode
0.5mAcm-2
0
Eh, V
1.0
0.75
0.5
0.25
0.0

the reaction mechanism (and consequently products) may be controlled by the adjustment of the electrochemical parameters. Tertiary amines (R_3N) react very slowly, as do alcohols.

The fundamental difference in reaction rate between amines (excluding R_3N) and alcohols is probably due to differences in adsorption at the electrode (the formation of an N → Ag bond for amines and adsorption by R-O-H-O-Ag bonds for alcohols). The presence of N-H or $\overset{H}{N}$-H groups appears to be prerequisite for the rapid oxidation of amines.

The kinetics of the oxidation of amine are very difficult to elucidate due to the simultaneous formation of complexes (soluble in the case of primary amines) with Ag^{I}. Also aliphatic amines of relatively high molecular weight (C_5 and above) and aromatic amines are only very slightly soluble in aqueous electrolytes which severely limits the range of applicability of this technique.

Non-aqueous organic solvents could be used with a suitable (quaternary ammonium salt) electrolyte, however, difficulties are immediately apparent in that the conductivities of such systems are generally low, silver oxides may not be formed at the working electrode and a careful choice of counter electrode has to be made to ensure a fast faradaic reaction at this electrode. Semi-aqueous solvent systems would overcome many of these difficulties, but 'salting out' of the reactant compound

may occur. It is clear that a careful choice of solvent/electrolyte system would be needed to realise the full electrocatalytic potential of the silver electrode.

REFERENCES

1. N. K. ADAM 'Physical Chemistry', p. 451, O.U.P. (1956)

2. W. J. ALBERY, S. BRUCKENSTEIN, D. T. NAPP Trans. Farad. Soc., 62, 1932 (1966)

3. J. A. ALLEN Aus. J. Chem. 13, 431 (1960)

4. J. A. ALLEN Aus. J. Chem. 14, 20 (1961)

5. J. A. ALLEN Proc. 1st Aus. Conf. Electrochem., p.76 Pergamon Press, (1965).

6. D. J. ASTLEY, J. A. HARRISON, H. R. THIRSK J. Electroanal. Chem. 19, 325 (1968)

7. G. ATHERTON, M. FLEISCHMANN, F. GOODRIDGE Trans. Farad. Soc. 63, 1468 (1967)

8. F. T. BACON Electrochim. Acta. 14, 569 (1969)

9. R. G. R. BACON, W. HANNA J. Chem. Soc (C), 4962 (1965)

10. R. G. R. BACON, D. STEWART J. Chem Soc (C), 1384 (1966)

11. C. BARBIERI, L. MALAGUTI Atti. Acad. Lincei. Rend. Classe. Sci. Fiz. Mat. e Nat. 8, 619 (1950)

12. G. C. BARKER, 'Modern Electroanalytical Methods' (ed. G. Charlot) P.112, Elsevier (1958).

13. K. K. BARNES, C. K. MANN J. Org. Chem. 32, 1474 (1967)

14. R. BARRADAS, G. FRAZER Can. J. Chem. 42, 2488 (1964)

15. R. BARRADAS, G. FRAZER Can. J. Chem. 43, 446 (1965)

16. F. BASOLO, R. G. PEARSON 'Mechansims of Inorganic Reactions', P. 303, J. Wiley (1958)

17. H. H. BAUER J. Electroanal. Chem. 16, 419 (1968)

18. A. von BAYER, V. WILLIGER Berichte 32, 3625 (1899)

19. W. BECK, R. LIND, W. F. K. WYNNE-JONES Trans. Farad. Soc. 50, 147 (1954).

20. N. P. BEREZINA, N. V. NICOLAEVA-FEDOROVICH Elektrokhimiya 3, 3 (1967).

21. T. BERZINS, P. DELAHAY J. Amer. Chem. Soc. 77, 6448 (1955).

22. A. BEWICK, M. FLEISCHMANN Electrochim. Acta. 11, 1397 (1966)

23. K. F. BLURTON, A. C. RIDDIFORD J. Electroanal. Chem. 10, 457 (1965).

24. J. O'M BOCKRIS, DEVANATHAN, K. MÜLLER Proc. Roy. Soc. A274, 55 (1963).

25. J. O'M BOCKRIS, E. GILEADI, K. MÜLLER Electrochim. Acta. 12, 1301 (1967).

26. G. C. BOND 'Catalysis By Metals', Academic Press (1962).

27. P. F. BOWDEN, E. K. RIDEAL Proc. Roy. Soc. A120, 59 (1928)

28. G. W. BRIGGS, M. FLEISCHMANN, D. J. LAX, H. R. THIRSK Trans. Farad. Soc. 64, 3120 (1968).

29. M. W. BREITER Disc. Farad. Soc. 45, 79 (1968)

30. S. B. BRUMMER, C. CAHILL Disc. Farad. Soc. 45, 67 (1968)

31. G. M. BUDOV, W.W. LOSEV Doklady. Akad. Nauk. S.S.S.R. 126, 1029, (1959)

32. J. A. V. BUTLER Trans. Farad. Soc. 19, 734 (1924)

33. J. A. V. BUTLER Proc. Roy. Soc. A122,399 (1929)

34. B. D. CAHAN, J. B. OCKERMANN, R. F. AMLIE, P. RUETSCHI J. Electrochem. Soc. 107,725 (1960)

35. D. L. CHAPMAN Phil. Mag. 25, 475 (1913)

36. T. G. CLARKE, N. A. HAMPSON, J. B. LEE, J. R. MORLEY, B. SCANLON Can. J. Chem. 46, 3437 (1968)

37. T. G. CLARKE, N. A. HAMPSON, J.B. LEE, J. R. MORLEY, B. SCANLON Tet. Letters 54, 5685 (1968)

38. T. G. CLARKE, N. A. HAMPSON, J. B. LEE, J. R. MORLEY, B. SCANLON Ber Bunsenge, Phys. Chem 73, 279 (1969)

39. T. G. CLARKE, N. A. HAMPSON, J. B. LEE, J. R. MORLEY, B. SCANLON Can. J. Chem. 47, 1649 (1969)

40. T. G. CLARKE, N. A. HAMPSON, J. B. LEE, J. R. MORLEY, B. SCANLON, Can J. Chem. in press

41. G. L. COHEN, G. ATKINSON J. Electrochem. Soc. 115, 1236 (1968).

42. B. E. CONWAY, J. O'M BOCKRIS J. Chem Phys. 26, 532 (1957).

43. B. E. CONWAY 'Electrode Processes' Ch.6, Ronald Press Ltd. (1964).

44. F. COTTON, G. WILKINSON 'Advanced Inorganic Chemistry' p.1144, Interscience (1966).

45. W. COWDREY, S. DAVIES Quart. Revs. 6, 358 (1952).

46. G. CROFT J. Electrochem. Soc. 106, 278 (1959)

47. B. B. DAMASKIN Electrochim Acta 9, 231 (1964)

48. P. DELAHAY J. Amer. Soc. 75, 1190 (1953)

49. P. DELAHAY 'Double Layer and Electrode Kinetics' p. 10, Interscience (1965)

50. P. DELAHAY, ibid., Ch. 9.

51. R. DeLEVIE 'Advances in Electrochemistry and Electrochemical Engineering' (ed. P. Delahay and C. W. Tabias) Vol. 6, Interscience (1967)

52. T. P. DIRKSE J. Electrochem. Soc. 106, 920 (1959)

53. T. P. DIRKSE J. Chem. Eng. Data 6, 538 (1961)

54. T. P. DIRKSE J. Electrochem. Soc. 109, 173 (1962)

55. T. P. DIRKSE, D. DeWIT, R. SCHOEMAKER J. Electrochem Soc. 114, 1196 (1967).

56. T. P. DIRKSE, D. B. DeVRIES J. Phys. Chem. 63, 107 (1959)

57. T. P. DIRKSE, L. Van Der LUGT, H. SCHNYDERS J. Inorg. Nucl. Chem. 25, 859 (1963).

58. O. A. ESSIN, B. J. MARKHOV Acta. Physicochim. U.R.S.S. 10, 353 (1939)

59. J. P. G. FARR, N. A. HAMPSON J. Electroanal. Chem. 13, 433 (1967)

60. E. FICK Ann. Physik 94, 59 (1855)

61. I. L. FINAR 'Organic Chemistry' Vol. 1,P.136 Longmans (1959)

62. A. FLEISCHER J. Electrochem. Soc. 115,816 (1968)

63. M. FLEISCHMANN, D. J. LAX, H. R. THIRSK Trans. Farad. Soc. 64, 3128 (1968)

64. M. FLEISCHMANN, D. J. LAX, H. R. THIRSK Trans. Farad. Soc. 64, 3137 (1968)

65. M. FLEISCHMANN, I. PETROV, W. F. K. WYNNE-JONES Proc. 1st Aus. Conf. Electrochem, p. 500 Pergamon Press (1965)

66. M. FLEISCHMANN, H. R. THIRSK J. Electrochem. Soc. 110, 688 (1963).

67. A. N. FRUMKIN Z. Phys. Chem. 116, 466 (1925).

68. A. N. FRUMKIN Svensk Kemishe Tideschrift 77, 300 (1965)

69. A. N. FRUMKIN, L. I. NEKRASSOV Dokl. Akad. Nauk. S.S.S.R. 126, 115 (1959)

70. H. GERISCHER Z. Electrochem 62 , 256 (1958)

71. H. GERISCHER Anal. Chem. 31, 33 (1959)

72. H. GERISCHER, H. KRAUSE Z. Physik. Chem. 10,264 (1957)

73. S. GLASSTONE 'Physical Chemistry', p. 1196, Macmillan (1953)

74. W. S. GRAFF, H. H. STADELMAIER J. Electrochem. Soc. 105, 446, (1958).

75. D. C. GRAHAME Chem. Rev. 41, 441 (1947)

76. D. C. GRAHAME J. Electrochem. Soc. 99, 370 (1952)

77. D. C. GRAHAME Anal. Chem. 30, 1736 (1958)

78. A. GOUY J. Phys. 9, 457 (1910)

79. B. HAGUE 'A. C. Bridge Techniques' p. 350, Pitman Press (1943)

80. J. M. HALE, R. GREEF Electrochim. Acta 12, 1409 (1967)

81. W. G. HAMER, D. N. CRAIG J. Electrochem. Soc. 104, 206, (1957)

82. L. P. HAMMETT 'Physical Organic Chemistry', p. 142 McGraw Hill (1940)

83. N. A. HAMPSON, P. C. JONES, R. F. PHILLIPS Can J. Chem. 45, 2045 (1967)

84. N. A. HAMPSON, D. LARKIN J. Electroanal. Chem. 18, 401 (1968)

85. N. A. HAMPSON, D. LARKIN, J. R. MORLEY J. Electrochem Soc. 114,817 (1967)

86. J. A. HARRISON J. Electroanal. Chem. 18,377 (1968)

87. H. von HELMHOLTZ Wied. Ann. 7, 337 (1879)

88. D. A. HOUSE Chem. Rev. 62, 185 (1962)

89. J. HORIUTI, M. POLANYI Acta. Physicochim. U.R.S.S. 2, 505 (1935).

90. T. HURLEN, Y. SANDLER, E. PANTIER Electrochim. Acta 11, 1463 (1966)

91. N. IBL Prot. Corros. Met. Finish. Proc. Int. Conf. Basel 1966, p. 48 (1967)

92. C. A. JOHNSON, S. BARNARTT J. Electrochem. Soc. 114, 1256 (1967).

93. C. A. JOHNSON, S. BARNARTT J. Phys. Chem. 71, 1637 (1967)

94. H. JOHNSON, F. CUTA, A. GARRETT J. Amer. Chem. Soc. 55, 2311 (1933).

95. K. M. JOHNSON Education in Chem. 4, 299 (1967)

96. P. JONES, H. R. THIRSK Trans. Farad. Soc. 50,732 (1954)

97. P. JONES, H. R. THIRSK, W. F. K. WYNNE-JONES Trans. Farad. Soc. 52, 1003 (1956).

98. B. N. KABANOV, D. I. LEIKIS Z. Electrochem 62, 660 (1958)

99. G. KORTUM 'Treatise on Electrochemistry' p. 510 Elsevier (1965)

100. F. I. KUKOZ, N. Yu. OSIPCHUK, M. SKALOZUBOV Tr. Novocherkasck. Politekh Inst. 170,84 (1967)

101. H. A. LAITINEN, J. E.B. RANDLES Trans. Farad. Soc. 51, 54 (1955)

102. E. LARSEN 'Transitional Elements' P. 170, W. A. Benjamin Inc. (1965).

103. M. Le BLANC, H. SACHSE Z. Physik 32, 887 (1931)

104. J. B. LEE, T. G. CLARKE Tet. Letts. 5, 415 (1967)

105. D. I. LEIKIS, E. S. SEVASTIANOV, I. G. DAGAEVA J. Electrochem. Soc. 113, 1341 (1966)

106. V. G. LEVICH 'Physicochemical Hydrodynamics' p. 286, Prentice Hall (1962).

107. G. N. LEWIS Z. Phys. Chem. 55, 449 (1906)

108. W. LORENZ Z. Phys. Chem. 202, 275 (1953).

109. W. LORENZ Z. Naturf. 9, 716 (1954).

110. W. LORENZ Z. Phys. Chem (N.F.) 17, 136 (1958)

111. R. LUTHER, F. POKORNEY Z. Anor. Chem. 57, 290 (1908).

112. C. K. MANN Anal. Chem. 36, 2424 (1964)

113. R. A. MARCUS J. Chem. Phys. 43, 679 (1965)

114. M. MASUI, H. SAYO, Y. TSUDA J. Chem. Soc. (B) 9736 (1968)

115. J. McMULLEN, N. HACKERMAN J. Electrochem. Soc. 106, 341 (1959)

116. R. MEMMING, G. SCHWANDT Angew. Chem. 6, 851 (1967)

117. T. MOELLER 'Inorganic Chemistry' p. 302, J. Wiley (1952)

118. T. MOELLER ibid., p. 839

119. G. NATTA Angew. Chem. 68, 393 (1956).

120. A. NEIDING. A. KAZARNOVSKII Dokl. Akad. Nauk. S.S.S.R. 78, 713 (1951)

121. W. NERST Z. Phys. Chem 2, 613, (1888)

122. R. S. NICHOLSON, I. SHAIN Anal. Chem. 36, 706 (1964)

123. A. I. OSHE Elektrokhimiya 4, 1214 (1968)

124. V. OSTROVSKII, M. TEMKIN Kinetics and Catalysis 7, 466 (1966)

125. H. G. OSWIN, M. SALOMON Can. J. Chem 41, 1686 (1963)

126. R. PARSONS 'Handbook of Electrochemical Constants' p. 70, Butterworths (1959)

127. M. E. PEOVER Chemical Engineer 211, 192 (1967)

128. B. PIERSMR, E. GILEADI 'Modern Aspects of Electro chemistry' (ed. J. O'M Bockris) Vol. 4, Elsevier (1966)

129. Y. PLESKOV Dokl. Akad. Nauk. S.S.S.R. 117, 645 (1957)

130. M. PROSKURNIN, A. N. FRUMKIN Z. Phys. Chem. 155, 29 (1931)

131. M. PROSKURNIN, A. N. FRUMKIN Trans. Farad. Soc. 31, 110 (1935).

132. L. RAMALEY, C. G. ENKE J. Electrochem. Soc. 112, 947 (1965)

133. J. E. B. RANDLES Disc. Farad. Soc. 1, 11 (1947)

134. J. E. B. RANDLES 'Trans. Symp Electrode Processes Philadephia 1959 (ed. E. Yeager), p. 209 (1961)

135. S. K. RANGARAJAN J. Electroanl. Chem. 16, 485 (1968)

136. A. C. RIDDIFORD 'Advances in Electrochem. and Electrochem. Eng.' (ed. P. Delahay, C. W. Tobias) Vol. 4, Interscience (1966).

137. J. M. SAVEANT, E. VIANELLO Electrochim. Acta 12, 629 (1967)

138. V. SCATTURIN, P. BELLON J. Electrochem. Soc. 108, 819 (1961)

139. J. SHORTER Chem. in Brit. 5, 269 (1969)

140. C. S. SMITHELLS 'Metals Reference Book' p. 160 Butterworths (1967)

141. C. S. SMITHELLS ibid, p. 685

142. S. SRINIVASAN, E. GILEADI Electrochim Acta. 11, 321, (1966)

143. O. STERN, Z. Electrochem. 56, 822 (1952)

144. P. STONEHART, Electrochim. Acta 13, 1789 (1968)

145. P. STONEHART, F. P. PORTANTE ibid, p. 1805

146. D. SWERN, Chem. Revs. 45, 6 (1949).

147. L. SYPER Tet. Letters 5, 4193 (1967)

148. Z. TAKEHARA, Y. NAMBA, S. YOSHIZAWA Electrochim. Acta. 13, 1395 (1968)

149. V. I. VESELOVSKII Acta Physiochim U.R.S.S. 11,815 (1939)

150. K. J. VETTER 'Electrochemical Kinetics (Theoretical Aspects)', P. 285 Academic Press (1967)

151. K. J. VETTER ibid, p. 347

152. K. J. VETTER ibid, p. 354

153. A. I. VOGEL 'Quantitative Inorganic Analysis' p. 257 Longmans (1959).

154. C. WAGNER J. Electrochem. Soc. 97, 71 (1950)

155. W. A. WATERS 'Mechanisms of Oxidation of Organic Compounds', p.1 Methuen (1964)

156. N. L. WEINBERG. H. L. WEINBERG Chem. Revs 68, 449 (1968)

157. A. WERNER 'Anorganischen Chemie' p. 82, Friedr. Vieweg und Sohn (1913)

158. F. G. WILL, C. A. KNORR Z. Electrotech. 64, 258 (1960)

159. R. H. WOPSCHALL, I. SHAIN Anal. Chem. 36,706 (1964)

160. G. V. ZHUTAEVA, N. A. SHUMILOVA Electrokhimiya 4,99 (1968)

161. G. V. ZHUTAEVA, N.A. SHUMILOVA, V.I. LUK'YANYCHEVA ibid, p. 196

162. H. E. ZITTEL, F. J. MILLER Anal. Chem 37,200 (1965)

163. P. ZUMAN 'Progress in Physical Organic Chemistry' (ed. A. Streitweiser, R. W. Taft), Vol. 5,p. 81, Interscience (1967)

APPENDIX 1

ELECTROCHEMICAL CELLS

All electrochemical cells were made from borosilicate glass. Moveable components were connected to the cells by means of conical ground glass joints (with P.T.F.E. sleeves) or (Quickfit Ltd. type) screw joints with P.T.F.E. washers.

Cell type I (Figs. 46 and 49) consisted of a single compartment of $\sim$350 ml capacity and was fitted with a side-arm for charcoal and a nitrogen lift pump to circulate electrolyte through the side arm. This cell was used for A.C. measurements.

Cell type II (Figs. 47 and 49) consisted of a large main compartment ($\sim$300 ml) with a removable lid carrying ground glass joints for the support of the test electrode. A vertical, moveable 'J' Luggin capillary passed through a screw joint in the lid and could be manoevered to within $\sim\frac{1}{2}$ mm of the test electrode. The main compartment was fitted with a similar electrolyte purification system to Type I cells. The small counter electrode compartment was isolated from the main compartment by means of a frit (porosity 2) to minimise the diffusion of Hydrogen to the working electrode. This cell was used for kinetic measurements at silver electrodes.

Type III cells (Fig. 48 and 49) were used in conjunction with a large vertical working electrode (see Appendix 3)

Fig. 46 Type I Cell. C-Activated Charcoal; S- Counter Electrode; R- Reference Electrode; T- Working Electrode

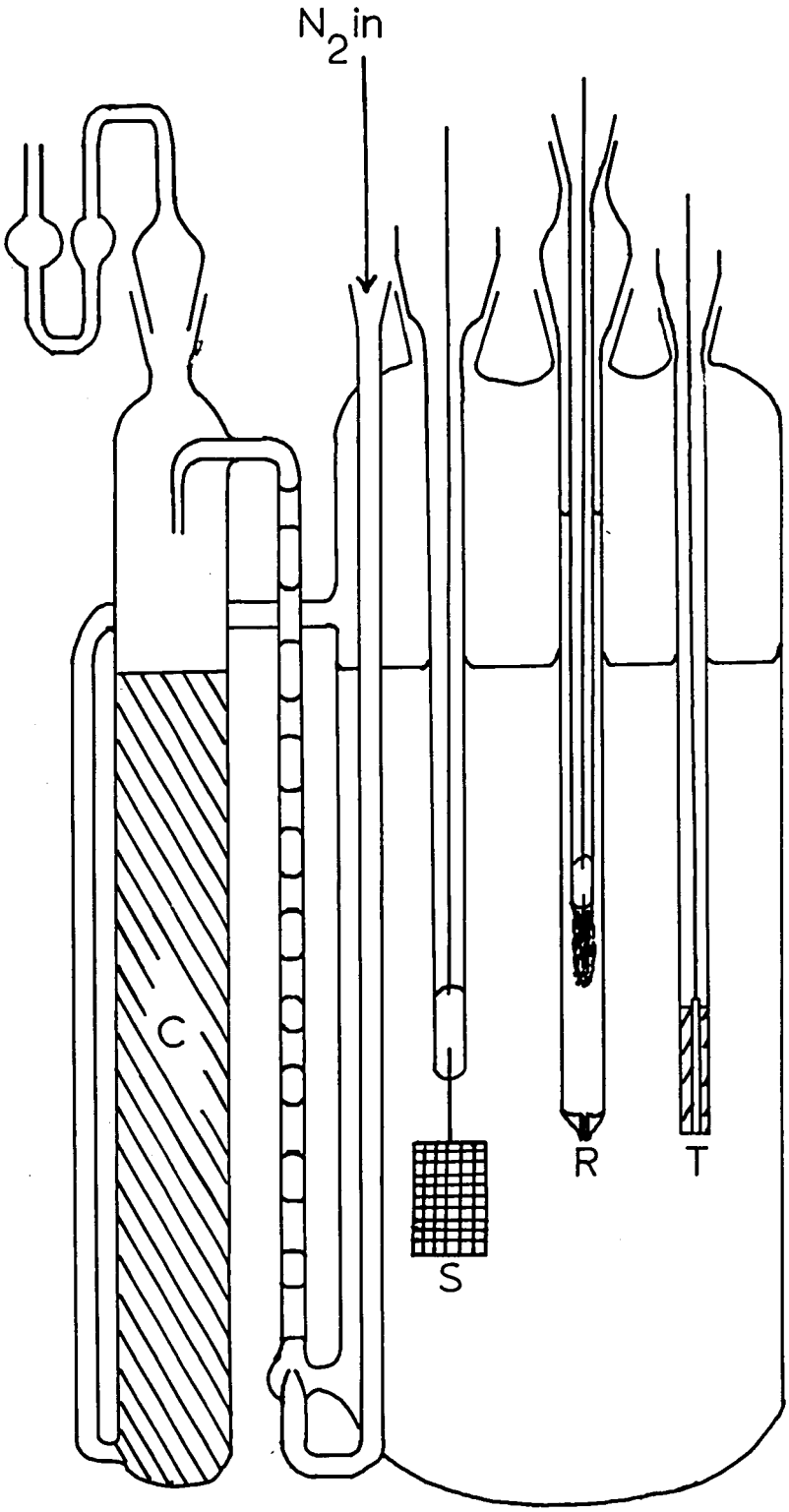
N_2 in
C
S
R
T

Fig. 47 Cell Type II. a joins with a′ . A-reference compartment; B-Counter Electrode Compartment; C-Working Electrode; D-Luggin Probe; E-Electrolyte Circulation System.

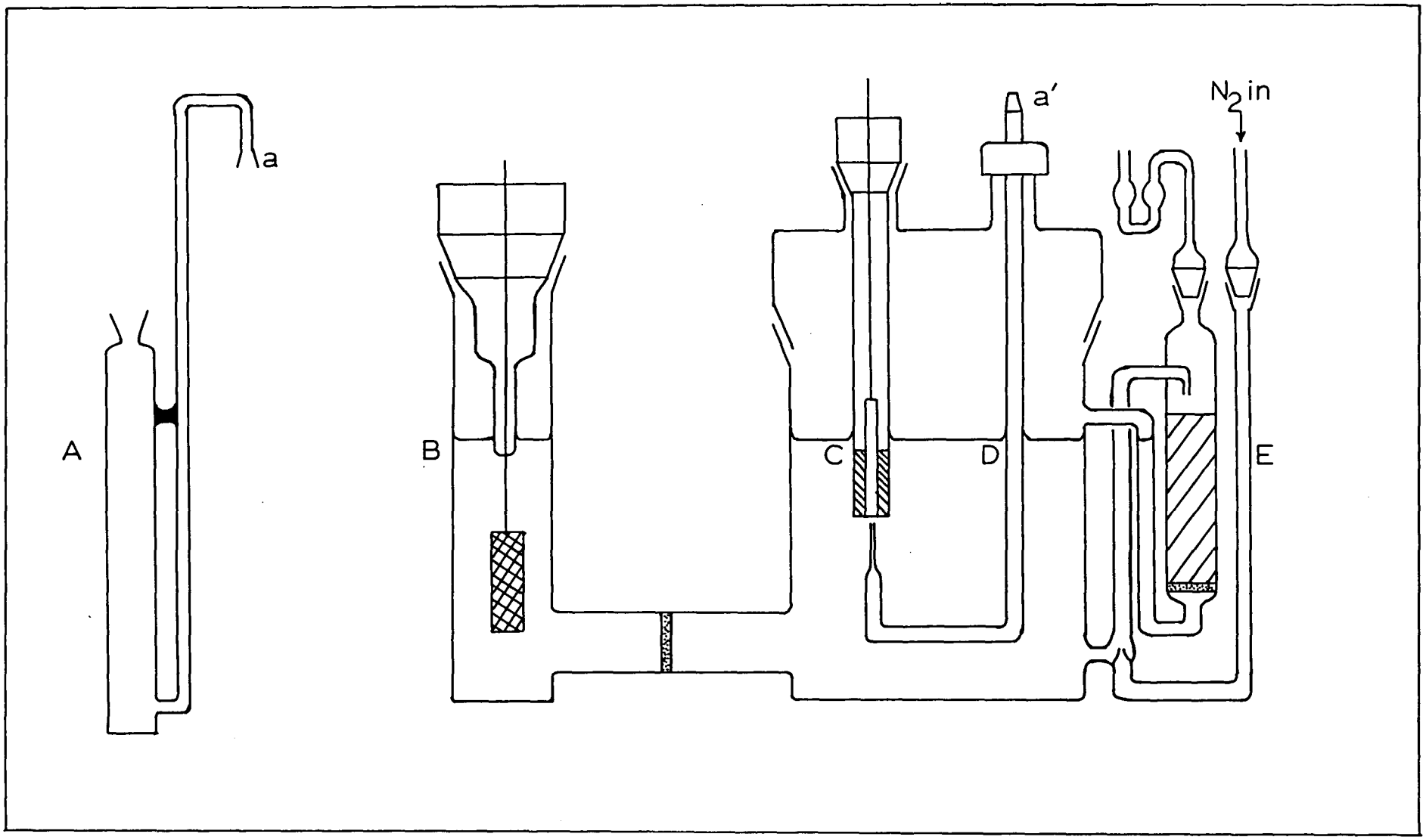
a
A
B
C
D
a'
N2 in
E

Fig. 48. Cell Type III Showing Vertical Planar Working Electrode.

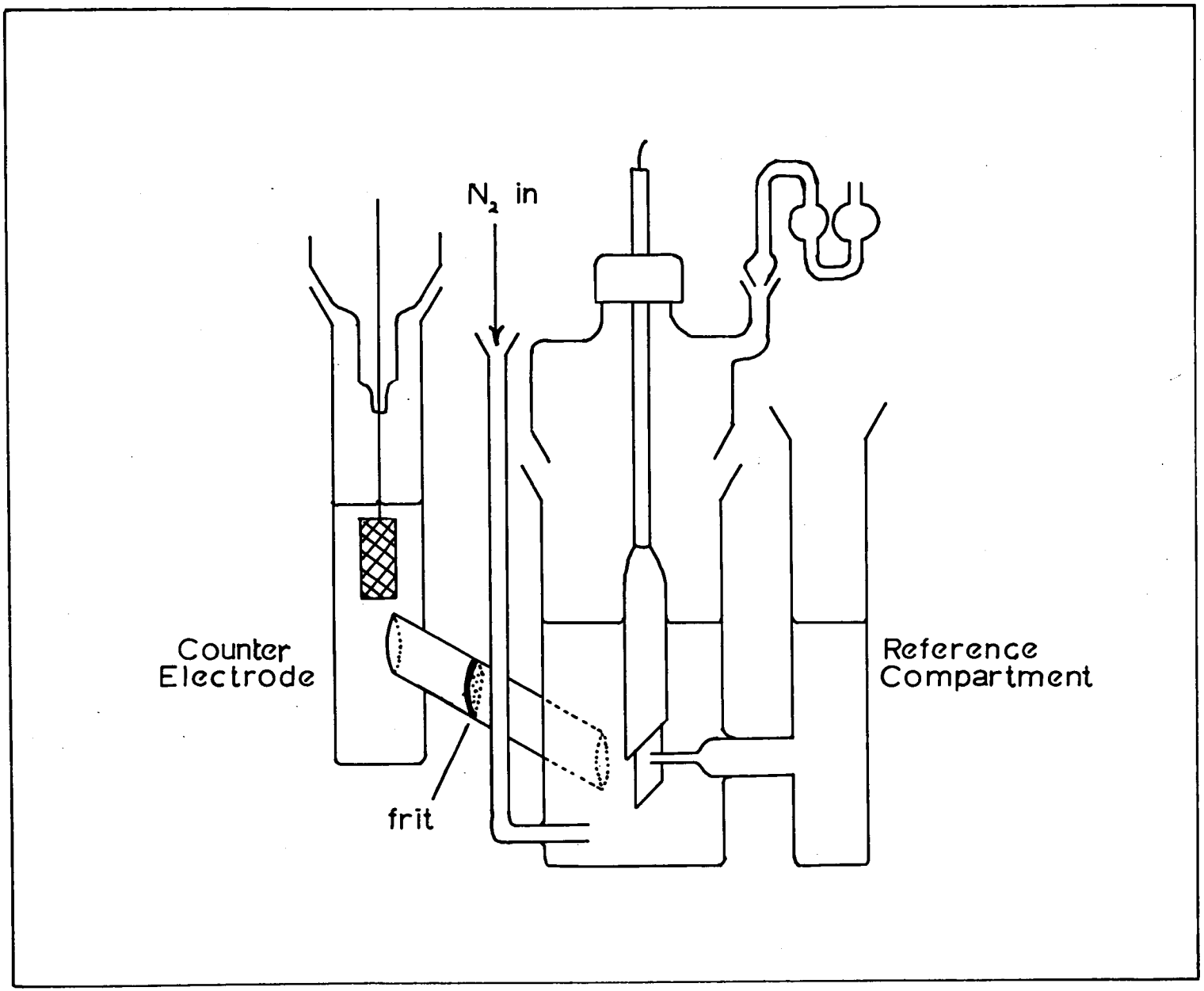
N_2 in
Counter Electrode
frit
Reference Compartment

Fig. 49 Photographs of Actual Cells

Type 1

Type 2

Type 3

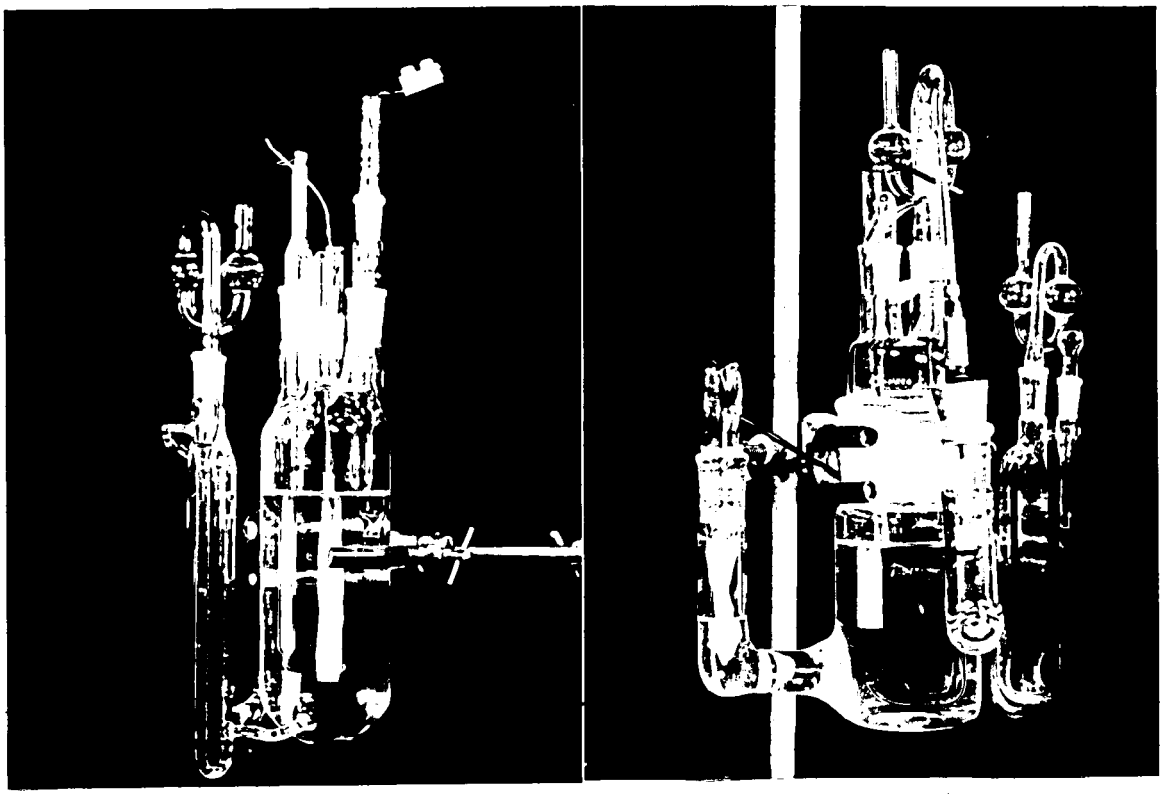

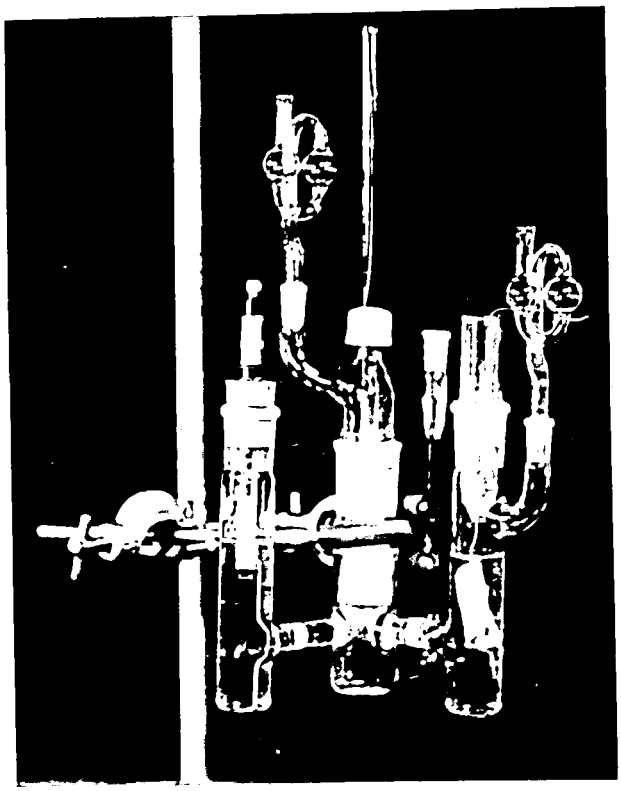

for studies of the oxidation of organic compounds. The working compartment (~25 ml) held a fixed horizontal Luggin capillary. The test electrode was supported, in the removable lid, by means of a screw joint and could be adjusted to within close proximity of the tip of the Luggin capillary. This cell was not fitted with a charcoal side arm but with a nitrogen purge tube. The counter electrode was contained in a compartment separated from the working compartment by means of a frit to prevent possible reduction of the organic compounds.

APPENDIX 2

$Ag_2O/Ag/OH^-$ REFERENCE ELECTRODES

Silver oxide reference electrodes were prepared by thermally decomposing Ag_2O (prepared by precipitation from $AgNO_3$) onto a platinum wire sealed into soda glass. A thick coating of partially decomposed oxide was built up on the wire and this microporous electrode was inserted into 1.0M NaOH and alternately cycled (galvanostatically) between oxidised (Ag_2O) and reduced forms. After 4-5 cycles the electrode (in the oxidised state) was held in 1.0M NaOH for ~6 weeks before use as a reference electrode.

Potentiometric measurements show that while the potentials of electrodes prepared in this manner are initially erratic (c.f. HAMER and CRAIG (81)) after 4-5 weeks a stable reversible potential is attained. $Ag_2O/Ag/OH^-$ electrodes prepared in this manner obey the expected $E - [OH^-]$ relationship (Fig. 50) and are stable for long periods with $E^\circ = +0.338V$ N.H.E.

Fig. 50 Potential Dependence on $[OH^-]$ for a typical Ag_2O Reference Electrode.

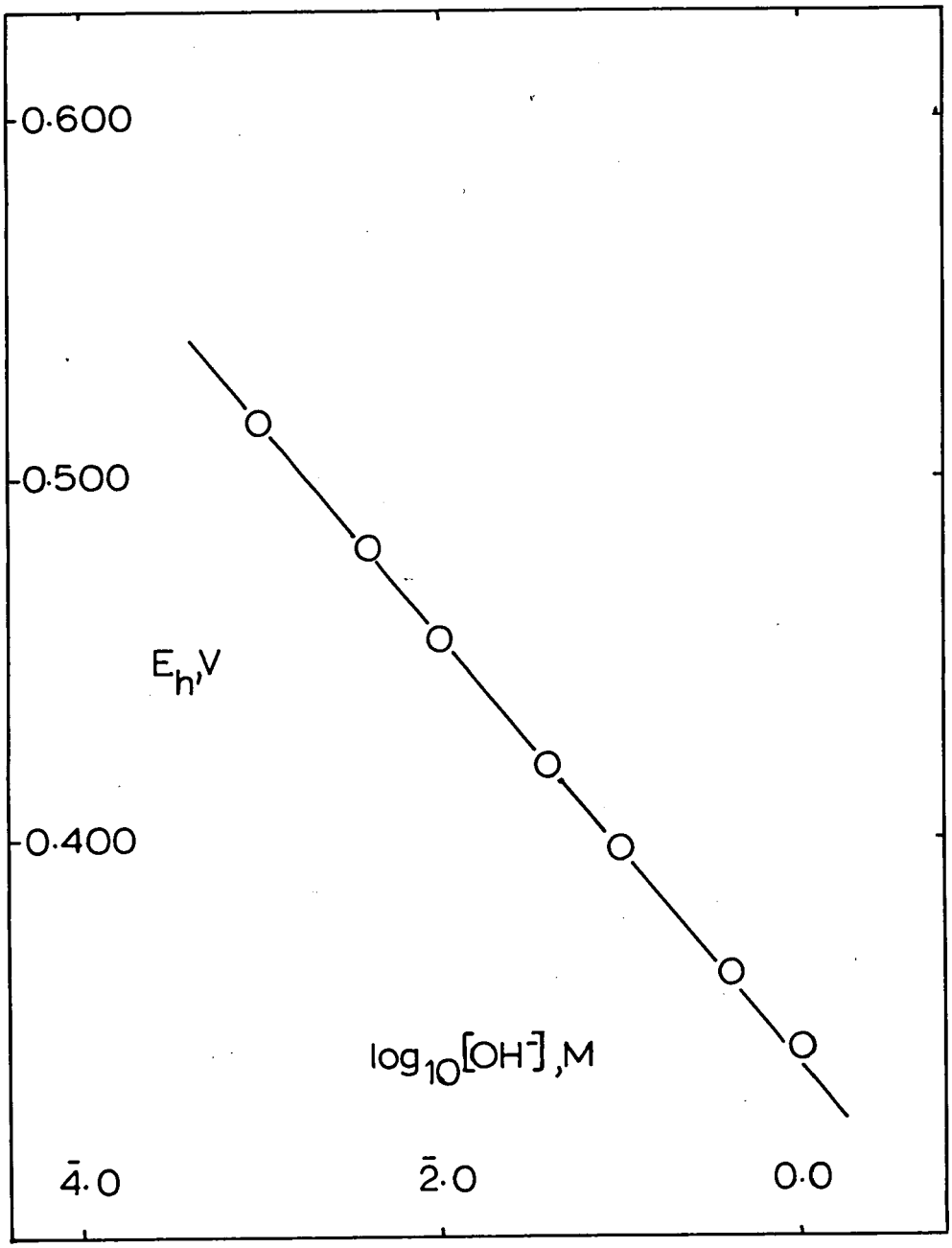
0·600
0·500
0·400
E_h,V
$\log_{10}[OH^-]$,M
4·0
2·0
0·0

APPENDIX 3

THE PREPARATION OF SILVER WORKING ELECTRODES

Silver working electrodes were made from 99.999% silver (Messrs. Johnson Matthey Ltd) in either rod or sheet form.

Micro electrodes for kinetic and electrode capacitance measurements were the exposed cross-section of a silver rod. The silver rod (with a wire soldered on for electrical connection) was mounted in a suitable glass-tube holder, warmed over a radiant heat source, and coated with additive free polythene powder (I.C.I. Plastics Div. grade 6830Ø). This was repeated until a thick coating (typically $\sim \frac{1}{8}$" thick) of melted polythene had built up around the electrode which was then allowed to cool. When completely cool the cross-section of the silver rod was exposed by careful grinding on roughened glass.

Working electrodes for preparative oxidations, made from a 1 c.m. wide strip of silver sheet, were coated with polythene as described above. The required surface area of electrode was exposed by careful paring of the polythene with a razor blade.

Each batch of polythene powder was checked for possible electrode contaminants by adding a quantity to a cell with a sitting mercury drop electrode in 1.0M $NaClO_4$. If the capacitance of the electrode deviated by $>1\%$ from its standard (75) value within 24 hrs of addition

the polythene, the sample was deemed unsuitable for the fabrication of electrodes.

Electrodes prepared in this manner gave time stable differential capacitance (Chapter 6) and kinetic (Chapter 7) data.

APPENDIX 4

THE PURIFICATION OF ELECTROLYTES

Electrolytes, prepared from A.R. chemicals and conductivity water were freed from trace amounts (to $< 10^{-9}$M) of surfactants by continuous circulation, within the cell, over activated charcoal.

The charcoal, 20 mesh gas absorption charcoal, was first purified by soxhlet extraction (with constant boiling HCL) of the cations present (predominantly iron). This process was continued until no trace of iron could be detected in the extractant liquor (KCNS test). The HCL was then removed by soxhlet extraction with water until the extractant gave a negative test for Cl^- with silver nitrate. The complete process of charcoal purification took 8-12 months. The purified charcoal was stored under conductivity water in stoppered flasks until required.

The electrolyte in the cells was circulated through the charcoal by means of a nitrogen lift pump. The nitrogen (B.O.C. Ltd. Oxygen free) was purified by passage over copper rods at $\sim 500^{\circ}C$, and then saturated with water vapour by passage through a bubbler of conductivity water.

APPENDIX 5

ELECTRICAL ANALOGUES FOR ELECTRODE REACTIONS AND ASSOCIATED AC CIRCUIT TRANSFORMS

There are three established analogues for an electrode reaction: the simple RANDLES (133) analogue (Fig. 51) which is for a reaction controlled solely by charge transfer/diffusion, and two analogues for mixed rate control, involving an alternative reaction path, due to LAITINEN and RANDLES (101), Fig. 52 and to GRAHAME (76) Fig. 53. These analogues are readily derived from the schering bridge measurements by means of a series of vector circuit transformations (Figs. 51, 52 and 53). The values for the various components of each transformation are given in Tables IX, X + XI respectively.

Fig. 51 A.C. Circuit Transforms to Derive the Elementary C.T. Analogue

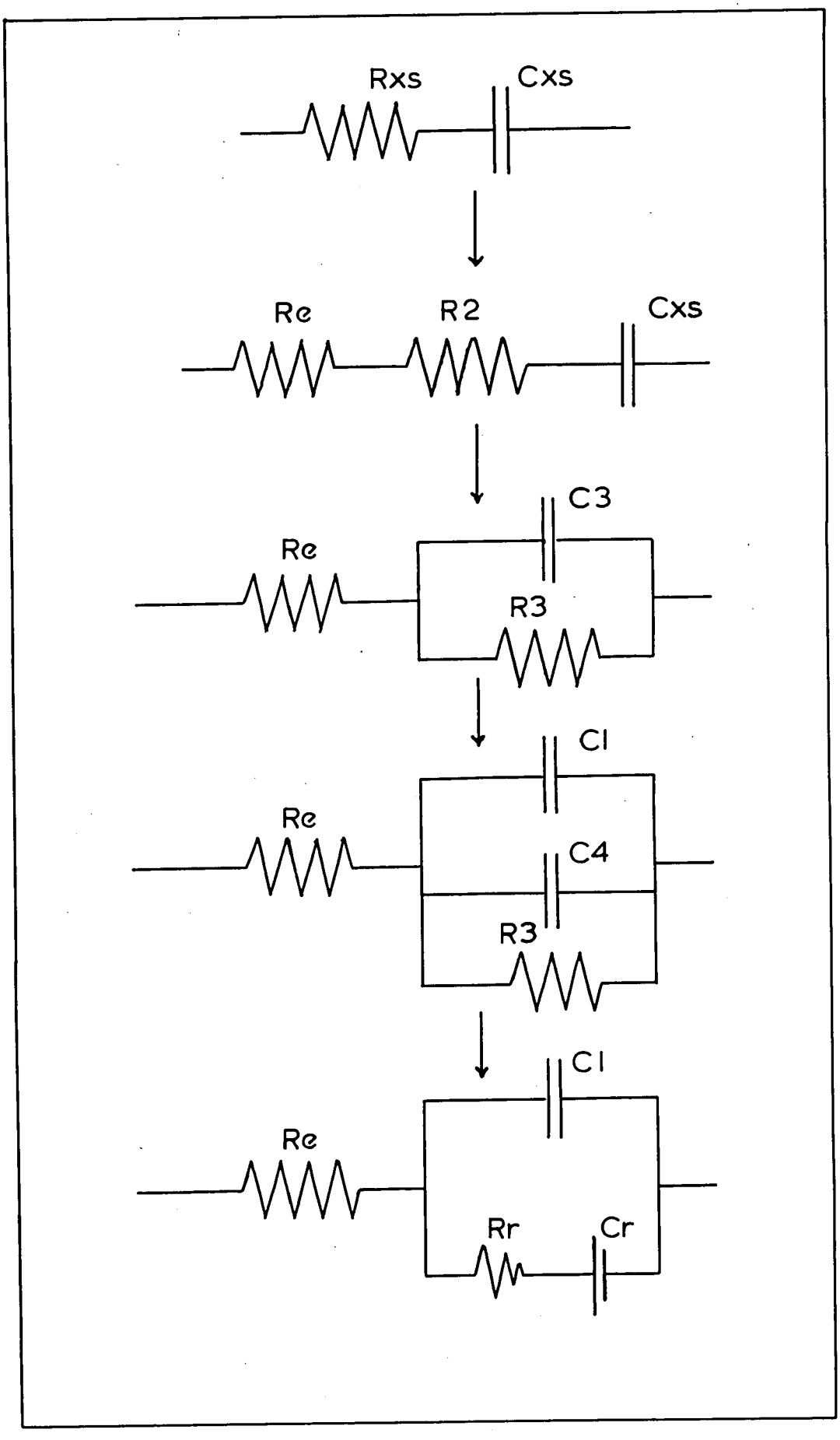
Rxs
Cxs
Re
R2
Cxs
C3
Re
R3
C1
Re
C4
R3
C1
Re
Rr
Cr

TABLE IX

DERIVATION OF COMPONENTS IN FIG 51

$$\omega = 2\pi \cdot \text{Frequency}$$

$$R_2 = R_{xs} - R_e$$

$$\beta = (\omega \cdot C_{xs} \cdot R_2)^{-1}$$

$$C_3 = C_{xs} \cdot \frac{\beta^2}{1 + \beta^2}$$

$$R_3 = R_2 (1 + \beta^2)$$

$$C_4 = C_3 - C1$$

$$\gamma = \omega \cdot C_4 \cdot R_3$$

$$R_R = \frac{R_3}{1 + \gamma^2}$$

$$1/\omega C_R = \gamma \cdot R_R$$

Fig. 52 A.C. Circuit Transforms to Derive the LAITINEN and RANDLES Analogue for a C.T. reaction with Adsorption.

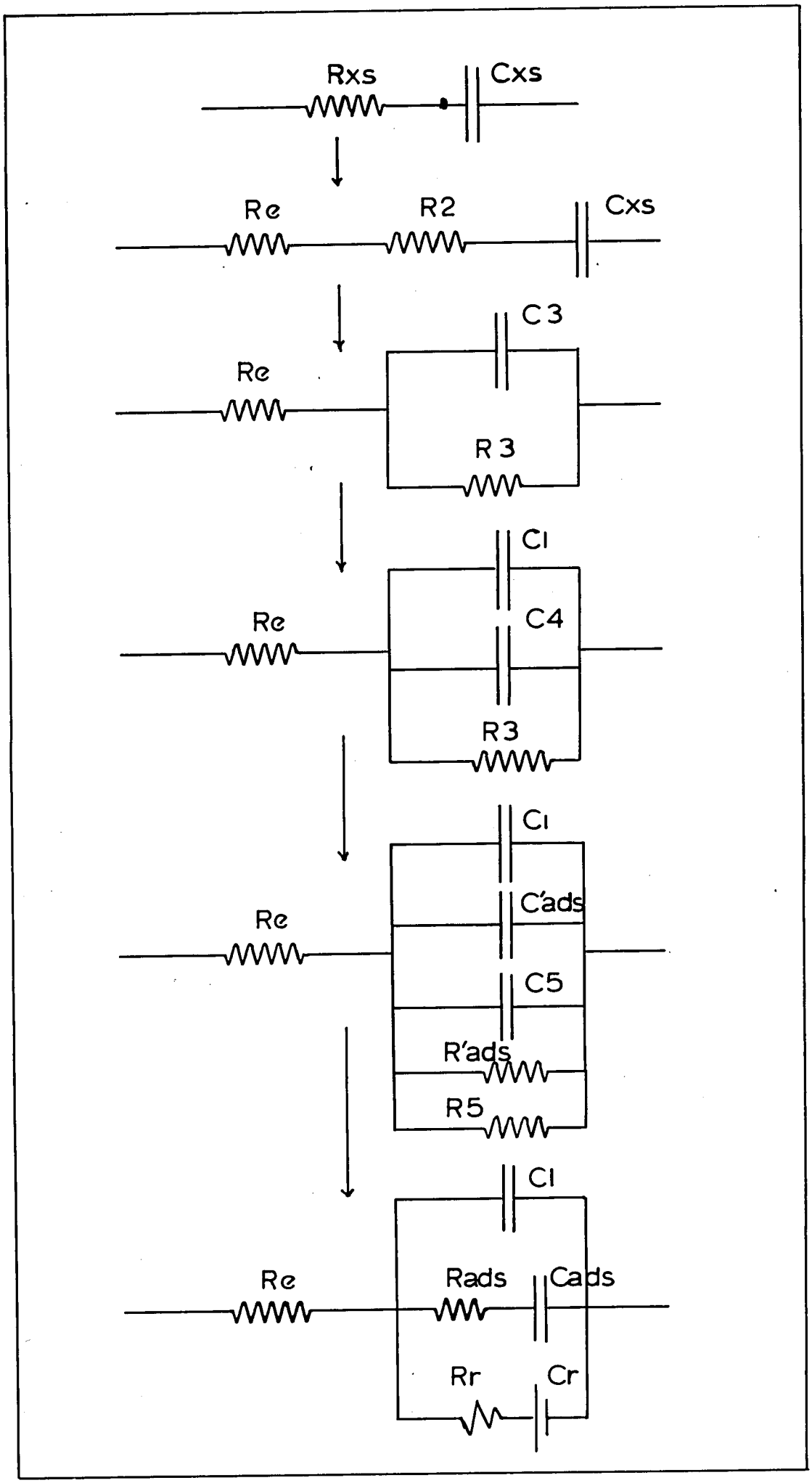
Rxs
Cxs
Re
R2
Cxs
C3
Re
R3
C1
Re
C4
R3
C1
C'ads
Re
C5
R'ads
R5
C1
Re
Rads
Cads
Rr
Cr

TABLE X

DERIVATION OF COMPONENTS IN FIG. 52

$$\omega = 2\pi \cdot \text{Frequency}$$

$$R_2 = R_{xs} - Re$$

$$\beta = (\omega \cdot R_2 \cdot C_{xs})^{-1}$$

$$C_3 = C_{xs} \cdot \frac{\beta^2}{1 + \beta^2}$$

$$R_3 = R_2 \ (1 + \beta^2)$$

$$C_4 = C_3 + C1$$

$$\delta = (\ \cdot Rads \cdot Cads)^{-1}$$

$$C\acute{a}ds = Cads \cdot \frac{\delta^2}{1 + \delta^2}$$

$$R\acute{a}ds = Rads \ (1 + \delta^2)$$

$$C_5 = C_4 - C\acute{a}ds$$

$$R_5 = \frac{R\acute{a}ds \cdot R_3}{R\acute{a}ds - R_3}$$

$$\epsilon = \omega \cdot R_5 \cdot C_5$$

$$R_R = \frac{R_5}{1 + \epsilon^2}$$

$$1/\omega C_R = \epsilon \cdot R_R$$

Fig. 53 A.C. Circuit Transforms to Derive the GRAHAME Analogue for a C.T. Reaction with Adsorption .

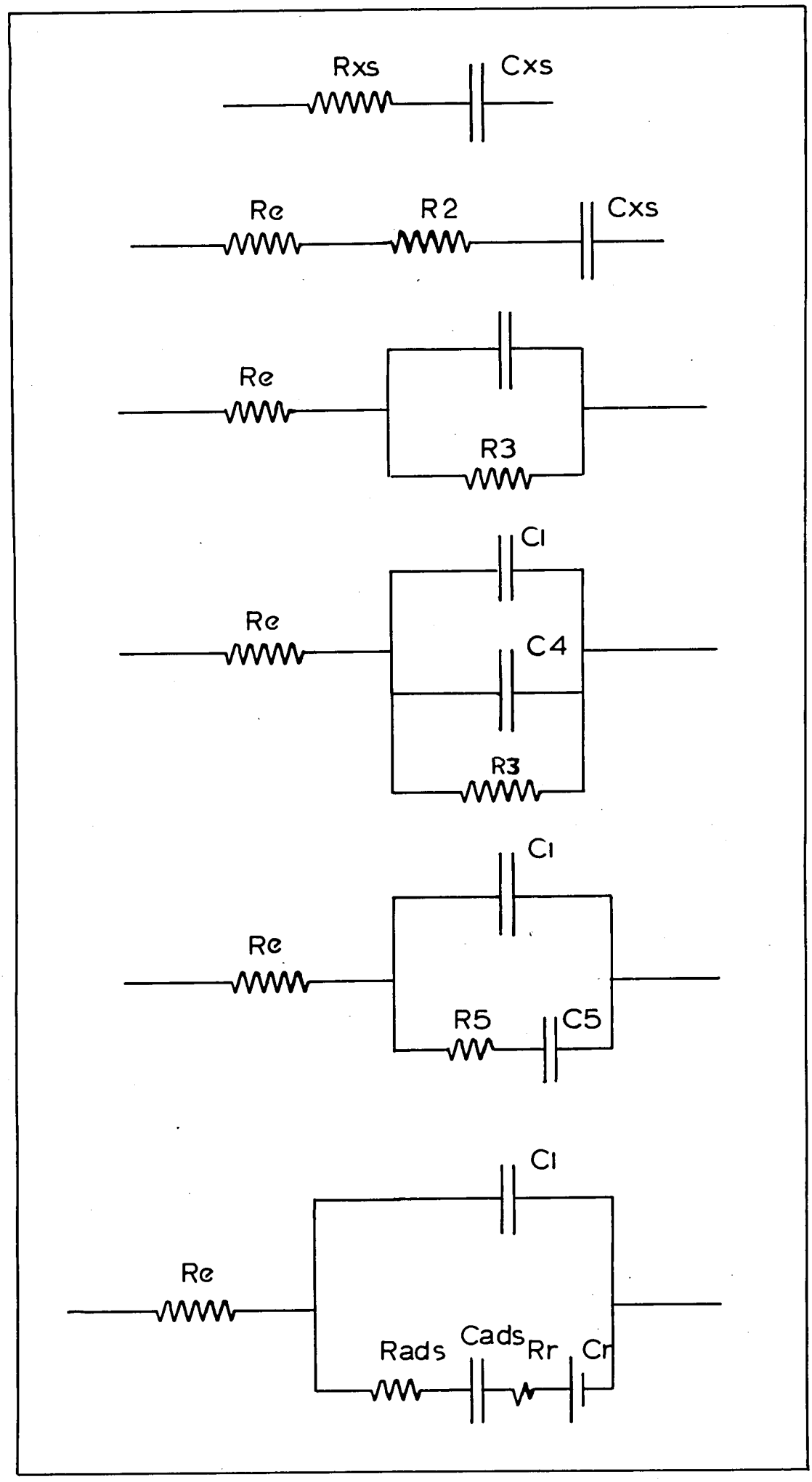
Rxs
Cxs
Re
R2
Cxs
Re
R3
Cl
Re
C4
R3
Cl
Re
R5
C5
Cl
Re
Rads
Cads
Rr
Cr

TABLE XI

DERIVATION OF COMPONENTS IN FIG. 53

$$\omega = 2\pi \cdot \text{Frequency}$$

$$R_2 = Rxs - Re$$

$$\beta = (\omega \cdot R_2 \cdot Cxs)^{-1}$$

$$C_3 = Cxs \cdot \frac{\beta^2}{1 + \beta^2}$$

$$R_3 = R_2 (1 + \beta^2)$$

$$C_4 = C_3 - C1$$

$$C_5 = C_4 \cdot \frac{1 + \gamma^2}{\gamma^2}$$

$$R_5 = \frac{R_3}{1 + \gamma^2}$$

$$Rp = R_5 - Rads$$

$$1/\omega Cr = 1/\omega C_5 - 1/\omega Cads$$

$$\gamma = \omega \cdot C_4 \cdot R_3$$

APPENDIX 6

COMPUTER PROGRAMS

These computer programs, written in FORTRAN IV for an ICT Series 1900 computer carry out the transforms given in Appendix 5.

Program H085 is elementary. Arrays of estimated CL and RE values, estimated CADS and RADS values and experimental FREQUENCY, RXS and CXS values are read in and an array of $W^{-\frac{1}{2}}$, R_R and $1/WC_R$ is calculated for each combination of CL, RE, RADS and CADS. The array which gives the best fit to the faradaic components (straight parallel Rr + $1/\omega$Cr vs. $\omega^{-\frac{1}{2}}$ plots) is chosen by inspection. This program will calculate on the basis of the three analogues given in Appendix 5, the analogue being selected by the value given to the logical 'switch' INDIC

This program which is cumbersome to use when the simple RANDLES analogue (Fig. 8) is chosen, becomes very difficult indeed when either of the adsorption analogues is used. The optimum array has to be chosen from a very large number of arrays (the number of arrays produced is the product of the number of estimated RE, CL, CADS and RADS values used), which is a very time consuming process.

It was to overcome these difficulties that programs H097 was written. This program uses an L.U.T. Computer Centre optimisation program PXS6D. PXS6D will minimise

(or maximise) a function, F, of any number of variables X_i, which are subject to lower and upper constraints G_i and H_i. The function, F, has to be calculated in a subroutine, CALXGH. The data, numbers of variables and contraints and software instructions are given in the Master segment which calls PXS6D.

In this application (H097) of PXS6D there are 5 variables:- RE, CL, RADS, CADS and the slope of R_R and $1/\omega CR$ vs. $\omega^{-\frac{1}{2}}$. F is chosen as the weighted sum of three diagnostic criteria: Fa, Fb, Fc. a - the criterion that the in-phase and out-phase components shall be parallel when plotted against $\omega^{-\frac{1}{2}}$ (this achieved by putting $Fa = \sum_i (R_R + 1/\omega C_R)_i^2$. b - that $1/\omega Cr$ vs. $\omega^{-\frac{1}{2}}$ shall be a straight line passing through the origin ($F_b = \sum (1/\omega Cr - x(5)\cdot\omega^{-\frac{1}{2}})_i^2$). c - the Tangent of the phase angle, ϵ (γ in the simple analogue), shall be less than 1.0 ($F_c = \sum \epsilon_i^4$ -a high even power was chosen so that the optimisation would not yeild -ve values for ϵ and to enable relatively smallweight factors to be used).

The limits are set such that for C_L and R_E: G_i is $\frac{1}{2}$ the initial value of X_i while H_i is double the initial value of X_i. For RADS, CADS and SLOPE only a lower constraint $G_i = 0$ is set. (H_i is given as double any value for X_i that may be calculated).

This program with suitable weighting factors has worked very well with data on the Zn^{2+}/Zn exchange (kindly supplied by Mr. J. T. Clark) but would not optimise properly the data for the Ag_2O/Ag exchange as discussed in Ch. 7.

PROGRAM H085

```
      MASTER  H085
      DIMENSION W(3,50),X(2,50),Y(2,50)
      COMMON LFREQ,M,N
      READ(1,1) KCASE
    1 FORMAT(I4)
      DO 75 K=1,KCASE
      READ(1,2) LFREQ,MNO,NNO,INDIC
      READ(1,3) (W(1,L),W(2,L),W(3,L),L=1,LFREQ)
      READ(1,4) (X(1,M),X(2,M),M=1,MNO)
    2 FORMAT(4I4)
    3 FORMAT(F7.1,F7.2,E10.4)
    4 FORMAT(2E10.4)
      IF(NNO)20,20,21
   20 WRITE(2,50)
   50 FORMAT(//20X,2HNO,2X,10HADSORPTION,2X,5HTERMS/)
      DO 74 M=1,MNO
      WRITE(2,51) X(1,M),X(2,M)
   51 FORMAT (/10X,3HRE=F7.2/10X,3HCL=E10.4/)
      WRITE(2,52)
   52 FORMAT(3X,4HFREQ,11X,3HRXS,12X,3HCXS,15X,5HGAMMA,10X,2HRR,14X,3HGR
     1R,13X,3HRRW)
      CALL CAL1(W,X)
   74 CONTINUE
      GO TO 75
   21 READ(1,5) (Y(1,N),Y(2,N),N=1,NNO)
    5 FORMAT(2E10.4)
      IF(INDIC)22,22,23
   22 WRITE(2,53)
   53 FORMAT(//20X,8HPARALLEL,2X,8HANALOGUE)
      DO 73 M=1,MNO
      DO 72 N=1,NNO
      WRITE(2,54) X(1,M),X(2,M),Y(1,N),Y(2,N)
   54 FORMAT(///10X,3HRE=F7.2/10X,3HCL=E10.4/8X,5HRADS=E10.4/8X,5HCADS=E
     110.4/)
      WRITE(2,52)
      CALL CAL2(W,X,Y)
   72 CONTINUE
   73 CONTINUE
      GO TO 75
   23 WRITE(2,55)
   55 FORMAT(//20X,6HSERIES,2X,8HANALOGUE)
      DO 71 M=1,MNO
      DO 70 N=1,NNO
      WRITE(2,54) X(1,M),X(2,M),Y(1,N),Y(2,N)
      WRITE(2,52)
      CALL CAL3(W,X,Y)
   70 CONTINUE
   71 CONTINUE
   75 CONTINUE
      STOP
      END
```

```
      SUBROUTINE CAL1(W,X)
      DIMENSION W(3,50),X(2,50),Y(2,50)
      COMMON LFREQ,M,N
      DO 101 L=1,LFREQ
      A=2.*3.14159*W(1,L)
      P=1./SQRT(A)
      R2=W(2,L)-X(1,M)
      IF(R2)30,101,30
   30 B=1./(A*R2*W(3,L))
      B2=B**2
      C3=W(3,L)*B2/(1.+B2)
      R3=R2*(1.+B2)
      C4=C3-X(2,M)
      G=A*C4*R3
      RR=R3/(1.+G**2)
      GRR=G*RR
      WRITE(2,56) W(1,L),W(2,L),W(3,L),G,RR,GRR,P
   56 FORMAT(3X,F7.1,3X,F7.2,3X,E10.4,3X,F7.4,3X,F8.2,3X,F8.2,3X,F8.6)
  101 CONTINUE
      RETURN
      END

      SUBROUTINE CAL2(W,X,Y)
      DIMENSION W(3,50),X(2,50),Y(2,50)
      COMMON LFREQ,M,N
      DO 102 L=1,LFREQ
      A=2.*3.14159*W(1,L)
      P=1./SQRT(A)
      R2=W(2,L)-X(1,M)
      IF(R2)31,102,31
   31 B=1./(A*R2*W(3,L))
      B2=B**2
      C3=W(3,L)*B2/(1.+B2)
      C4=C3-X(2,M)
      R3=R2*(1.+B2)
      D=1./(A*Y(1,N)*Y(2,N))
      D2=D**2
      CD=Y(2,N)*D2/(1.+D2)
      RD=Y(1,N)*(1.+D2)
      C5=C4-CD
      R5R=RD-R3
      R5=R3*RD/R5R
      G=A*R5*C5
      RR=R5/(1.+G**2)
      GRR=G*RR
      WRITE(2,57) W(1,L),W(2,L),W(3,L),G,RR,GRR,P
   57 FORMAT(3X,F7.1,3X,F7.2,3X,E10.4,3X,F7.4,3X,F8.2,3X,F8.2,3X,F8.6)
  102 CONTINUE
      RETURN
      END
```

```
      SUBROUTINE CALS(W,X,Y)
      DIMENSION W(3,50),X(2,50),Y(2,50)
      COMMON LFREQ,M,N
      DO 103 L=1,LFREQ
      A=2.*3.14159*W(1,L)
      P=1./SQRT(A)
      R2=W(2,L)-X(1,M)
      IF (R2)32,103,32
   32 B=1./(A*R2*W(3,L))
      B2=B**2
      C3=W(3,L)*B2/(1.+B2)
      R3=R2*(1.+B2)
      C4=C3-X(2,M)
      GA=A*R3*C4
      G2=GA**2
      C5=C4*(1.+G2)/G2
      R5=R3/(1.+G2)
      RR=R5-Y(2,N)
      GRR=(1./(A*C5))-(1./(A*Y(2,N)))
      G=GRR/RR
      WRITE(2,58) W(1,L),W(2,L),W(3,L),G,RR,GRR,P
   58 FORMAT(8X,F7.1,8X,F7.2,8X,E10.4,8X,F7.4,8X,F8.2,8X,F8.2,8X,F8.6)
  103 CONTINUE
      RETURN
      END
```

PROGRAM H097

```
      MASTER H097
      DIMENSION X(5),G(10),H(10),A(30),D(5),E(5),W(8,50),DIFF(50)
      COMMON JFREQ,K,FACT1,FACT2
C W1=FREQ,W2=RXS,W3=CXS,W4=RR,W5=GRR,W6=GAMMA,W7=W,W8=RRW
C X1=RE,X2=CL,X3=RADS,X4=CADS,X5=SLOPE
      READ(1,2) IPRINT,JFREQ,KNO
      READ(1,3) FACT1,FACT2
      READ(1,4) R1,R2
      READ(1,6) (X(I),I=3,5)
      READ(1,5) (W(1,J),W(2,J),W(3,J),J=1,JFREQ)
    2 FORMAT(I2/2I4)
    3 FORMAT(2E7.1)
    4 FORMAT(E10.4/E10.4)
    5 FORMAT(F7.1,F7.2,E10.4)
    6 FORMAT(E10.4)
      WRITE(2,54) FACT1,FACT2
   54 FORMAT(//8X,9HWEIGHTING,2X,6HFACTOR,2X,3HFOR,2X,8HSTRAIGHT,2X,4HGR
     1R=E9.1/8X,9HWEIGHTING,2X,6HFACTOR,2X,3HFOR,5HGAMMA,2X,4HLESS,2X,4H
     2THAN,2X,4HONE=E9.1)
      X(1)=R1
      X(2)=R2
      G(1)=0.5*R1
      G(2)=0.5*R2
      H(1)=2.*R1
      H(2)=2.*R2
      DO 13 I=3,5
   11 G(I)=0.
   13 H(I)=X(I)*2.
      N=5
      M=5
      KMAX=200
      BJ=-1
      NA=30
      NG=10
      DO 12 K=1,KNO
      DO 10 J=K,JFREQ
      W(7,J)=2.*3.14159*W(1,J)
   10 W(8,J)=1./SQRT(W(7,J))
      CALL PXS6D(N,M,KMAX,IPRINT,BJ,F,X,G,H,W,NW,NA,NG,A,D,E)
      WRITE(2,51) (X(I),I=1,5)
      WRITE(2,52)
      WRITE(2,53) (W(1,J),W(2,J),W(3,J),W(6,J),W(4,J),W(5,J),W(8,J),J=K,
     1JFREQ)
   51 FORMAT(//8X,11HOPTIMUM RE=F7.2/8X,11HOPTIMUM CL=E10.4/6X,13HOPTIMU
     1M RADS=E10.4/6X,13HOPTIMUM CADS=E10.4/5X,14HOPTIMUM SLOPE=E10.4)
   52 FORMAT(3X,4HFREQ,11X,3HRXS,12X,3HCXS,15X,5HGAMMA,10X,2HRR,14X,3HGR
     1R,13X,3HRRW/)
   53 FORMAT(3X,F7.1,8X,F7.2,8X,E10.4,8X,F7.4,8X,F8.2,8X,F8.2,8X,F8.6)
   12 CONTINUE
      STOP
      END
```

```
      SUBROUTINE CALXGH(N,M,IT,F,X,G,H,W)
      DIMENSION X(5),G(10),H(10),A(30),D(5),E(5),W(8,50),DIFF(50)
      COMMON JFREQ,K,FACT1,FACT2
      SW5=0.
      SW6=0.
      DO 90 J=K,JFREQ
      R2=W(2,J)-X(1)
      IF(R2)30,90,30
   30 B=1./(W(7,J)*R2*W(3,J))
      B2=B**2
      C3=W(3,J)*B2/(1.+B2)
      C4=C3-X(2)
      R3=R2*(1.+B2)
      DA=1./(W(7,J)*X(3)*X(4))
      D2=DA**2
      CD=X(4)*D2/(1.+D2)
      C5=C4-CD
      RD=X(3)*(1.+D2)
      R5R=RD-R3
      R5=RD*R3/R5R
      W(6,J)=W(7,J)*C5*R5
      EP2=W(6,J)**2
      W(4,J)=R5/(1.+EP2)
      W(5,J)=W(4,J)*W(6,J)
      SW5=SW5+(W(5,J)-X(5)*W(8,J))**2
      SW6=SW6+W(6,J)**2
      DIFF(J)=W(4,J)-W(5,J)
   90 CONTINUE
      F=(FACT1*SW5)+(FACT2*SW6**2)+(DIFF(JFREQ)-DIFF(JFREQ-4))**2
      RETURN
      END
```

```
PXS6D          (SEMI-COMPILED)

PXS6C1         (SEMI-COMPILED)

PXS6C2         (SEMI-COMPILED)

PXS6C3         (SEMI-COMPILED)

PXS6C4         (SEMI-COMPILED)

       FINISH
```

SYMBOLS

A	Nucleation exponent
C_L	Differential capacitance
C_R	Reaction capacitance
C_{XS}	Measured total capacitance
C_i^*	Concentration of species i
C_o^*	Concentration of oxidised species
C_R^*	Concentration of reduced species
D_i	Diffusion coefficient of species i
E	Electrode Potential
E_h	Electrode Potential referred to N.H.E.
E_m	Potential of current maximum (P.S.V. experiments)
E_r	Reversible electrode potential
E_z	Potential at which $q_o = 0$
F	Faraday ($\sim$96,500 coulombs)
h	Thickness of a 2-D nucleus
h	Plank's Constant ($\backsim 6.6 \times 10^{-27}$) e.s.u.)
I	Current
i	Current density
i_o	Exchange current density
I_m	Current maximum (P.S.V. experiments)
k_o	Standard rate constant (apparent)
$\vec{k}$	Rate constant for forward change transfer reaction
$\overleftarrow{k}$	Rate constant for reverse change transfer reaction
M	Initial diameter of a 2-D nucleus
N	Number of nuclei per unit area
No	Limiting number of nuclei per unit area

n	Number of electrons transferred in one unit reaction
n_a	Number of electrons transferred in rate controlling stage.
p	Freundlich exponent
q	Charge density
q_e	Charge denisty of electrode ($\equiv q_s$)
q_i	Charge density at electrode side of interphase
q_o	Charge density of metal side of interphase
R_D	Charge transfer resistance
R_E	Electrolyte resistance
R_R	Reaction resistance
R_{XS}	Measured resistive component of electrode impedance
S	Cross sectional area of growing needle
T	Temperature (^oK)
t	time
v	Potential sweep rate
v_e	Electrode reaction rate
α	Transfer coefficient
ΔG_e^*	Electrochemical free enthalpy of activation
ΔH^*	Enthalpy of activation
$\Delta \phi$	Galvani Potential Difference
$\Delta \psi$	Volta Potential Difference
δ	Double Layer "thickness"
ϵ	Dielectric constant
χ	Boltzmann's constant ($\sim 1.38 \times 10^{-16}$ e.s.u.)
η	Overpotential

η_D Charge transfer overpotential

η_Ω Ohmic potential

θ_i Degree of Coverance of species i

ν_i Stoichometric factor of species i

ρ Density of the solid phase

τ Transmission Coefficient

ω Angular frequency